January 2020

Evaluation Of Autoantibodies To Paraneoplastic Antigens As Early Detection Biomarkers For High-Grade Serous Ovarian Cancer

Laura Catherine Hurley
Wayne State University

EVALUATION OF AUTOANTIBODIES TO PARANEOPLASTIC ANTIGENS AS EARLY DETECTION BIOMARKERS FOR HIGH-GRADE SEROUS OVARIAN CANCER

by

LAURA CATHERINE HURLEY

DISSERTATION

Submitted to the Graduate School

of Wayne State University,

Detroit, Michigan

in partial fulfillment of the requirements

for the degree of

DOCTOR OF PHILOSOPHY

2020

MAJOR: CANCER BIOLOGY

Approved By:

_____

Advisor Date

_____

_____

_____

_____

DEDICATION

This dissertation is dedicated to my family,

especially

to Will Hurley.

to Bob Garela.

to Dovi Afesi.

and to Josephine Jannetta.

ACKNOWLEDGEMENTS

I would like to thank my mentor, Dr. Michael Tainsky, for his support and guidance throughout my PhD. He has provided the perspective to balance curiosity with focus. I am so appreciative of my time in such a positive and productive laboratory. Nancy Levin's attention to detail and organization of patient samples was instrumental in these studies. I would like to thank her for her excellent RD-debugging skills, which were an immense help in experimental design and data analysis, and for her help in processing large volumes of patient samples. Dr. Mita Chatterjee worked on the discovery stages and on the development of these biomarker studies and I would like to thank her for training me in the processes of protein purification. Dr. Greg Dyson provided expert statistical test planning and data analysis. Dr. Kristen Purrington provided guidance on issues concerning population science and disease prevalence.

I would like to thank J'nice Stork for all of her assistance and for being a source of motivation in the form of baked goods, and Dr. Rita Rosita for all of her helpful advice. A special thank you to Dr. Maggie Purcell and Dr. Sidra Ahsan for being there every step. I have been lucky to be surrounded by the encouragement of fellow students and friends in the laboratory including Dr. Jaime Lopes, Scott Baughan, Douglas Depoorter, Dr. Marufa Rumman and Sophia Chaudhry. Thank you for helping me to prepare presentations, troubleshoot experiments, and go for coffee. Thank you to the undergraduate students I have had the honor of working with, including Jasmine Coles, Shlomo Muszkat, Morena Tinaj, and Zachary Haworth, for their roles in moving the projects forward.

I especially want to thank the Cancer Biology Graduate Program including Dr. Larry Matherly, Dr. George Brush, and Nadia Daniel and the Foreign Exchange Student

Program at Okayama University, Okayama, Japan, for facilitating my studies through the Okayama Research Exchange Program. I am incredibly grateful for this experience. Thank you to Dr. Masaharu Seno for welcoming me into your laboratory. I have learned so much from excellent scientists including Dr. Anna Sanchez Calle, Dr. Neha Nair, Dr. Maram Zahra, Dr. Marta Prieto Villa, Dr. Tsukasa Shigehiro, Dr. Arun Vaidyanath, Dr. Apriliana Cahya, Dr. Hafizah Binti Mahmud, Dr. Akimasa Seno, and Dr. Oo Aung. Thank you Dr. Tomonari Kasai for teaching me stem cell culture techniques.

Thank you to my committee, Dr. Russ Finley, Dr. Geng Shen Wu, and Dr. Benjamin Kidder, for your feedback and advice. Thank you to Dr. Yubin Ge and Dr. Isabela Podgorski for aiding in public speaking development. Thank you to my colleagues in the WSU IBS graduate school for the exam study sessions and also for inspiring me with your work. Thank you also to my friends and family who have helped with editing manuscripts, rehearsing talks, formatting figures, and especially to Paul Hurley for providing consultation on statistical analyses. Also thanks to Louie and Antonio Conti for without them I wouldn't know research or real pasta. Finally, I would like to thank my funding, the Ruth L. Kirschenstein Research Training Grant (T32 CA009531), Okayama University Research Exchange Fellowship, Wayne State University Rumble Graduate Research Assistantship, DeRoy Testamentary Foundation Predoctoral Fellowship in Cancer Research, and the Wayne State Cancer Biology Graduate program for support in traveling to the American Association for Cancer Research Annual Meeting 2018 and the American Society of Clinical Oncology/Society for Immunotherapy of Cancer Clinical Immuno-Oncology Symposium 2017.

TABLE OF CONTENTS

LIST OF TABLES

LIST OF FIGURES

LIST OF ABBREVIATIONS

AChR	Acetylcholine receptor
Anti-NMDAR	anti-*N*-methyl-d-aspartate receptor
BAFF	B-cell-activating factor
CA125	Cancer Antigen 125
CAR-T	Chimeric antigen receptor T
CARP VIII	Carbonic anhydrase-related protein VIII
CDR2	Cerebellar degeneration related protein 2
CDR2L	Cerebellar degeneration related protein 2-like
CHTN	Cooperative Human Tissue Network
CKB	Creatine kinase brain type
CSF	Cerebrospinal fluid
CTA	Cancer-testis antigen
CTCs	Circulating Tumor Cells
cDNA	Circulating Tumor DNA
CV	Coefficients of variation
EPIC	European Prospective Investigation into Cancer
ESCC	Esophageal squamous cell carcinoma
GABA	Gamma-aminobutyric acid
HA	Hemagglutinin antigen
HGSOC	High grade serous ovarian cancer
HARS	Histidyl-tRNA synthetase
IDO	Indole-amine-2,3,-dioxygenase

IGluRs	Ionotropic glutamate receptor
IGCNU	Intratubular germ-cell neoplasm unclassified type
IA	Immunoadsorption
IgG	Immunoglobulin
IPTG	β-D-1-thiogalactopyranoside
irAE	Immune Related Adverse Event
IVIg	Intravenous immunoglobulin
KLH	Keyhole limpet haemocyanin
LSPR	Localized surface plasmon resonance
NAPPA	Nucleic Acid Programmable Protein Arrays
NMDAR	*N*-methyl-d-aspartate receptor
NXP-2	Nuclear matrix protein 2
MGluR	Metabotropic glutamate receptor
OD	Optical Density
PCA-1	Purkinje cell antibody 1
PE	Plasma exchange
PID	Pelvic inflammatory disease
PLCO	Prostate, Lung, Colon, Ovarian Cancer
PPV	Positive predictive value
RAG1	Recombination-activating gene 1
RAG2	Recombination-activating gene 2
ROCA	Risk of Ovarian Cancer Algorithm
RRSO	Risk-reducing salpingo-oopherectomy

SCSOCS	Shizuoka Cohort Study of Ovarian Cancer Screening
SEREX	Serological analysis of recombinant cDNA expression libraries
SERPA	Serologic Proteome Analysis
SERS	Surface enhanced Raman spectroscopy
SI-NET	Small intestine neuroendocrine tumor
SPR	Surface plasmon resonance
TMB	3.3', 5.5'-tetramethylbenzidine
TLS	Tertiary Lymphoid Structure
TIF1-GAMMA	Transcription intermediary factor-1 gamma
TVUS	Transvaginal Ultrasound
UKCTOKS	UK Collaborative Trial of Ovarian Cancer Screening
VEGF	Vascular endothelial growth factor
VGKC	Voltage-gated potassium channel

1. CHAPTER 1: Introduction

1.1. Early Detection of Ovarian Cancer

1.1.1. Ovarian Cancer Subtypes, Stages, and Survival

Ovarian cancer is the fifth leading cause of cancer-related deaths in women. Stage I ovarian cancer is defined by localized cancer in the ovaries or fallopian tubes, with only 15% of cases diagnosed at this stage [143]. The majority of cases are diagnosed at an advanced stage, defined as stage II when the tumor has spread to organs within the pelvis, stage III which involves the peritoneal surface of the pelvis or abdomen and surrounding lymph nodes, and stage IV with metastasis beyond the abdominal cavity [143]. Worldwide, the 5-year age-standardized net survival for stage I ovarian cancer is 80%, which decreases to 30% for advanced disease defined as stage II-IV for all subtypes [119]. Standard of care is primary optimal debulking surgery followed by platinum-based chemotherapy [9, 106]. The most significant prognostic factor is degree of residual disease following surgery [106]. The majority of patients with advanced disease experience a recurrence, of which 75% of recurrent cases cannot be cured [106]. The presence of chemoresistant stem-like cells contributes to tumor recurrence [96].

Ovarian cancer is classified as Type I and Type II, which represents 20% and 80% of cases, respectively. Type I ovarian cancer is less aggressive, low grade, is associated with ARIDA1, BRAF, PIK3CA, PTEN, and KRAS mutations, and is comprised of mucinous, clear cell, and endometrioid tumor subtypes. Type II ovarian cancer has more aggressive, high grade tumors most commonly comprised of the serous subtype, and is associated with p53 mutations [101]. The site of origin differs

between Type I and Type II tumors; Type I tumors originate as atypical benign conditions such as endometriosis which can implant on the ovary and transform, whereas Type II tumors originate in the fallopian tube as serous tubal intraepithelial carcinoma. Type I ovarian cancer is largely diagnosed at stage I or II whereas Type II ovarian cancer is most often diagnosed at stage III or IV with decreased overall survival [101]. Seventy percent of all epithelial ovarian cancer cases are high-grade serous ovarian cancer (HGSOC); the present study evaluates a series of autoantibodies for use as diagnostic biomarkers in serum samples from patients with HGSOC [143].

1.1.2. Early Detection in the General Population

Three large randomized control trials have evaluated the effectiveness of screening for ovarian cancer in the general population. In the Prostate, Lung, Colon, and Ovarian (PLCO) cancer trial, 68,557 women were followed [23]. Screening for ovarian cancer was performed with both Cancer Antigen 125 (CA125) and transvaginal ultrasound (TVUS). Abnormal findings on either test prompted surgery, with no observed mortality benefit compared with the control arm with no screening. CA125 is a glycoprotein that was identified as a biomarker for ovarian cancer and is elevated in 80% of late stage cases and 50% of early stage cases [153]. It is also elevated in other benign gynecological conditions such as uterine fibroids, endometriosis, as well as other diseases such as cirrhosis and interstitial lung disease [4]. Alone, it is not an adequate biomarker due to insufficient sensitivity and specificity. When measured at a single time point, CA125 has historically been considered elevated at a level >35 U/mL, and has been used to monitor recurrent disease. The PLCO trial utilized a single measurement of CA125, and in the same time frame women underwent imaging with TVUS. Results

of the PLCO trial showed no difference in mortality for this screening method [23]. A randomized control study in Japan titled the Shizuoka Cohort Study of Ovarian Cancer Screening (SCSOCS) enrolled 41,688 women who were either screened annually with TVUS and CA125 interpreted at a single time point at the cutoff value of 35 U/mL [97]. An increased proportion of stage I cases was observed, though this finding was not significant, and mortality was not reported [97].

Improvements in early detection were observed in the UK Collaborative Trial of Ovarian Cancer Screening (UKCTOCS) due to improved screening methods by incorporation of the Risk of Ovarian Cancer Algorithm (ROCA). ROCA detects increases in CA125 values over time relative to each patient's baseline value, which improves specificity. Additionally, imaging with TVUS is only initiated by increasing CA125 values, which greatly reduces false-positives. The UKCTOS study enrolled over 200,000 patients, divided into a multi-modal screening arm using ROCA, a screening arm with yearly TVUS, and a non-screening arm [86]. Multi-modal screening with ROCA resulted in a stage shift with 36.1% detected at stages I-II [85]. Initial analysis at 7 years suggests there may be a mortality benefit in the ROCA screening arm, and while follow-up long term analysis at 14 years remains to be reported, if trends observed at 7 years continue there is predicted to be an observed mortality decrease in the screening arm [86].

1.1.3. Early Detection in High Risk Population

Screening in increased-risk populations has the potential to be beneficial given a higher prevalence relative to the general population [75, 147, 166]. Those with a family history of ovarian cancer are at an increased-risk, including hereditary breast and

ovarian cancer patients with BRCA1 and BRCA2 mutations that are frequently found in the germline of Type II HGSOC, and Lynch syndrome with mismatch repair gene mutations [43]. The clinical recommendation for women with known BRCA1 or BRCA2 mutations or family history of ovarian cancer is prophylactic removal of the ovary and fallopian tubes. Risk-reducing salpingo-oopherectomy (RRSO) reduces ovarian cancer incidence in high risk women [146]. Among patients with BRCA1/2 mutations, those who completed RRSO have reduced incidence of ovarian cancer and cancer-related mortality rates [112]. However, the decision to undergo surgery is complex, and there remains a population of women who choose not to undergo surgery. In a study of 2,287 women with increased familial risk of ovarian cancer, 40% of patients chose RRSO, while 60% chose ovarian cancer screening with the ROCA screening strategy [112]. Risk of surgery, maintaining the option to have children, and both physiological and psychological side effects of removal of the ovary and fallopian tube stemming from surgical menopause including bone density loss and hormonal changes are factors that patients consider. [56, 112, 123]. An increased risk of multi-morbidity has been reported for patients undergoing bilateral salpingo-oopherectomy in a study comparing 1,653 women retaining ovaries with 1,653 women at average risk for ovarian cancer who underwent surgery [144]. Women with the oophorectomy performed between the ages of 46-49 had a significantly increased risk of anxiety, depression, hyperlipidemia, diabetes, arthritis, and cancer. Women who underwent surgery before the age of 46 were also at a significantly increased risk for depression and hyperlipidemia, as well as for cardiac arrhythmias, coronary artery disease, arthritis, asthma, chronic obstructive pulmonary disease, and osteoporosis [144].

For women who decide to not have surgery, 3 prospective trials have recently examined the benefit of screening more frequently than once a year, and a stage shift was observed in cases detected. In the UK Familial Ovarian Cancer Screening Study phase II trial, 4, 348 women at high-risk for ovarian cancer were screened for CA125 every 4 months with yearly TVUS, which resulted in a significant stage shift in diagnosis. Of the 19 total cases detected during the 5 years of screening, 10 were stage I-II [147]. Two prospective trials from the Cancer Genetics Network and the Gynecologic Oncology Group together screened 3, 962 women at high-risk for ovarian cancer with CA125 screening every 3 months, followed by TVUS upon increases in CA125 above the patient's baseline. In these trials, 3 of the 6 incident cases were stage I-II [166]. These trials also demonstrated compliance with frequent screening among high-risk women. Additional biomarkers such as autoantibodies can be combined with CA125 to improve upon sensitivity in early detection. For women at high-risk for ovarian cancer, an improved early detection method would provide the option of frequent screening for those who decline or delay prophylactic surgery.

1.1.4. Strategies for Early Detection

Although screening in high-risk women who decline surgery using the two-step ROCA as described above is an acceptable method for early detection in terms of sensitivity, specificity, and positive predictive value (PPV), there are limitations in both steps. In the first step of CA125 detection, 20% of all cases will not express CA125, and 50% of early stage cases will not present with detectable levels of CA125 and are missed by ROCA [5, 164]. In the second step, TVUS has limitations of detecting early stage disease at low tumor volume as well as errors in interpretation. Improvement of

the first step by additional biomarkers to complement CA125 and novel imaging technologies can further develop early detection strategies. For example, additional circulating antigens as well as circulating autoantibodies have been measured in samples without detectable CA125 in retrospective studies. Novel biomarkers, imaging technology, and CA125 companion markers are outlined below.

TVUS is the standard technique for imaging of the ovaries, however it is limited in visualization of the fimbriae of the fallopian tubes and is unable to detect small lesions [54]. Light-induced endogenous fluorescence can detect serous tubal intraepithelial carcinomas from surgically removed tissue with 73% sensitivity. In vivo, falloposcopy has been proposed to detect serous tubal intraepithelial carcinoma with light-induced endogenous fluorescence [128].

Circulating tumor cells (CTCs) can be isolated from blood by targeting epithelial antigens on the cell surface followed by sequencing. In a study measuring both CA125 and CTCs in 153 serial serum samples from 51 patients with epithelial ovarian cancer, CTCs were demonstrated to be superior to CA125 detection with 90% sensitivity [208]. CTCs detected 93% of stage I disease compared with CA125 which detected 64% of stage I samples. However the ability to implement detection of CTCs into routine practice is limited.

Cell-free circulating tumor DNA (ctDNA) can be amplified from blood samples and sequenced for mutations as well as analysis of DNA hypermethylation, copy number variation, and loss of heterozygosity [54]. CancerSEEK is a test combining ctDNA and protein biomarkers, which demonstrated 98% sensitivity, however the

majority of cases were advanced stage. The limitation however is in the time frame required to process blood samples [114].

miRNA can be detected in circulation within extracellular vesicles or bound to chaperone proteins, which make them stable analytes. Multiple panels of miRNA have been identified with high performance of sensitivities of 62.4%, 86%, 75% and specificities ranging from 92.9%, 83%, and 100%, respectively [53, 198, 209]. The complementation of these panels with CA125 is not yet known, however in limited cases it was shown that CA125 positivity was independent of miRNA panel positivity, suggesting that these two strategies could be combined for an enhanced test.

Methods of detection using body fluids in proximity to the ovaries such as isolation of DNA from tampons as well as uterine lavage have been performed to detect TP53 mutations [54]. Endocervical brushings were analyzed from 245 patients with ovarian cancer using PapSEEK, a test which examines 18 mutations or aneuploidy, and resulted in 99% specificity relative to 714 healthy controls with 33% sensitivity for all ovarian cancer cases, as well as 34% sensitivity among early stage cases. When using intrauterine brushing, PapSEEK resulted in 100% specificity with 45% sensitivity for 51 ovarian cancer patients relative to 125 healthy controls; this study did not measure CA125 [54].

There have been extensive studies of additional circulating antigens to complement CA125, of which the antigen HE4 has been most promising. The European Prospective Investigation into Cancer (EPIC) cohort study enrolled over 200,000 women, of which 810 developed ovarian cancer [165]. CA125, CA72.4, CA15.3, and HE4 were evaluated with the banked serum samples, and none of the

markers performed better than CA125. HE4 was the only marker to marginally increase sensitivity in combination with CA125 [165]. The advantage of H4 is the superior specificity to CA125 [74]. Evaluation of serum samples from the UKCTOCS study, the combination of HE4 and CA72.4 was able to detect 16% of CA125-negative cases, however they were not detected with additional lead-time relative to CA125 [164].

1.1.4.1. Autoantibody Biomarkers

When the tumor is at a small size, there may be insufficient amount of circulating antigens to be detectable in serum or plasma. Autoantibodies are attractive biomarkers as they can be detected from a simple blood test, and they are more stable than circulating antigens. The long-term stability of autoantibodies in frozen serum allow for prospective-retrospective research in biomarker discovery and validation stages using banked serum samples. Studies of autoantibody tests for ovarian cancer to complement CA125 measurements and TVUS are currently ongoing. A detailed literature review revealed that eighty-five autoantigens have been evaluated for the early diagnosis of ovarian cancer with ongoing studies seeking an optimal panel [61, 92]. Due to inter-tumor heterogeneity and variable immune responses, it will be necessary to combine markers with the sensitivities of individual autoantibodies ranging from 10-30% to create a panel of antigens with sufficient sensitivity.

An autoantibody response can be detected from microscopic lesions that are undetectable with imaging. For example, the antibody associated with paraneoplastic encephalitis, Ma2, has been detected in patients with pre-invasive, microscopic intratubular germ-cell neoplasm unclassified type (IGCNU) [118]. In a study of 6 patients with encephalitis and positive for anti-Ma2 antibodies with no apparent tumor,

all 6 patients were found to have pre-invasive, microscopic IGCNU [118]. In this study we evaluated a set of antigens associated with paraneoplastic syndromes for their use in the detection of autoantibodies for the early detection of ovarian cancer. In a prospective study of serum samples from the UKCTOCS study, autoantibodies to TP53 were detected 8.1 months prior to elevated CA125 detection and 9.2 months prior to ROCA detection in 34 cases that were screen-positive with ROCA, and 22.9 moths prior to diagnosis of ovarian cancer in the 9 cases that were screen-negative with ROCA [194]. Autoantibodies to tumor antigens, produced at small tumor volumes, can be combined with serum screening of CA125 to improve sensitivity in early detection.

1.2. Tumor Immunology

The immune response to a transformed cells has been described by Schreiber et al. as a multistep process named “cancer immuno-editing” [154]. This theory describes the complex interaction of the immune system components of the microenvironment during tumor development, and the subsequent selection of tumor cells which evade the immune response. The three stages of immuno-editing are defined as elimination, equilibrium, and escape, and are critical components of tumor biology.

1.2.1. Immunotherapy and Ovarian Cancer

The immune response and tumor immune microenvironment influence tumor development and patient survival. Ovarian cancer has been shown to be immunogenic, and trials are currently evaluating the potential for both immunotherapies targeting tumor antigens and checkpoint blockade strategies [90, 116, 131]. The immune microenvironment has reproducibly been associated with prognosis in ovarian cancer; infiltration of lymphocytes correlates with survival [99, 207]. Presence of tertiary

lymphoid structures (TLSs) in the tumor periphery is associated with improved prognosis for lung, colorectal, breast, prostate, and ovarian cancer [72, 125]. TLSs in ovarian cancer are associated with local memory B cells at the tumor site, as well as increased levels of immunoglobulin (IgG) [72, 125]. The presence of B cells at TLS is associated with increased patient survival in ovarian cancer [72].

Treatment strategies involving adoptive transfer of T cells have been developed for antigens associated with ovarian cancer, particularly NY-ESO-1. Cancer-testis antigens (CTAs) are ideal targets for immunotherapy due to their restricted expression in healthy tissue and overexpression in the tumor. The quantity of available T cells limits adoptive transfer therapy, whereas chimeric antigen receptor T (CAR-T) cells do not have this limitation. Targets for CAR-T cell therapy include NY-ESO-1, MUC16, Mesothelin, HER2, and folate receptor-alpha [89, 192].

NY-ESO-1 is also a target for cancer vaccines. A group that is pioneering strategies for immunotherapy in ovarian cancer has developed NY-ESO-1 vaccines currently being evaluated in phase 3 trials. Usage of DNA methylation inhibitors to epigenetically enhance expression of cancer testis antigens such as NY-ESO-1 and LAGE-1 in combination with NY-ESO-1 vaccine and chemotherapy resulted in 6/10 patients with partial clinical response or disease stabilization [132, 190]. Response was associated with increased NY-ESO-1 autoantibodies and NY-ESO-1 specific T-cells. This group has also demonstrated an upregulation of immune checkpoint pathways when either PD-1, LAG-3, or CTLA-4 were blocked by genetic ablation or antibodies in a mouse model [81]. These studies indicate that combination of blockade strategies can overcome local T-cell suppression.

Other targets of local immune suppression in ovarian cancer include indole-amine-2,3,-dioxygenase (IDO) and vascular endothelial growth factor (VEGF). Macrophages secrete VEGF. IDO promotes T cell differentiation to T-regs. One trial in ovarian cancer patients in remission is evaluating the combination of an IDO inhibitor with an NY-ESO-1 vaccine in effort to extend rates of remission [131].

Anti-PD-1 and anti-PD-L1 therapies as single agents have not been successful in ovarian cancer. However combination of PD-L1 and CTLA-4 showed improved outcome relative to either agent alone. CTLA-4 antibodies in combination with chemotherapy, radiotherapy, and PARP-inhibitors have shown improved efficacy, due to the enhanced immune response driven by presentation of tumor cell antigens during cell death. In a phase I/II clinical trial, the overall response rate for recurrent ovarian cancer patients receiving the combination of Parp-inhibition and PD-1-inhibition was 45% for ovarian cancer patients with BRCA1/2 mutations compared with 25% for overall patients with ovarian cancer [107].

Importantly, the success of immunotherapy has been seen primarily in recurrent ovarian cancer patients, as these treatment strategies are in early clinical trial stages. After several lines of chemotherapy, which is enrollment criteria for the majority of the trials, patients can have T cell exhaustion and emergence of an immunosuppressive tumor microenvironment. There is rational hope that immunotherapy as a frontline treatment could provide optimal outcomes [90, 116].

1.2.2. Normal B-Cell Development and Generation of Antibody Diversity

B cell receptors undergo two mechanisms of somatic mutation, recombination of the heavy and light chain in the central immune system followed by somatic

hypermutation in the peripheral immune system [82]. These mechanisms generate random combinations at a scale to match the enormous diversity of possible amino acid combinations encountered in the body. Generation of autoantibodies, or antibodies against non-foreign self-antigens, occurs when there is a breakdown of central or peripheral tolerance mechanisms. Tolerance to a particular antigen is defined by lymphocytes with receptors specific to the antigen that remain alive but not active. There are a series of checks against auto-reactive IgG, but despite these checks, healthy individuals can harbor low titers of antibody against self-antigens without escalation of the response to autoimmune symptoms.

In the bone marrow, developing B cells generate unique receptors with recombination from three gene segments, called V(D)J recombination. T cells also undergo V(D)J recombination in the thymus. Up to half of the B cell receptors and T cell receptors that result from V(D)J recombination bind with self-antigen [64]. In the bone marrow, when an immature B cell binds with self antigen, recombination-activating gene 1 and 2 (*RAG1* and *RAG2*) maintain expression and continue to participate in V(D)J rearrangement in effort to edit the B cell receptor [64]. Should the B cell receptor remain reactive with native self-antigen, the cell will be removed via clonal deletion. Cell death is mediated by decreased expression of the B-cell-activating factor receptor, which binds the growth factor B-cell-activating factor (BAFF), as well as increased expression of the pro-apoptotic factor BIM [64].

T cell receptors recognize linear peptide fragments that are presented on MHC molecules. In the thymus, T cell receptors that weakly bind MHC with self-peptide survive receptor selection and are not further edited by V(D)J recombination, as *RAG1*

and *RAG2* genes are no longer expressed, whereas those that bind self-peptide too tightly activate cell death [64]. Genetic susceptibility to autoimmune diseases can be due to mutations in MHC molecules resulting in defective MHC binding to peptide and therefore ineffective deletion of self-reactive T cell receptors. The autoimmune regulator protein, or AIRE, is a transcription factor responsible for expressing proteins that are organ-specific to present to developing T cells. Genetic defects in *AIRE* can also result in autoimmunity, a prominent example being decreased expression of insulin in the thymus due to specific *AIRE* variants resulting in autoimmune diabetes [64].

The second mechanism that generates B cell receptor diversity is somatic hypermutation of the B cell receptor, which occurs in germinal center follicles in the peripheral lymphoid tissues [64, 82]. During this process, antibodies are edited to increase the affinity for antigen binding, which is called affinity maturation. At this stage B-cells differentiate to antibody-producing plasma cells and memory B cells. Furthermore, antibodies can undergo class switch recombination in which the of the heavy chain switches from IgM to IgA, IgH, IgE, IgD, and IgG with different effector functions [82]. Loss of immune tolerance can occur at multiple stages of B and T cell development.

1.2.3. Development of an Autoimmune Response

Both genetic and environmental factors contribute to the breakdown of central or peripheral tolerance and the development of autoimmune conditions. Multiple genes associated with antigen processing or immunoregulatory mechanisms are involved in genetic susceptibility to autoimmune disease. In patients with autoimmune disease, often it is not a single gene but an accumulation of defects in immunoregulatory genes

that are epigenetically deregulated or harbor mutations. Variants in *HLA* genes that are involved in antigen processing and presentation via the MHC complex account for half of the known genetic risk loci for autoimmune diseases [156].

In addition to MHC alleles associated with inefficient epitope binding, it has also been theorized that epitope conformation can reduce or enhance the interaction with MHC. Antigens that are intrinsically disordered have reduced affinity to MHC. In particular, nuclear antigens have been characterized as having disordered epitope fragments, which is suggested to affect binding to MHC and may contribute to their escape from deletion in draining lymph nodes [24, 139]. These structural characteristics partially explain the overlap of those autoantibodies to nuclear complex proteins, DNA binding proteins and RNA binding proteins detected in autoimmune conditions and in cancer, where immune regulation is disrupted. DNA-binding proteins and dsDNA and ssDNA when bound to antibodies can also form immune complexes that can trigger stimulatory receptors. Additionally, the protein structure can contribute to the propensity of certain antigens to become recognized as non-self proteins. This includes regions prone to cleavage by Granzyme B, caspases, or cathepsins, which can expose otherwise hidden epitopes [16].

Environmental factors include both the creation of an inflammatory and immuno-stimulatory microenvironment with cytokines and activating signals, as well as exposure of cryptic epitopes via toxins or apoptosis. Bacteria or virus can contain epitopes that are shared with self-antigens, and trigger an immune response against self-antigens through molecular mimicry [16, 24].

1.2.4. Tumor Associated Antigens

There are several conditions that can generate an antibody or immune response to a tumor. This includes a breakdown of immune tolerance including genetic defects in antigen processing and presentation or down regulation of regulatory mechanisms, antigen overexpression or expression of an organ-specific antigen, changes in protein structure resulting from mutations and post-translational modifications, and cell death through tissue injury causing exposure of intracellular antigens [13].

CTAs are a highly immunogenic class of tumor-associated antigens, with expression often restricted to germ cells of the testis at various stages of differentiation [59]. Cancer stem cells express CTAs at higher levels compared with the bulk tumor population [110, 163, 196]; several CTAs have been shown to be involved in early stages of embryonic development. There are a number of antibodies shared by autoimmune disease and cancer. For example TP53 autoantibodies have been detected in systemic sclerosis and systemic lupus erythematosus, and autoantibodies to c-myc have been detected in systemic lupus erythematosus and dermatomyositis as well as several tumor types [15].

Normal expression of onconeuronal antigens is restricted to the brain and therefore expression of these antigens by a tumor can trigger an immune response; unregulated autoimmunity in this context results in a paraneoplastic neurological syndrome.

1.3. Paraneoplastic Syndromes

Paraneoplastic syndromes are a form of autoimmunity driven by antigen expression by the tumor, which directly demonstrates the anti-tumor immune response. Paraneoplastic neurological syndromes manifest when an unregulated immune

response targets tumor antigens that are also expressed by neuronal or muscle cells. These syndromes are diagnosed before detection of the tumor in 70% of cases [66]. In cases where tumor antigens are shared with neuronal cells, referred to as onconeuronal antigens, patients have symptoms affecting the central nervous system. When the antigen is shared with antigens in muscle cells or at the neuro-muscular junction, patients have symptoms affecting the peripheral nervous system. The antibodies associated with these syndromes are more specific for the tumor type than for the resulting syndrome.

Interestingly, paraneoplastic syndromes can result in spontaneous regression of the tumor, and immunological symptoms can resolve upon surgical removal of the tumor. Return of paraneoplastic syndrome symptoms can indicate recurrence of the tumor. Although paraneoplastic syndromes are rare, paraneoplastic autoantibodies have been reported in patients with lung, breast and ovarian cancer without a paraneoplastic syndrome. For example, 16-25% of SCLC patients without a paraneoplastic syndrome were found to have autoantibodies to the paraneoplastic antigen HuD [93].

Paraneoplastic syndromes are categorized by neurologists into classical and non-classical syndromes, as described in **Table 1.1** and **Table 1.2** [67]. These definitions guide diagnosis of a definite paraneoplastic syndrome as being caused by an underlying tumor. In addition to the following criteria, other known causes of neurological syndromes must be excluded to diagnose a definite paraneoplastic syndrome. Classical paraneoplastic syndromes are highly associated with cancer, and in diagnosis of classical syndromes investigation for tumor with imaging and other

diagnostic tests is undertaken immediately. Classical syndromes with diagnosis of tumor within five years of presentation of symptoms with or without paraneoplastic antibodies are considered definite paraneoplastic syndromes. Non-classical syndromes are less often caused by an underlying tumor and therefore to be categorized as paraneoplastic in origin, the syndrome should be accompanied by presence of paraneoplastic antibodies and tumor diagnosis within five years of presentation of symptoms. Non-classical syndromes without presence of paraneoplastic antibodies that resolve upon treatment of tumor may also be considered definite paraneoplastic syndromes. Diagnosis of a classical or non-classical syndrome with no tumor detection but with presence of well-characterized paraneoplastic antibodies can be considered definite paraneoplastic syndrome; these cases may represent an effective immunological tumor clearance [67].

1.3.1. Tumors Associated with Paraneoplastic Syndromes

The main tumor types associated with paraneoplastic syndromes are small cell lung cancer, thymoma, breast, and ovarian cancer. SCLC is the tumor type most frequently detected in patients with paraneoplastic syndromes. The syndromes associated with SCLC are encephalomyelitis, cerebellar degeneration, opsoclonus-myoclonus, sensory neuropathy, Lambert-Eaton myasthenic syndrome, and polymyositis as outlined in **Table 1.1**. The paraneoplastic autoantibodies associated with SCLC are well characterized and can therefore be detected in 90% of SCLC case with paraneoplastic neurological syndromes [65]. In a prospective study which included n=240 SLCC cases without a paraneoplastic syndrome, 28.8% had detectable SOX2, HuD, or P/Q voltage-gated calcium channel autoantibodies [65]. Of the 24 patients with

a paraneoplastic neurological syndrome in the study, 87.5% were positive for at least one those three paraneoplastic autoantibodies.

Thymoma is the second most common malignancy associated with paraneoplastic syndromes. It has been reported that 30-47% of all patients with thymic epithelial tumors, predominantly thymoma, develop the paraneoplastic syndrome myasthenia gravis. Myasthenia gravis is the result of autoantibody interference in the neuromuscular junction on skeletal muscle cells, which targets the acetylcholine receptor (AChR) in 85% of cases. Autoantibodies against striated muscle antigens are detected in the majority of patients with thymoma and myasthenia gravis.

Breast and ovarian cancer are associated with paraneoplastic cerebellar degeneration with majority of the cases reporting with anti-Yo autoantibodies. Yo autoantibodies target both CDR2 (cerebellar degeneration related protein 2), also called PCA-1 (purkinje cell antibody 1), and CDR2L (cerebellar degeneration related protein 2-like), which shares 50% homology to CDR2 [52]. It has recently been reported that CDR2L is the main target in paraneoplastic cerebellar degeneration, though Yo autoantibodies can be detected with both antigens [52]. Benign teratoma, a non-epithelial ovarian germ cell cancer, is the tumor type most commonly associated with anti-*N*-methyl-d-aspartate receptor (anti-NMDAR) encephalitis, with reported 90% of tumor-associated anti-NMDAR encephalitis cases having ovarian teratoma [32, 83, 202].

1.3.2. Etiology of Paraneoplastic Syndromes

The development of a paraneoplastic syndrome is a result of autoimmunity; tumor associated antigens elicit an immune response to antigens also expressed in

Table 1.1: Classical Paraneoplastic Neurological Syndromes.

Classical Neurological Syndrome	PNS in association with Cancer and Onconeural Antibodies	References
Syndromes of Central Nervous System		
Encephalomyelitis	Esophageal small cell carcinoma (anti-Hu), SCLC (anti-Amphiphysin)	[70, 161]
Limbic encephalitis	SCLC, breast (anti-Hu, anti-ANNA-3); Testicular cancer (anti-Ma2)	[71, 105]
Subacute cerebellar degeneration	Gynecological and breast cancer (anti-Yo, anti-Ri); Lung (anti-Hu); Hodgkin's lymphoma (anti-Tr and anti-mGluR1); SCLC (anti-Zic4, anti-ANNA-3)	[105, 158]
Opsoclonus-myoclonus	Lung cancer (anti-Ri, anti-Hu, anti-Amphiphysin, anti-P/Q-type Voltage-gated calcium channel (VGCC), breast and ovarian cancer (anti-Ri, anti-Yo), testicular cancer (anti-Ma-2)	[14, 19, 77, 126]
Syndromes of Peripheral Nervous System		
Subacute sensory neuropathy	SCLC (anti-Hu, anti-CV2(CRMP5), anti-Amphiphysin, anti-Yo)	[8, 47]
Chronic gastrointestinal pseudo-obstruction	Thymoma (anti-Voltage gated potassium channel (VGKC))	[184]
Syndromes of Neuromuscular Junction and Muscle		
Lambert-Eaton myasthenic syndrome	SCLC (anti-P/Q type VGCC, anti-N-type VGCC, anti-SOX1, anti-PCA2)	[105, 142, 150]
Dermatomyositis - Polymyositis	Lung, ovarian and breast adenocarcinoma (anti-Jo-1, anti-Mi-2)	[26, 203]

Table 1.1: Paraneoplastic Syndromes and Associated Autoantibodies and Tumor Type.

Table 1.2: Non-classical Paraneoplastic Neurological Syndromes.

Non-classical Neurological Syndrome	PNS in association with Cancer and Onconeural Antibodies	References
Syndromes of Central Nervous System		
Brainstem encephalitis	Lung carcinoma (anti-Ri, anti-Hu)	[19, 122]
Optic neuritis caused by Neuromyelitis optica	Lung adenocarcinoma (anti-Aquaporin-4)	[183]
Cancer-associated retinopathy	Lung cancer (anti-recoverin)	[140]
Melanoma-associated retinopathy	Melanoma (autoantibodies against rod bipolar cells)	[170]
Stiff person syndrome	Breast cancer, thymoma, and colon cancer (anti-Amphiphysin)	[170]
Necrotizing myelopathy	Leukemia (No reports on well characterized onconeural antibodies)	[63]
Motor neuron diseases	Thymoma (anti-CV2(CRMP5))	[182]
Syndromes of Peripheral Nervous System		
Acute sensorimotor neuropathy	SCLC (anti-Hu)	[151]
Guillain-Barre syndrome	Lung adenocarcinoma (anti-CASPR2)	[176]
Brachial neuritis	Breast cancer (No reports on well characterized onconeural antibodies)	[109]
Subacute/chronic sensorimotor neuropathies	SCLC (anti-Hu)	[113]
Neuropathy and paraproteinaemia	Multiple Myeloma, non-Hodgkin's lymphoma, chronic leukemias (anti-MAG)	[145]
Neuropathy with vasculitis	Gastric cancer (antinuclear cytoplasmic antibody (ANCA))	[36]
Autonomic neuropathies	SCLC (anti-collapsin response mediator protein 5 (CRMP-5))	[127]
Acute pandysautonomia	NSCLC (No reports on well characterized onconeural antibodies)	[178]
Syndromes of Neuromuscular Junction and Muscle		
Myasthenia gravis	Thymoma (anti-acetylcholine receptor (AChR))	[206]
Acquired neuromyotonia	Thymoma (anti-VGKC)	[58]
Acute necrotizing myopathy	Merkel cell carcinoma (MCC) (anti-Hu)	[78]

Table 1.2: Non-classical Paraneoplastic Syndromes and Associated Autoantibodies and Tumor Type.

neuronal or muscle tissues, breaking immune tolerance and resulting in autoimmune tissue damage. The occurrence of antibodies in serum and cerebrospinal fluid (CSF) that recognize the antigens shared by neurons and tumor cells has been reported, however only a fraction of tumor-bearing patients with elevated titers of paraneoplastic autoantibodies will develop a neurological syndrome. Cross-reactivity of tumor and nervous tissue alone is insufficient to cause a paraneoplastic neurological syndrome and other factors are necessary including enhanced cytokine production, increased MHC-1 expression, and infiltration of $CD8^+$ T-cells to the tissue site [44]. Like other autoimmune diseases, development of paraneoplastic neurological syndrome is due to a combination of environmental and genetic factors. There have been associations with HLA haplotypes with increases susceptibility to paraneoplastic syndromes [162, 201]. Presumably, in patients with insufficient binding of epitopes to MHC proteins, there can be errors in clearance and these epitopes can be allowed to persist undetected as a self-antigen.

Somatic mutations in target antigens for paraneoplastic cerebellar degeneration, CDR2 and CDR2L have been reported. Of 26 ovarian cancer cases with antibody-positive cerebellar degeneration, 65% of cases had at least one somatic mutation, and 59% also had CDR2L gene amplification [167]. All 26 cases had either gene amplification or somatic mutation in the CDR2/CDR2L genes. Additionally, missense mutations were predicted to have enhanced binding to MHC I. None of the 116 control samples from patients with ovarian cancer without paraneoplastic cerebellar degeneration harbored mutations in these genes [167].

1.3.3. Autoantibodies Associated with Paraneoplastic Syndromes

1.3.3.1. Intracellular Antigens

Intracellular antigens include anti-nuclear antibodies, such as DNA and RNA binding proteins, and cytoplasmic antigens including tRNA synthetase antibodies, and syndrome-specific antibodies. The symptoms of paraneoplastic syndromes involving intracellular antigens are primarily the result of T-cell mediated destruction of healthy tissue. This is evidenced by infiltration of CD8+ T cells in autopsied and biopsied tissue. In patients with paraneoplastic cerebellar degeneration, paraneoplastic Yo antigen specific cytotoxic T-cells have been detected in patient blood samples [2]. Symptoms of paraneoplastic syndromes that target intracellular antigens including onconeural antigens can be irreversible due to T-cell mediated death of neurons.

Studies have also shown antibody-uptake in rat brain neurons with functional consequences, suggesting possible additional methods of neuronal death in addition to cytotoxic T-cell targeted attack. Intracellular uptake and demonstrated binding of anti-Yo antibodies resulted in disruption of calcium homeostasis in rat cerebellar slice culture [155]. Greenlee et al. has reported cellular uptake of both anti-Yo and anti-Hu patient antibodies in rat slice culture [68, 69].

1.3.3.2. Extracellular Antigens

In paraneoplastic syndromes that target membrane bound proteins, the antibodies can be directly pathogenic. Antibodies target various neuronal cell surface channels and receptors including: voltage-gated potassium channel-complex, ionotropic glutamate receptors (iGluRs), metabotropic glutamate receptors (mGluRs), gamma-aminobutyric acid (GABA), glycine receptor, and water channels [83]. Antibodies

targeting the neuromuscular junction include voltage-gated calcium channels, muscle AChR, and ganglionic AChR, as outlined in **Tables 1.1 and 1.2** [83].

1.3.3.3. Treatment

Autoantibodies targeting antigens located extracellularly on the cell membrane can directly cause symptoms. Dalmau et al. reported that in paraneoplastic encephalitis associated with NMDAR antibodies, a rapid correction of symptoms after surgery for ovarian teratoma was observed [45]. The target antigens include extracellular receptors, and in most cases the antibodies are directly pathogenic. Therefore removing or diluting circulating IgG provides benefit to these patients. Paraneoplastic syndromes that target extracellular antigens are easier to manage with treatment options such as intravenous immunoglobulin (IVIg) and plasma exchange therapy (PE). IVIg consists of a blood-derived product collected from humans. The mechanisms of action are not completely understood, but IVIg is involved in the inhibition of B cells and production of autoantibodies as well as saturation of FcRn receptor, which is involved in recycling of IgG through protection from lysosomal degradation [17, 168]. IVIgs have been used in the treatment of some autoimmune diseases like Guillain-Barré. Syndrome, chronic demyelinating polyneuropathy, and systemic lupus erythematosus [168]. PE and immunoadsorption (IA) are procedures that help to remove circulating antibodies. PE removes antibodies in a non-specific manner, whereas IA removes antibodies with a high specificity due to the presence of an adsorber (commonly tryptophan). A retrospective study revealed that in a study population of 31 patients who had autoimmune encephalitis, 22/31 had autoantibodies against N-methyl-d-aspartate receptor (NMDA-R), voltage-gated potassium channel (VGKC), Hu and GABA, and

treatment with PE and IA showed an improvement in modified ranking score in 67% of the patient population [51].

In contrast, the evaluation of IVIg treatment was reported by Uchuya et al. in a retrospective study including 22 patients with anti-Yo and anti-Hu PEM and sensory neuropathy, both intracellular targets. Stabilization was observed in 10% of patients who received IVIg at a dose of 0.5 g/kg/day for 5 days, and was carried on for 3 months [177]. Due to the primary involvement of CD8+ T cells and permanent loss of neuronal cells, paraneoplastic syndromes targeting intracellular antigens such as cerebellar degeneration have poor prognosis and can often be fatal. Treatment with IVIg or PE is of little benefit for cases targeting intracellular antigens. Instead, immunosuppression via steroids or depletion of lymphoid populations with immunotherapeutics such as Rituximab can alleviate some symptoms.

1.3.4. Immunotherapy and Neurological Adverse Events

1.3.4.1. Mouse Models

The presence of autoantibodies alone is not sufficient to cause paraneoplastic syndromes. This is reflected by the fact that the frequency of patients with cancer positive for paraneoplastic autoantibodies is higher than the frequency of patients with cancer who develop paraneoplastic syndromes as well as directly demonstrated by mouse models where administration of autoantibodies is insufficient to cause disease. A model involving CTLA4, however, was shown to invoke paraneoplastic syndrome [200]. In this model, breast cancer cells expressing influenza hemagglutinin antigen (HA) were implanted into balb/c mice. The mice expressed HA with cre recombinase in Purkinje cells in the cerebellum. CD4+ and CD8+ T cells with anti-hemagglutinin

receptors were injected intravenously, and the tumor growth was decreased relative to controls. The mice however did not express any neurological symptoms. When this syngeneic mouse model was treated with anti-CTLA4, the anti-tumor response was increased and in addition the mice displayed evidence of cerebellar degeneration both behaviorally and with Purkinje cell loss with inflammation of the cerebellum. When mice with HA-expressing tumor cells but without HA expressing purkinje cells were injected with anti-hemagglutinin CD4+ and CD8+ T cells, treatment with anti-CTLA4 had comparable affect on tumor regression but did not result in any neurological symptoms.

Similarly, administration of anti-PDL1 antibody in a mouse model for autoimmune encephalomyelitis exacerbated the neurological symptoms. This mouse model for autoimmune encephalomyelitis is initiated by immunization to myelin oligodendroctye glycoprotein peptide [152]. Increased infiltration of lymphocytes to the CNS as well as increased antigen-specific T cell expansion and cytokine production were observed after PD-1 blockade [152].

Mouse models with antibodies that target cell surface antigens however can induce neurologic symptoms without inhibition of immune checkpoints. Autoantibodies targeting mGluR from patients with paraneoplastic cerebellar degeneration were injected into mice intrathecally and resulted in severe cerebellar ataxia in mice, which was reversible with removal of the autoantibodies [205].

1.3.4.2. Case Reports

Paraneoplastic syndromes are a form of autoimmunity driven by antigen expression on the tumor, and they are a demonstration of the mechanisms of tumor immunity. CAR T cell therapy can result in neurotoxicity, however this neurotoxicity is

not caused by a paraneoplastic syndrome. Neurotoxicity associated with CAR T cell therapies includes CAR T cell- related encephalopathy syndrome and cytokine-release syndrome [129]. Therapies targeting immune checkpoints can result in immune-related adverse events (irAEs), which includes paraneoplastic syndromes. Use of checkpoint inhibitors has resulted in paraneoplastic syndromes to arise in tumor types not otherwise associated with paraneoplastic syndromes, such as melanoma [205]. Dermatomyositis was diagnosed in a woman with metastatic melanoma who was treated with CTLA-4 inhibitor ipilimumab. The dermatomyositis symptoms resolved when therapy was discontinued, and they returned when ipilimumab was again administered [159]. In another case report of metastatic melanoma, a patient was treated with both ipilimumab and nivolumab. Within two weeks of treatment, the woman developed symptoms indicative of autoimmune encephalitis, and was treated with IVIG and methylprednisolone [188]. The patient was tested for presence of paraneoplastic antibodies, and NMDAR antibodies were detected in the cerebrospinal fluid. After treatment with rituximab, the patient's symptoms improved [188].

A phase 2 clinical trial measured correlation of paraneoplastic antibodies with neurotoxicity when SCLC patients were treated with the immuostimulatory agent ipilimumab, which is an anti-CTLA-4 antibody targeting T-regulatory cells [10]. Results indicated that presence of paraneoplastic syndrome associated autoantibodies at the start of treatment correlated with severe paraneoplastic neurotoxic effects [10]. In addition to early detection, assessment of paraneoplastic autoantibodies may provide candidate biomarkers as there are increasing calls for predictive baseline biomarkers to

identify patients at risk for developing neurologic irAEs prior to treatment with checkpoint inhibitor immunotherapies.

1.3.5. Paraneoplastic Syndromes Associated with Ovarian Cancer

The paraneoplastic syndromes most commonly associated with ovarian carcinoma include paraneoplastic cerebellar degeneration, dermatomyositis and polymyositis [202, 203]; women presenting with these syndromes are referred for evaluation of ovarian cancer. Symptoms of cerebellar degeneration include ataxia, lack of balance, speech dysfunction, and nystagmus. Antibodies associated with paraneoplastic cerebellar degeneration that have been detected in women with ovarian cancer include anti-Yo, anti-Ri, and anti-Amphiphysin [202]. Polymyositis is an inflammatory myopathy resulting in muscle weakness, in cases of dermatomyositis, skin rashes co-occur with muscle weakness. Patients with these symdromes are at higher risk for malignancy, with detection of a tumor in 30% of dermatomyositis cases and in 15% of polymyositis cases [157]; relevant antibodies include anti-Jo1, anti-mi2, and anti-SRP [105]. Paraneoplastic autoantibodies that have been reported in cases with ovarian cancer are listed in **Table 1.3**. The presence of paraneoplastic autoantibodies is criteria for diagnosis of a paraneoplastic syndrome in patients with neurological symptoms, meaning the neurological syndrome is caused by the tumor-initiated immune response. However, paraneoplastic autoantibodies can also be detected in serum from patients with a tumor that do not present with neurological symptoms. Therefore, detection of autoantibodies associated with paraneoplastic syndromes is an approach to the early detection of ovarian cancer in asymptomatic patients.

Table 1.3: PNS Autoantibodies Reported in Ovarian Cancer Cases.

PNS in association with ovarian cancer	Onconeural antibodies targeting paraneoplastic antigens in PNS-associated ovarian cancer	NCBI	Refs
Paraneoplastic cerebellar degeneration	Yo antibody or Purkinje cell cytoplasmic antibody type 1 (PCA-1/CDR2)	NM_001802	[130]
Paraneoplastic cerebellar degeneration	Zic-4 antibodies	BC136339	[80, 95]
Paraneoplastic cerebellar degeneration	Carbonic anhydrase-related protein VIII (CARP VIII) antibodies	NM_004056	[1, 11]
Paraneoplastic Cerebellar Degeneration	Creatine kinase B (CKB) antibodies	NM_001823	[174]
Paraneoplastic encephalomyeloneuropathy	P/Q and N type calcium-channel antibodies	X99897 M94172	[104]
Encephalomyelitis	Amphiphysin antibodies	NM_001635	[199]
Myositis	Jo-1 autoantibodies, Histidyl-tRNA synthetase (HARS)	AAX99363.1	[203]
Myositis	SRP-19 autoantibodies	U51920.1	[73]
Myositis, Myasthenia gravis	Cortactin antibodies	BC008799.2	[18]
Dermatomyositis	TIF1-γ (TRIM33) autoantibodies or anti-p155/140	NG_023287.1	[117]
Dermatomyositis	NXP-2 autoantibodies, or anti-MJ antibodies	NM_015358.2	[84]
Paraneoplastic Cerebellar Degeneration	Yo antibody (CDR2L)	NM_014603	[52]
Idiopathic inflammatory myopathy, Sjogren's syndrome and SLE	Ro52 autoantibodies (TRIM21)	NM_003141.3	[55, 149]
Antiphospholipid antibody syndrome	Phospholipid antibodies	N/A	[148]

Table 1.3: Paraneoplastic Autoantibodies Reported in Ovarian Cancer. Table adapted from "Chatterjee M, Hurley LC, Tainsky MA. Paraneoplastic antigens as biomarkers for early diagnosis of ovarian cancer. *Gynecol Oncol Rep*. 2017;21:37–44.".

1.3.6. Polymyositis/Dermatomyositis

Dermatomyositis and less commonly polymyositis are paraneoplastic syndromes that can precede the diagnosis of ovarian cancer. The pathogenesis of polymyositis is mediated by cytotoxic T-cells, as evidenced by an infiltration of CD8 + T-cells in the muscle of myositis patients, which are recruited by local inflammation [25]. Additional symptoms in dermatomyositis are caused by immune-complexes binding to endothelial cells, activating the complement system and resulting in cell lysis and capillary destruction through the membrane attack complex [25].

In paraneoplastic myositis, the target of immune attack is regenerating muscle tissue, where in times of injury and muscle repair there is exposure of intracellular antigens. It has been shown that the paraneoplastic antigens HARS and mi-2 are found at high levels in developing muscle and myositis muscle, compared with low levels in healthy muscle [26]. In vitro studies demonstrated that HARS and mi-2 were expressed at high levels in myoblasts, and decreased as these cells differentiated to form myotubes [26]. In addition to analysis of antigens in myositis muscle tissue and human myotube cell culture, increased expression of myositis-associated antigens was observed in regenerating mouse muscle [138]. Additionally, HARS expression was found to be higher in the muscle of newborn rats compared with adult tissue [204].

1.3.6.1. Myositis-Associated and Myositis-Specific Autoantibodies

The Jo-1 autoantibody that recognizes the Histidyl-tRNA synthetase (HARS) is an antibody specific to myositis [203]. Chatterjee et al. have independently identified an epitope of the anti-Jo-1 target, HARS, through a phage-display screening of serum IgGs obtained from ovarian cancer patients. This epitope, when combined in a panel of 3

antigens, had the ability to predict ovarian cancer recurrence 9 months prior to the standard clinical recurrence criteria including CA125 [27].

Other autoantibodies found in the serum of myositis patients include anti-Ro52, anti-PL-7, anti-PL-12, anti-Mi-2, anti-PM-Scl75, anti-PM-Scl100, and anti-Ku [41]. Patients with inflammatory myopathies that are positive for anti-Jo-1 are often positive for anti-Ro52 antibodies, which target the antigen TRIM21. In one study examining the sera of 112 patients with inflammatory myopathies, 21% of patients were anti-Jo-1 positive, 20% of patients were anti-Ro52 positive, and 58% of those anti-Jo-1 positive patients were also positive for anti-Ro52 [149]. In a study of 89 anti-Jo-1 positive patients with anti-synthetase syndromes including polymyositis and dermatomyositis, 36 were also Ro52 positive. It was also found that when Jo-1 and Ro52 antibodies co-occurred, the risk of malignancy was increased, with reported cases of colon, breast, ovarian, and esophageal cancer [115]. Therefore, these two antigens together on a panel could increase cancer diagnostic specificity of an autoantibody classifier. Ishikawa et al. reported a study of screening of patients with connective tissue disease including myositis and dermatomyositis for the detection of autoantibodies that target nuclear matrix protein 2 (NXP-2). Out of 206 patients screened, 6 were positive for NXP-2. The study showed that 1 out of these 6 patients had dermatomyositis diagnosed at the same time as diagnosis of ovarian cancer. The patient was negative for antibodies to transcription intermediary factor-1 gamma (Tif1-gamma) but positive for antibodies to NXP-2 [84]. In another study of patients with inflammatory myopathies screened against an inflammatory myopathy immunoprofile test, 11/80 patients tested positive for an inflammatory myopathy associated antibody, and 5/11 of those patients

had a cancer. Out of these 5 cancer cases with positive inflammatory myopathy immunoprofiles, 1 of the cases was a woman with ovarian cancer who tested positive for Tif1-gamma [117]. Fiorentino et al. reported that in a cohort of 111 patients at the Stanford University Dermatology Clinic and a cohort of 102 patients at the Johns Hopkins Myositis Center, positivity to either NXP-2 or Tif1-gamma was present in 83% of patients with Cancer-Associated Dermatomyositis [57]. Suzuki et al. reported the presence of anti-SRP54 antibodies in 100 patients who had an inflammatory myopathy, 5 of whom had a malignancy, including 1 ovarian cancer [169]. In these studies we investigated a panel of autoantibodies associated with myositis for potential ovarian cancer biomarkers.

1.3.7. Paraneoplastic Cerebellar Degeneration

In ovarian cancer-associated cerebellar degeneration, cytotoxic T-cell attack is targeted to the Purkinje cells of the cerebellum. Destruction of Purkinje cells affects speech and motility, and often results in patient death. Case reports have demonstrated otherwise undetectable microscopic ovarian cancer in patients with Yo-positive cerebellar degeneration, which was discovered upon laparotomy and pathological analysis of resected tissue, prompted by diagnosis of cerebellar degeneration [62, 135]

1.3.7.1. Autoantibodies Associated with Cerebellar Degeneration

Yo antibody is also known as Purkinje cell cytoplasmic antibody type 1 (PCA-1), is targeted against CDR2 antigen that with limited normal protein expression in the brain and testes, as well as overexpression in ovarian cancer with or without cerebellar degeneration [38]. CDR2L (a member of CDR family) has 50% amino acid sequence

homology to CDR2 and its expression has been observed in both ovarian tissue and cerebellar Purkinje cells. Eichler et al. has reported that in a study population comprising patients with ovarian cancer, breast cancer and paraneoplastic neurological syndrome patients with Yo-positive antibodies, those patients who had paraneoplastic cerebellar degeneration, harbored antibodies directed against both CDR2 and CDR2L [52]. Darnell et al. reported that the tumor-specific expression of CDR2 in neurologically normal patients with ovarian cancer. In this study, tumor specimen lysates were prepared from 20 ovarian cancer patients were probed with sera obtained from paraneoplastic cerebellar degeneration patients on western blot and 13/20 tumor lysates showed the expression of CDR2 (target of anti-Yo antibodies) both in cerebellar neuronal tissue and ovarian tumors [46]. Expression of CDR2 was also observed in ovarian cancer patients who had no clinical manifestation of paraneoplastic cerebellar degeneration or circulating anti-Yo antibodies [46]. Therefore, the expression of onconeural antigens and their association with their respective antibodies does not always associate with the appearance of paraneoplastic neurological syndrome [46]. Monstad et al. determined the prevalence of Yo antibodies in a study population comprising 557 ovarian cancer patients and 253 breast cancer patients, few of which were associated with paraneoplastic neurological syndrome. The frequency of Yo antibody association with ovarian cancer was found to be 13/557 (2.3%), as opposed to 4/253 (1.6%) patients with breast cancer. Only 2/13 ovarian cancer patients had paraneoplastic cerebellar degeneration prior to diagnosis of ovarian cancer [124]. For paraneoplastic autoantibodies to be clinically useful for ovarian cancer diagnostics, panels of multiple antibodies will need to be employed. Karasnoudis et al. reported a

case study of a 60-year patient who initially had paraneoplastic cerebellar degeneration. After performing paraneoplastic antibody screening, only Zic4 antibody titer in serum was found to be elevated. CSF also showed presence of Zic-4 antibodies. Thoracic and abdominal CT scans revealed the presence of a tumor in the right ovary and diagnosis of ovarian adenocarcinoma was confirmed [95]. Hoftberger et al. reported the appearance of carbonic anhydrase-related protein VIII (CARP VIII) antibodies in association with paraneoplastic cerebellar degeneration at the time of ovarian adenocarcinoma tumor recurrence in a 69-year woman [79]. CARP VIII protein is expressed in the brain Purkinje cells, however strong expression of CARP VIII protein has been observed in lung cancer and has been linked to its higher proliferative and invasive properties that are essential for tumor growth and progression [1]. Lennon et al. investigated the frequency of anti-P/Q and N type calcium-channel antibodies in a study population of cancer patients. Of 70 small-cell lung, ovarian or breast carcinoma patients who were associated with a paraneoplastic encephalomyeloneuropathy, 2/19 (5%) ovarian cancer patients were reported to harbor antibodies against P/Q-type and N-type calcium channels. The calcium channel antibodies were detected in human cerebellar and cerebral cortical tissues [104]. Antoine et al. reported the occurrence of Amphiphysin antibodies in ovarian cancer patients in a study comprised of 2800 patients but only 5 were selected after pre-screening the sera for the presence of Amphiphysin antibodies. Among 5 patients, who were diagnosed with encephalomyelitis prior to ovarian cancer diagnosis, one was found to have circulating Amphiphysin antibodies [7]. A case report by Forgy et al. revealed that an ovarian cancer patient developed paraneoplastic cerebellar degeneration symptoms at seven months post-

surgery despite the fact that her CT scan report, CA125 levels, and physical examinations indicated no recurrence of ovarian cancer, yet her levels of Yo antibodies in the serum and in the CSF were both > 320 U/ml (normal range is < 10 U/ml) [60].

1.3.8. Paraneoplastic Autoantibodies Previously Associated with Ovarian Cancer

In addition to classical paraneoplastic autoantibodies associated with myositis or cerebellar degeneration, additional paraneoplastic autoantibodies have been reported in ovarian cancer primarily in case studies as summarized in **Table 1.3**.

1.3.9. Sero-Negative Samples for Identification of Novel Paraneoplastic Antigens

Although paraneoplastic antibodies known to be associated with cancer have been studied in detail, the search for new paraneoplastic cancer associated autoantibodies is ongoing. Novel antigens involved in central nervous system synaptic or neuronal surface autoantibody disorders have recently been identified at an approximate rate of two per year [103]. Two recent findings include antibodies to cortactin and creatine kinase brain type (CKB) [18, 174]. Cortactin was recently identified as a paraneoplastic antigen in two independent studies [18]. Following identification, both groups screened paraneoplastic sera against cortactin; one group detected cortactin antibodies in 20% of polymyositis patients using ELISA with western blot confirmation, while the other group identified cortactin antibodies in 19.7% of myasthenia gravis patients who were sero-negative for classic paraneoplastic antigens [18]. Myositis is a paraneoplastic syndrome closely linked with ovarian cancer. Cortactin has been reported to be overexpressed in ovarian cancer by mRNA analysis

of tumor tissues as well as by immunohistochemical staining of cortactin on tumor histological sections, and its expression was associated with poor prognosis [108]. Another recently identified paraneoplastic antigen is creatine kinase brain type, CKB. In an effort to identify novel paraneoplastic antigens in patients with cerebellar degeneration that were sero-negative for classic paraneoplastic markers, 2D western blot of paraneoplastic antibody sero-negative sera followed by mass spectrometry identified CKB as a novel paraneoplastic cerebellar degeneration-associated antigen [174]. CKB serum antibody reactivity was demonstrated in the cytoplasm of mice Purkinje cells as well as urinary bladder cancer tissue samples. CKB was elevated in several cancers including stage 1 ovarian cancer patients and was demonstrated to contribute to cancer progression [108]. As more paraneoplastic antigens are discovered, the panel of antigens to use for diagnosis of ovarian cancer could be expanded.

1.4. Paraneoplastic Antibodies for Early Detection

1.4.1. Paraneoplastic Antibodies as Cancer Biomarkers

As lung cancer is associated with paraneoplastic syndromes, an FDA-approved ELISA based test for smokers at risk for lung cancer, the EarlyCDT-Lung panel of antigens for the autoantibody detection of lung cancer, includes the paraneoplastic autoantigens HuD and SOX2. HuD and SOX2 are associated with limbic encephalitis, sensory neuronopathy and Lambert-Eaton myasthenic syndrome, and HuD is also associated with paraneoplastic encephalomyelitis and paraneoplastic cerebellar degeneration [65]. The sensitivity of the EarlyCDT-Lung 7-marker panel including HuD

and SOX2 is 41%, and in an audit of its first 1,600 screenings in the clinic, 57% of test-positive cases were early stage I or stage II NSCLC [87].

Cui et al., reported a study on autoantibodies to the paraneoplastic antigen Ma2 for the early detection of recurrence for small intestine neuroendocrine tumors (SI-NETs). The study evaluated 124 serum samples obtained from patients diagnosed with SI-NETs on an ELISA platform with recombinant Ma2 protein, which resulted in high sensitivity and specificity as revealed by the ROC values between 0.734 and 0.816 [42].

1.4.2. Panel of Autoantibodies for Early Detection

It is well established that while individual autoantibodies have low frequency of positive titer among patient sera, a combination of autoantigens for detection of autoantibodies can greatly increase diagnostic sensitivity. Matt et al. developed a multiplex Luminex assay using six onconeuronal antigens, namely NOVA-1 (Ri antibodies), HuD, Ma2, CDR62 (Yo antibodies), CRMP-5 (CV2 antibodies), and Amphiphysin to immunoscreen 119 patients who had definite paraneoplastic syndrome. Their assay yielded a high sensitivity, such as 83% for Ri antigen, 91% for Ma2, 93% for HuD and 100% for Yo, CV2 and Amphiphysin. Higher specificity was also obtained, like 96% for CV2, 97% for HuD, Yo, Amphiphysin, 99% for Ma2 and 100% for Ri antigens [111]. In a review of 60 ovarian cancer biomarker publications, of the 27 studies involving TAA or autoantibody multi-analyte panels, it was demonstrated that improved sensitivity with a panel of markers can be achieved while maintaining specificity [160]. Therefore a panel of multiple antigens should increase the sensitivity of antibody-based tumor diagnostics*,* and in the case of ovarian cancer, a panel including paraneoplastic antigens could serve to detect autoantibodies in high-risk populations with family history

or known BRCA1/2 mutations. A panel of autoantibodies could be measured CA125; both the antigen and antibodies could be analyzed from a patient serum sample. Other cancers, especially those associated with paraneoplastic syndromes such as breast, lung, pancreatic, colon, and lymphoma, could benefit from TAA combined with autoantibody detection.

1.4.3. Methods of Detection of Autoantibodies

The evaluation of onconeural antibodies in ovarian cancer serum samples with or without paraneoplastic syndrome was used to generate a panel of paraneoplastic antigens to implement in screening on various clinical platforms. Standard approaches for the detection of autoantibodies in patient serum are ELISA and western blot [13]. Immunohistochemistry and cell-based fluorescence are also used in particular for intracellular onconeuronal antigens. Rat and primate brain slices are commonly used for expression patterns of neuronal cell-surface antigens [179] . Immunohistochemistry however is difficult to interpret and subject to user bias. Immunocytochemistry is also used on cultured rat hippocampal neurons. Cell-based assays using transformed cells such as HEK or HeLa cells overexpressing the target antigen can be incubated with patient serum and measured for staining [179].

More sensitive and rapid tests have recently been developed for autoantibody detection, including electrochemical, optical, and microfluidic approaches [191]. Optical approaches include surface plasmon resonance (SPR), localized surface plasmon resonance (LSPR), and surface enhanced Raman spectroscopy (SERS) [191].

For autoantibody discovery phases, mass spectrometry is a reliable method, particularly with Serologic Proteome Analysis (SERPA) in which tissue homogenate or

cell lysates are separated on a 2D SDS PAGE gel, and spots specific to disease samples are analyzed by mass spectrometry. Serological analysis of recombinant cDNA expression libraries (SEREX) has historically been used for discovery of many tumor-associated antigens, including NY-ESO-1 [13, 33]. Protein microarrays are an improvement from SEREX in that these arrays utilize purified recombinant protein, eliminating much of the background noise generated from using E. coli cell lysates in SEREX. A prominent example of a human protein microarray is Nucleic Acid Programmable Protein Arrays (NAPPA) [13].

1.5. Hypothesis: Autoantibodies Associated with Paraneoplastic Syndromes are Candidate Biomarkers for Early Detection of Ovarian Cancer

As paraneoplastic antigens initiate autoimmune responses, these are highly immunogenic proteins expressed by the tumor. While paraneoplastic syndromes are rare, autoantibodies associated with the syndromes are more common. In SCLC, 16-25% of cases without a paraneoplastic syndrome had detectable anti-Hu antibodies, and 40% of SCLC cases without a neurological syndrome had a detectable levels of at least one paraneoplastic antibody from a panel of intracellular and cell surface antigens [65, 93]. Therefore, we evaluated a set of myositis associated and onconeuronal autoantigens for detection of autoantibodies in serum from ovarian cancer patients without a known paraneoplastic syndrome.

The primary goal of this thesis is to identify candidate autoantibody biomarkers for early detection of ovarian cancer. In addition to early detection, understanding the distribution of autoantibodies in patients without neurological symptoms may help to further understand development of paraneoplastic syndromes as well as management

of immunotherapy neurologic irAEs. Baseline levels of paraneoplastic autoantibodies could serve to identify patients that would be at risk for developing neurologic irAEs as immunotherapies for ovarian cancer treatment continue to develop.

2. CHAPTER 2: Materials and Methods

2.1. Collection of patient samples

Samples were obtained from patients at Karmanos Cancer Institute, St. John Hospital and Oakwood Hospital in Detroit, MI, and at the Mayo Clinic, Rochester, MN. Additional specimens were provided by the Cooperative Human Tissue Network (CHTN) and Gynecologic Oncology Group specimen banks. All samples were collected prior to surgery or therapy. Healthy control sera were collected as part of a large-scale community outreach project. Blood was collected via venipuncture, centrifuged at 2,500 rpm at 4°C, and the resulting serum stored at -80°C. Protocols were approved by the Institutional Review Boards of Wayne State University and the individual hospitals. Each patient provided written informed consent.

For the Validation I and Validation II studies, the early and late stage HGSOC group is comprised of females age 18 and over diagnosed with epithelial ovarian cancer. In these studies we used serum collected from 19 early stage and 95 late stage serous ovarian cancer patients prior to treatment or surgery. The benign ovarian cyst group included 100 samples. One hundred healthy controls were self-reported to be free of cancer and potentially confounding benign conditions such as ovarian cysts, uterine fibroids, or endometriosis. The HARS antigen was not processed with the Validation II sample set, with the exception of n=5 early stage HGSOC samples. Sample usage tracking ensured that the 314 samples selected for the two validation studies were not used initially to identify the biomarkers.

2.2. Sub-cloning of Antigens

The tumor antigens were first PCR amplified using forward primers (containing 6X His tag and T7 tags) and reverse primers using cDNA template obtained from ovarian tumor samples or ovarian cancer cell lines SKOV3 or OVCAR3. The PCR products were column purified, digested with restriction endonucleases and ligated to pET-21b bacterial expression vector (EMD Millipore Corporation, San Diego, CA) (**Figure 2.1**). The ligated DNA was then transformed into the BL21-DE3 strain and positive colonies were selected; all cDNA expression plasmids used in this study were fully DNA sequenced. These expression vectors were employed for in *vivo* production of recombinant His-tagged proteins in Bl21-DE3 bacterial strain.

2.3. Purification of Antigens

The BL21-DE3 bacterial cells bearing clones were grown overnight in 5 mL LB with 50 µg/mL ampicillin at 37° C. 0.5 mL of the overnight culture was added to 500 mL LB with 50 µg/mL ampicillin and grown at 37° C to OD between 0.4-0.5, IPTG (β-D-1-thiogalactopyranoside) was added to a final concentration of 0.6 mM to induce the production of T7 RNA polymerase within the BL21-DE3 expression host, which is required for RNA and subsequent protein synthesis and the culture was grown at 37° C for three hours. The cells were pelleted at 1,200 X g for 15 minutes and supernatant was discarded. The pellet was frozen at -80°C for at least 30 minutes and then lysed with Thermo Scientific Bacterial Protein Extraction Reagent lysis buffer, centrifuged at 15,000 X g and then transferred the supernatant. The pellet, containing the target protein that forms within inclusion bodies, was solubilized in 8M urea.

2.3.1. HIS-Tag Purification

The crude His-tagged proteins were purified first using Ni-NTA beads (Thermo Fisher Scientific, Waltham, MA) following manufacturer's protocol. Ni-NTA beads bind to His residues that are attached to proteins and results in relatively pure protein. Western blot image of elutions of His-Purification are shown in **Figure 2.1**; elutions were pooled and quantified with Bio-Rad DC protein assay.

2.3.2. T7-Tag Purification

The Ni-NTA purified His-tagged proteins were further purified using T7•Tag® Antibody Agarose (MilliporeSigma, Burlington, MA) which bind the N-terminal 11 aa of the T7 gene 10 protein. The second round of purification with T7 Antibody bound agarose beads is necessary to remove any contaminating bacterial poly-His containing proteins from first round of Ni-NTA bead purification. Following purification, proteins were processed through Zeba desalting columns (Thermo Fisher Scientific, Waltham, MA). Western blot image of elutions of T7-Purification are shown in **Figure 2.1**; elutions were pooled and quantified with Bio-Rad DC protein assay.

2.3.3. Commercial Proteins

The recombinant proteins in this study are full-length, with the exception of the recombinant PAX8 protein that consists of the amino acids 1-287 (Sino Biological, Wayne, PA). The SRP-19 expression plasmid was kindly gifted by Dr. Howard M. Fried, University of North Carolina at Chapel Hill [76]. The human TP53 (1-393) expression plasmid was a gift from Cheryl Arrowsmith (Addgene plasmid #24859; RRID:Addgene_24859; http://n2t.net/addgene: 24859) [12].

Figure 2.1

A. PET-21b Bacterial Expression Vector

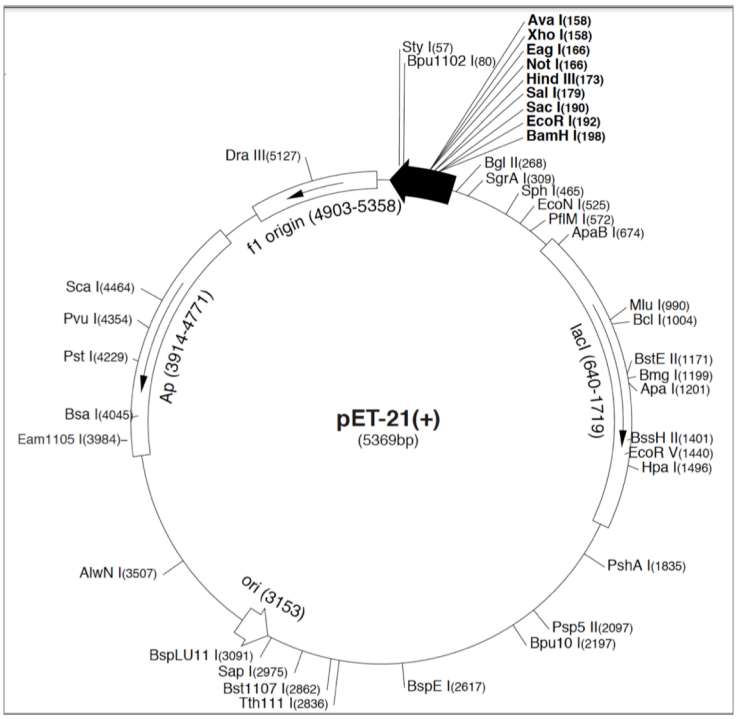

B. Antigen: T712A, HIS Column Elutions

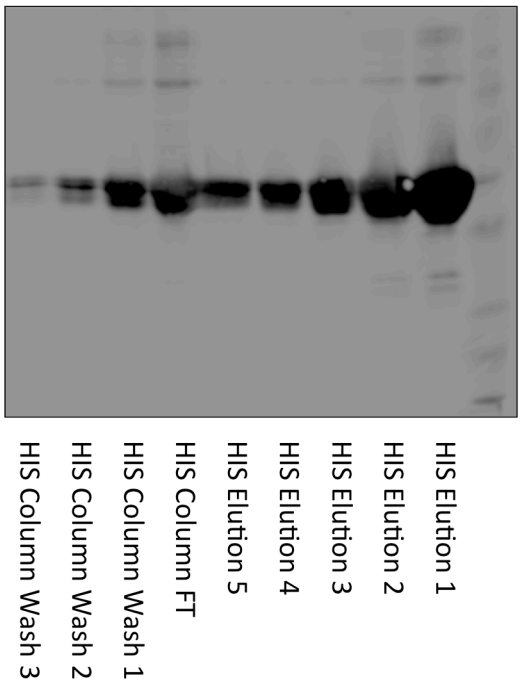

C. Antigen: T712A, T7 Column Elutions

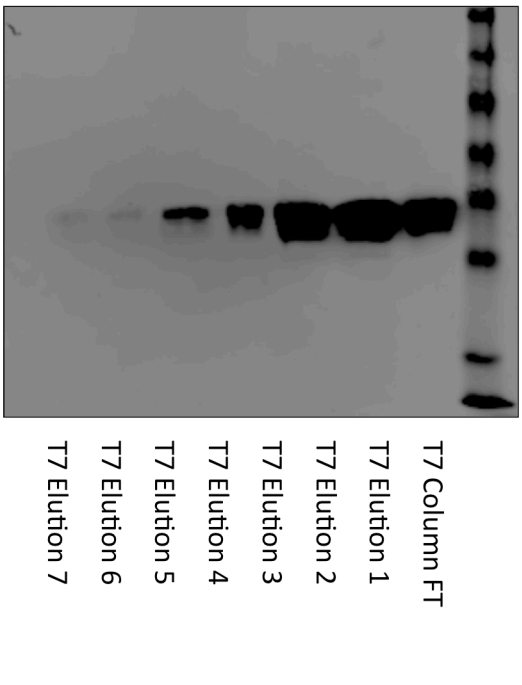

Figure 2.1: Protein Purification Overview.
A. PET-21b vector map. B. Elutions of T712A antigen, His-column purification, anti-HIS Ab 1:10,000. C. Elutions of T712A antigen, T7-agarose purification, anti-HIS Ab 1:10,000

2.4. Western Blot

Western blots were performed with 0.5 µg of purified recombinant proteins separated on a 10% acrylamide SDS-PAGE. Proteins were transferred onto nitrocellulose membranes for one hour on ice at 250mA. The membranes were blocked overnight at 4°C with 5% milk in TBS with 0.1% Tween20 (TBS-T). The next day, each serum sample was pre-incubated at a 1:300 dilution in 3 ml of 5% milk in TBS-T with 75 µg of BL21-DE3 E. coli lysate for one hour to reduce background reactions of human sera to E. coli proteins. The patient serum was then incubated with nitrocellulose membranes for one hour at room temperature. Following three washes with TBS-T, secondary IR-dye labeled mouse anti-His tag and goat anti-Human IgG antibodies were incubated for one hour at room temperature followed by three washes with TBS-T and two with PBS. Autoantibody binding to the antigens was quantified on LiCor Image Studio software (LI-COR Biosciences, Lincoln, NE) as background-corrected integrated intensity of anti-human IgG (IRDye800) normalized to anti-His tag antibody (IRDye700). Secondary anti-HIS tag antibody was quantified and used as a loading control to normalize each protein band to the anti-human IgG value. The same lot of each secondary antibody was used for the experiment, and separate preparations of secondary antibody had no significant effect. Day to day variation as calculated from the IRDye700 readings of the anti-His tag antibody was used to adjust data.

2.5. ELISA

2.5.1. Optimization of ELISA for Patient Serum Incubation

A semi-automated ELISA was developed using the Biomek3000 liquid pipetting robot for addition of blocking reagent, washing buffer, secondary antibody, TMB

substrate, and sulfuric acid. Plates were coated with antigen with multichannel pipette by hand, and primary antibody consisting of patient serum diluted in blocking buffer was added with a single channel pipette by hand. Optimization was performed for: concentration of coating antigen, dilution of patient samples, blocking reagent with patient samples, and timing of the washing procedure including plate drying times dependent on plate processing order.

2.5.1.1. Selection of Blocking Agent

In order to optimize ELISA conditions, we processed plates with a number of blocking reagents. The blocking reagents evaluated at various concentrations each included: casein, gelatin, donkey serum (Jackson Laboratories), Donkey Serum (Equitech-Bio, Kerrville, TX), Aves Blocking buffer, Chonblock, Seablock, BSA, Milk, and keyhole limpet haemocyanin (KLH). We found that the donkey serum from Equitech-Bio at 5% provided the lowest background.

2.5.1.2. Serum Sample Preparation

Our primary antibody in this indirect ELISA was patient serum diluted 1:300. Originally, patient serum was diluted in washing buffer. However we observed that a number of samples displayed reactivity with the various blocking agents used. We found that pre-incubation of the patient samples in blocking reagent reduced this background. Samples were incubated with blocking agent for one hour at room temperature with light rocking prior to addition to the ELISA plate, this incubation occurred simultaneously to the blocking agent on the ELISA plate. **Figure 2.2** shows the effects of pre-incubation of patient serum with blocking reagent: 5% Donkey Serum (Equitech-Bio, Kerrville, TX).

Figure 2.2

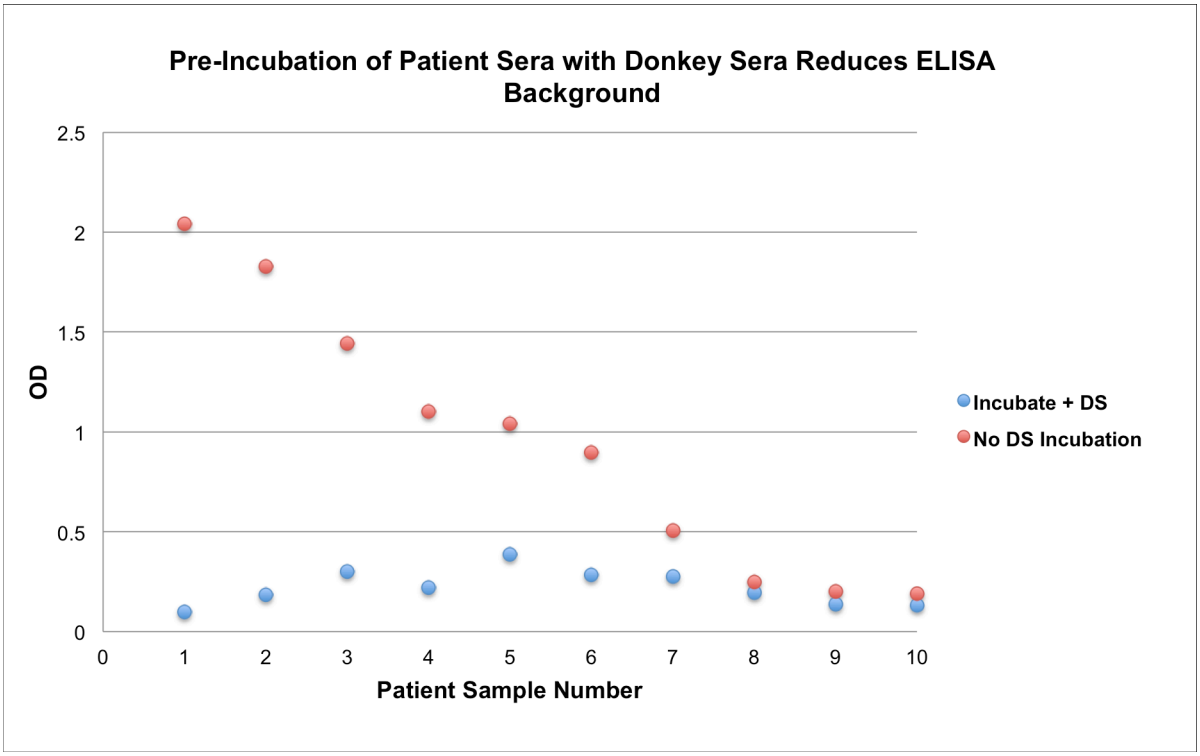

Figure 2.2: ELISA: Sample Pre-Incubation with Donkey Serum.
Pre-incubation of 10 patient samples for 1 hour at room temperature with blocking agent (5% donkey serum) reduced background reactivity. Background is measured on non-coated wells with only PBS, blocked with donkey serum, and incubated with patient serum followed by anti-human HRP-conjugated secondary antibody.

In addition to pre-incubation of each patient sample in blocking reagent, we found that although proteins were doubly purified using the HIS and T7 tag, we found a few samples on western blot exhibited non-specific bands. These bands were not associated with anti-His tag antibody signal on the IR700 channel, and were detectable only on the IR800 channel. On western blot, these non-specific bands were non-consequential, as quantification was only measure on that IR800 band which overlapped with IR700 anti-His tag signal. On ELISA however, these non-specific reactions create background noise. Pre-adsorption of our patient sample with 75ug/mL of E. coli bacterial extract reduced non-specific bands observed on western blot as well as reduced optical density measurement on ELISA.

2.5.1.3. ELISA Reproducibility

The serum set described in **Table 4.1** was processed on ELISA. Each measurement was run in duplicate per plate, with four plates processed per day over 11 days. For 88 replicate measurements of the 1:75 dilution of the positive control standard curve, the coefficients of variation (CV) for the variance components in the ELISA assay are as follows: Intra-assay CV (within plate) 0.0281; Inter-assay CV (plate to plate) 0.0749; and CV day-to-day 0.0898 [39]. Reproducibility within a single plate is shown in **Figure 2.3.**

2.5.1.4. Antigen Concentration

Optimal antigen concentration was determined using positive control serum purchased from The Binding Site (San Diego, CA). Various lots of these serum samples were positive for: CDR2, CDR2L, HARS, and TRIM21. For those antigens that did not have a commercially available positive control serum, we incubated various

Figure 2.3

A.

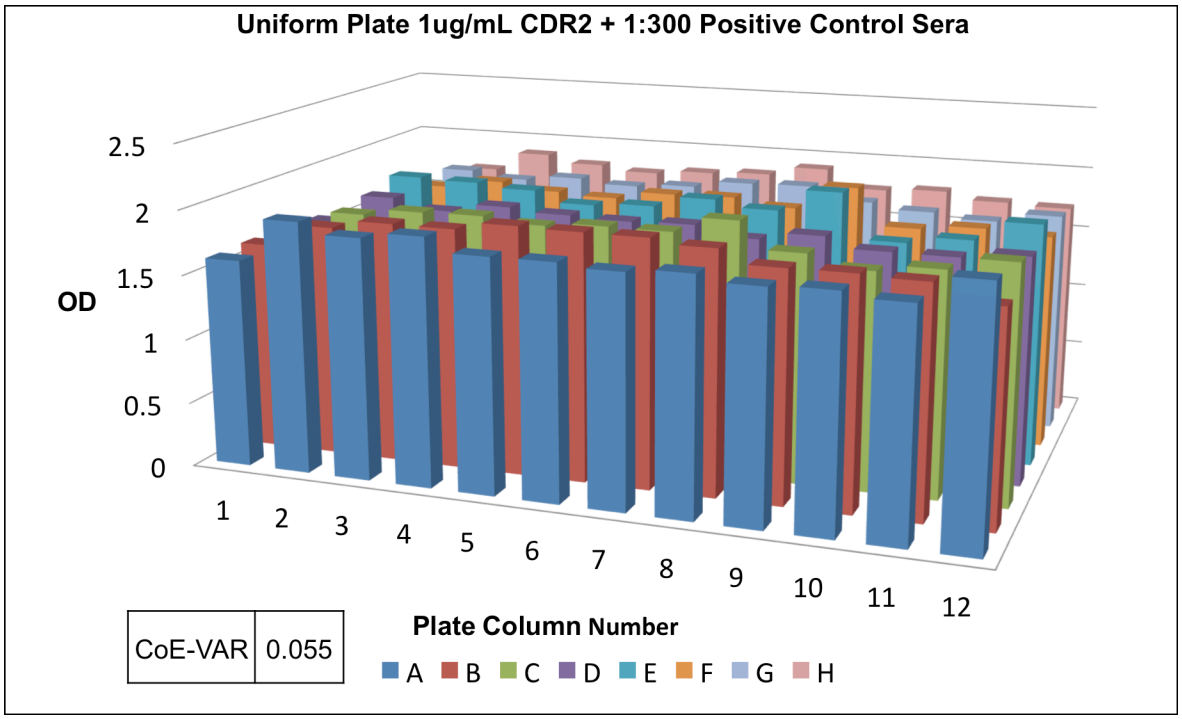

B.

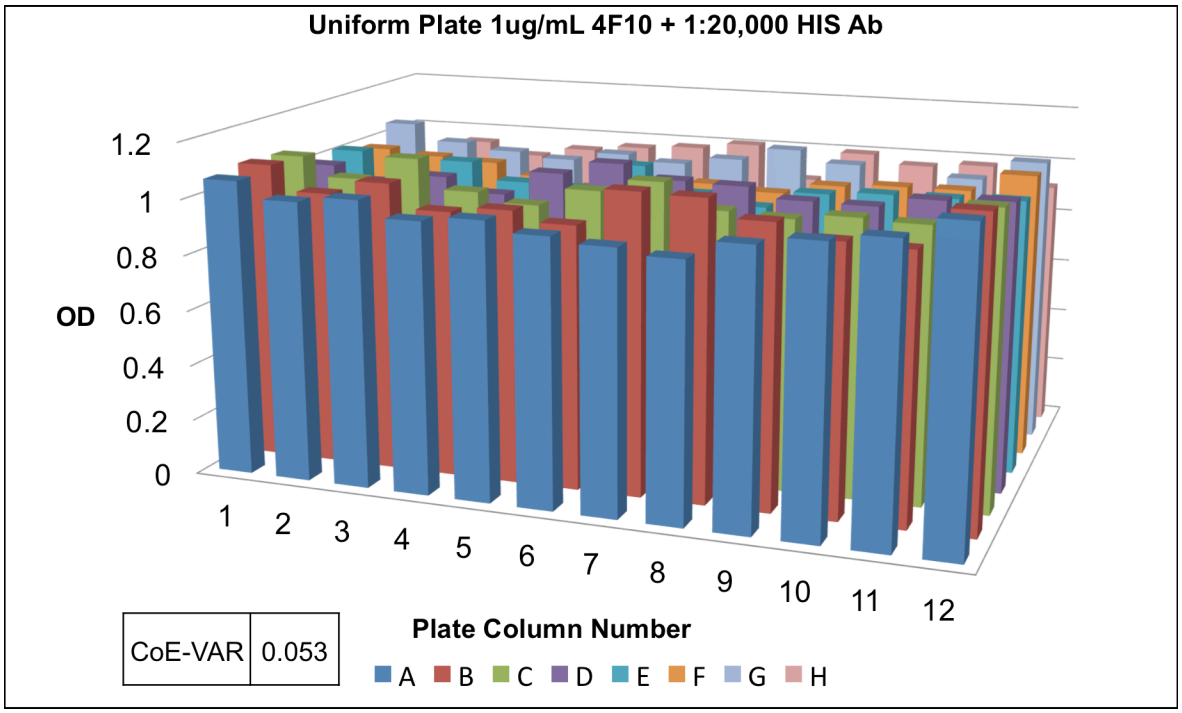

Figure 2.3: ELISA Uniform Plate. A. OD values from uniform CDR2-coated ELISA plate with positive control patient serum as primary antibody. B. OD values from uniform 4F10-coated ELISA plate with anti-HIS tag primary antibody.

concentrations of antigens with patient serum samples that were previously observed to react. The concentration of antigen that provided half-maximum signal was selected as the working antigen concentration for subsequent studies.

2.5.2. ELISA, Validation I

The serum set described in **Table 4.1** was processed on ELISA as follows: purified antigens were coated in duplicate wells at concentrations from 0.3-1.5 mg/mL (depending on the protein as determine from preliminary tests) in PBS and incubated overnight at 4°C. All subsequent steps took place at room temperature. Wells were blocked for one hour with 5% donkey serum in PBS. To eliminate background of patient sera reactivity with donkey serum and a lysate of nonspecific bacterial proteins, samples were diluted 1:100 in PBS with 5% donkey serum and 75 mg of BL21-DE3 E. coli lysate for one hour. Patient samples were incubated on the plate for one hour, followed by one-hour incubation of donkey anti-human HRP-conjugated secondary antibody. TMB substrate solution (Thermo Fisher Scientific, Waltham, MA), containing 3.3', 5.5'-tetramethylbenzidine (TMB) was added, followed by 0.45 M sulfuric acid to stop the reaction after 20 minutes. The addition of blocking solution, washing steps, TMB and sulfuric acid addition were performed on the Biomek2000 automated liquid handling robot (Beckman Coulter, Brea, CA).

A standard curve using serum with known reactivity to TRIM21 (The Binding Site, San Diego CA) at five dilutions ranging from 1:75 to 1:1200 was included on each plate to account for plate-to-plate and day-to-day variation. In addition, a pair of non-coated wells were blocked with donkey serum and incubated with each patient serum. These

patient serum specific background values were subtracted from the antigen values for each patient sample.

3. CHAPTER 3: Selection of Antigens by Detection of Paraneoplastic Autoantibodies in OVCA sera

3.1. Homology of OVCA Epitopes to Paraneoplastic Antigens

3.1.1. Background: Phage-Display Biopanning

OVCA-related epitopes were previously identified by screening unbiased random-peptide phage display cDNA libraries using ovarian cancer sera and selectively enriching reactive epitopes through biopanning with ovarian cancer and healthy control samples [27, 30]. Using this high throughput epitope cloning strategy, the Tainsky laboratory identified 56 autoantibody biomarkers for ovarian cancer, three of which predicted recurrent ovarian cancer 9 months prior to clinical recurrence [27]. One of these three biomarkers is homologous to paraneoplastic antigen HARS, which is associated with paraneoplastic myositis [27]. Using NCBI Protein Blast for the 56 sequences reactive with ovarian cancer patient serum, it was found that several epitopes shared amino acid sequence homology with paraneoplastic antigens [30]. Two epitopes, 4B7 and 3A9, displayed 100% homology to the myositis associated antigens HARS and SRP-19, respectively [27, 30]. Additionally, four ovarian cancer epitopes, 4F10, 4E8, 5H6, and 5A3 and showed partial homology to the paraneoplastic antigens TRIM21, Hu-D, MUSK, and CDR2. Alignments of the epitopes with the full-length antigen amino acid sequence are shown in **Figure 3.1**

3.1.2. OVCA epitopes incubated with paraneoplastic IgG on microarray

Commercially available positive control autoimmune serum samples were purchased from The Binding Site (San Diego, CA). Three control samples were utilized: positive for the antigens HARS, CDR2, and HU-D (**Figure 3.2:A**). Although information

Figure 3.1

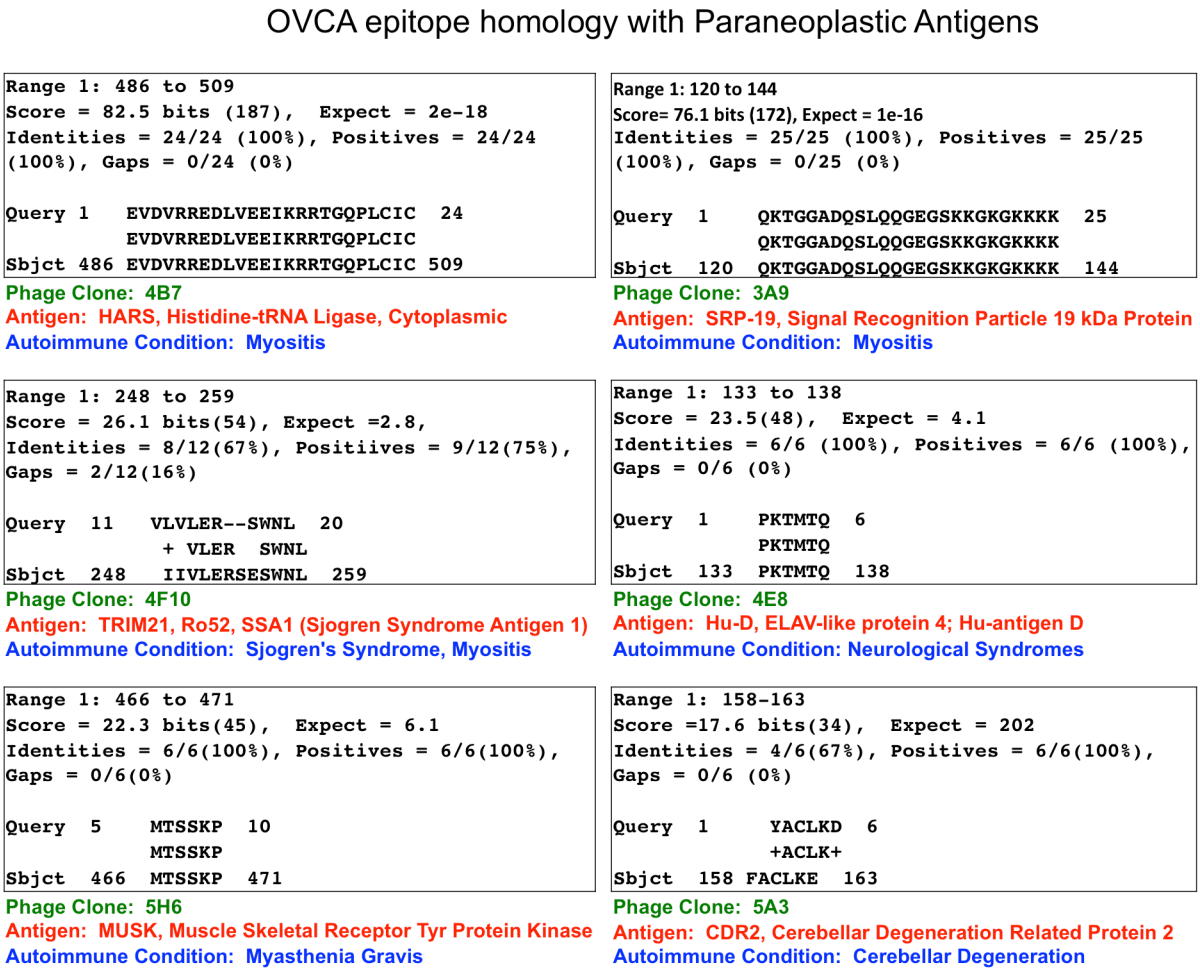

Figure 3.1: Homology of OVCA Epitopes to Paraneoplastic Antigens.
Alignments from NCBI protein-BLAST search for OVCA epitopes with proteins associated with paraneoplastic syndromes. Top sequence indicates OVCA epitope sequence; middle sequence indicates alignment; bottom sequence indicates full-length protein region of homology.

Figure 3.2

A.

Sera Title	Antibody (Antigen)	PN Syndrome	Cancer
BX104 (n=5)	Jo-1 (HARS)	Myositis	Breast/GYN, lung, gastric carcinoma
BX198 (n=1)	Yo-1 (CDR2)	Cerebellar Degeneration	Breast/GYN
BX199 (n=5)	ANNA-1 (HuD)	Sjogren's Syndrome	SCLC

(The Binding Site Ltd, Birmingham, UK)

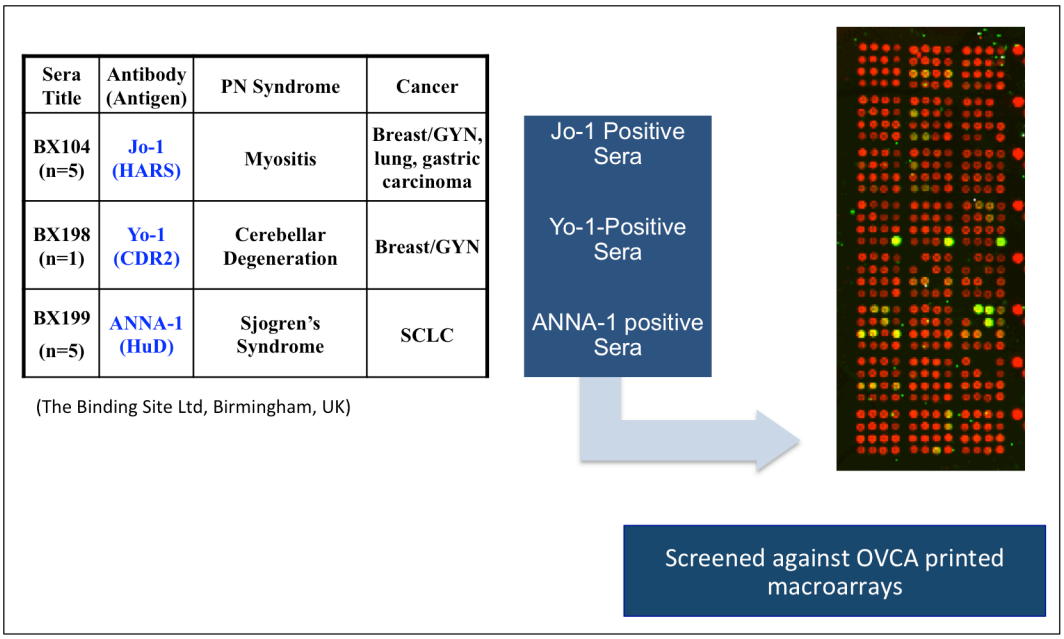

B.

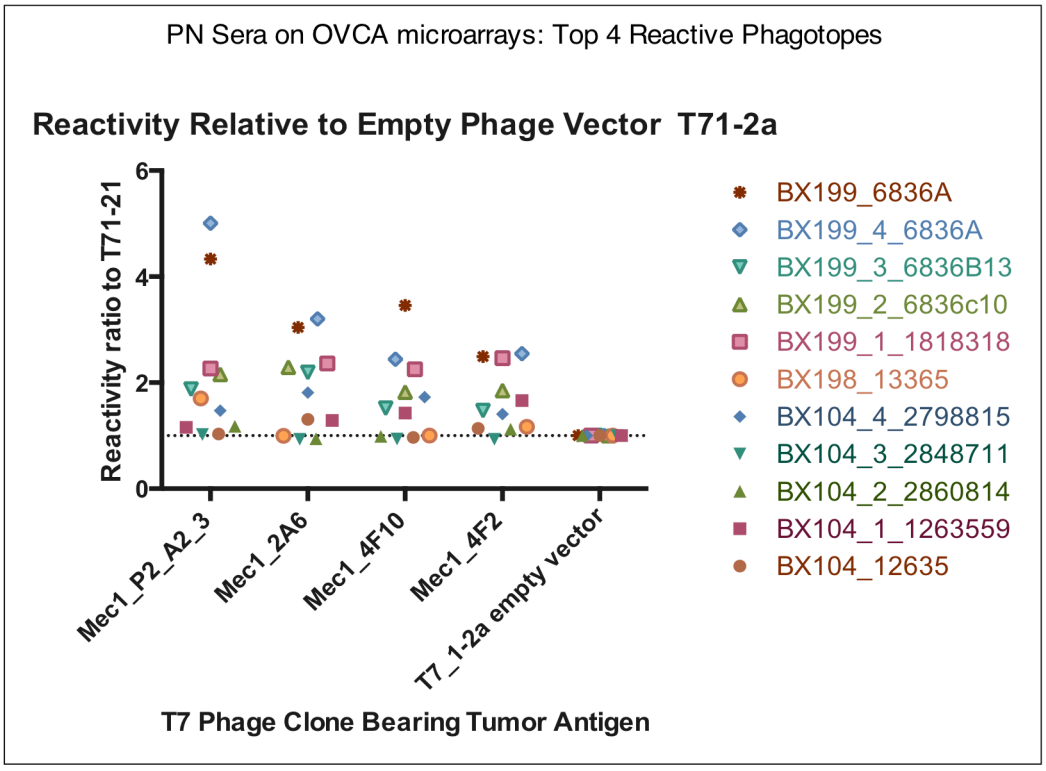

Figure 3.2: Autoimmune Patient Serum with OVCA IgG.
A. Overview of positive control serum incubated with OVCA macroarrays.
B. Reactivity of top 4 phage clones reactive with positive control autoimmune serum.

regarding the disease status of the donor patient was not available, these serum samples contained high titers of either anti-HARS antibodies, anti-CDR2 antibodies, or anti-HuD antibodies. Autoimmune sera were processed with OVCA epitope macroarrays, with 4 phage clones displaying high reactivity (**Figure 3.2:B**), confirming reactivity with both ovarian cancer patient sera and autoimmune condition patient sera. The 4 reactive phage clones were amplified and purified from E. coli for evaluation on western blot.

3.2. Paraneoplastic Line Blots

An initial survey of autoantibodies to 20 paraneoplastic antigens in HGSOC sera [29] [28] was performed, including the five antigens to which ovarian cancer epitopes showed homology; HARS, SRP-19, TRIM21, CDR2 and Hu-D (**Figure 3.3**). This study utilized two commercially available line blots in which recombinant antigens were spotted onto a membrane, with one line blot test consisting of myositis-associated antigens, and a second line blot test consisting of onconeuronal antigens associated with paraneoplastic neurological syndrome.

Myositis-associated antigens were evaluated on line blots from Euroimmun (EUROIMMUN, Leubeck, Germany) and onconeuronal antigens associated with paraneoplastic syndromes were evaluated on line blots from Ravo Diagnostika (Ravo Diagnostika, Freiburg, Germany). The antigens included on the Euroimmun myositis line blots are: TRIM21, OJ, EJ, PL-12, PL-7, SRP, HARS, PM-SCL75, PM-SCL100, KU, and MI-2. The antigens included on Ravo Diagnostika paraneoplastic antigen line blots are: Hu-D, CDR2, RI, CRMP5, AMPHIPHYSIN, MA1, MA2, SOX1, and GAD65. The

Figure 3.3

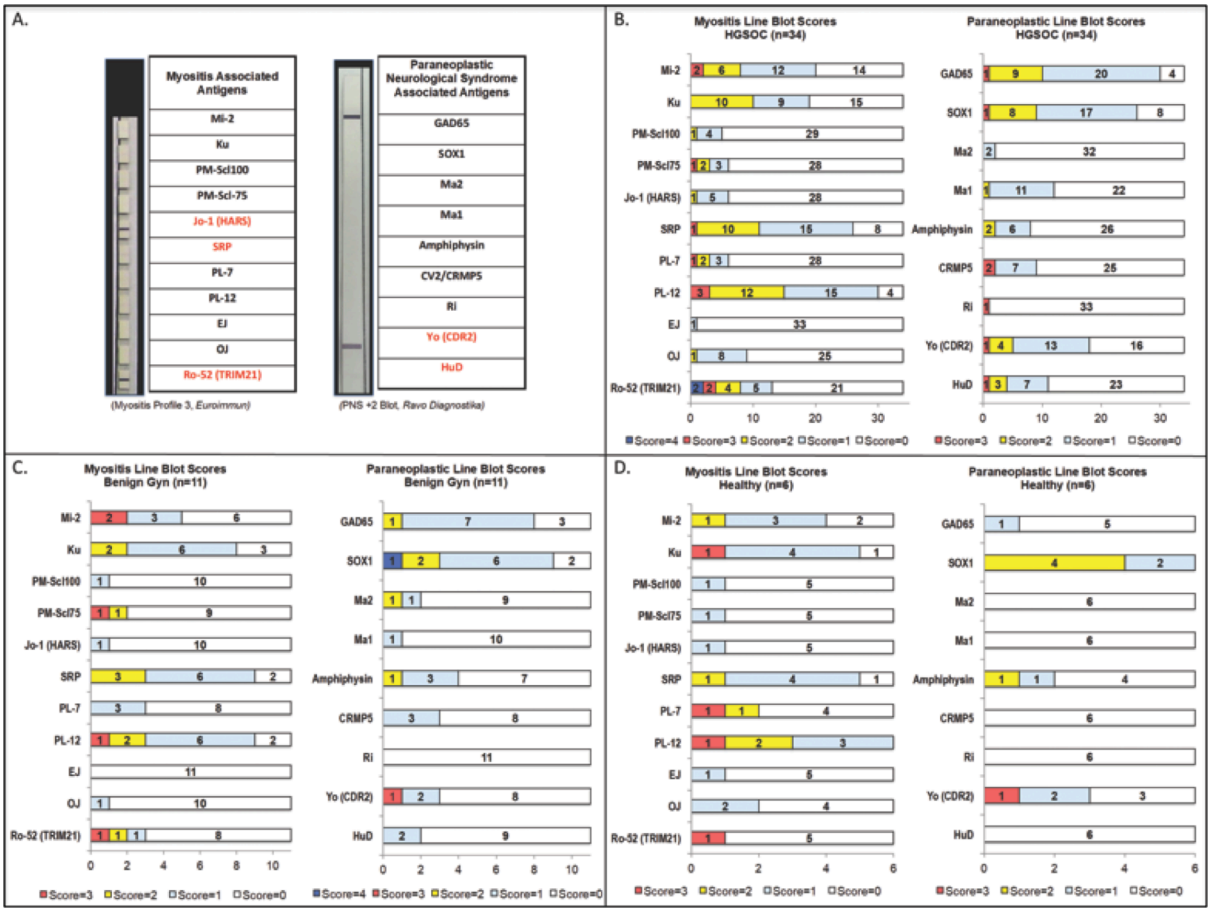

Figure 3.3: Paraneoplastic Antigen Line Blots.
Serum set of 34 HGSOC samples, 9 benign samples, and 11 healthy samples processed on Euroimmun and Ravo Diagnostika line blots, with 20 antigens total.
A: Image of Euroimmun myositis line blot and Ravo Diagnostika paraneoplastic antigen line blot with anti-HARS and anti-TRIM positive control serum and anti-CDR2 positive control serum, respectively.
B: Heat map of reactivity of line blots with HGSOC serum, as scored from 0-4.
C: Heat map of reactivity of line blots with benign serum, as scored from 0-4.
D: Heat map of reactivity of line blots with healthy serum, as scored from 0-4.

line blots were processed per manufacturer protocol, incubated with a serum sample diluted at 1:100.

3.2.1. Association of Western Blot results with Paraneoplastic Line Blots

There were ten samples processed on both the line blots and on western blot with the antigens HARS, CDR2, and TRIM21. Results from each platform are shown in **Table 3.1.**

3.3. Re-analysis of Recurrence Biomarker Study Data Set

We previously used phage-display screening to identify autoantibody biomarkers for both early detection and recurrence of ovarian cancer [27, 30]. Two of our identified markers were epitopes from myositis-associated antigens, HARS and SRP-19. We note that in our previous work, the antigens CDR2, TRIM21, and HARS were evaluated for reactivity to antibodies in sera from patients experiencing a recurrence of their HGSOC; however, in that study the levels of autoantibody were considered relative to a negative control antigen for each individual patient at three time points, with the goal of monitoring disease recurrence [28].

With the goal of early detection in the current study, autoantibodies were considered relative to healthy and benign control serum samples. We re-analyzed data from the recurrence study establishing a threshold using the healthy control samples within the sample set. The western blot was quantified as described in section 2.4, with the anti-Human IgG intensity normalized to the anti-His tag loading control per antigen; the resulting values are plotted in **Figure 3.4**. In the original data set, samples were taken from 3 time points for each patient, labeled as T1, T2, and T3. For this analysis, we used the second, T2, measurement as it is the time point closest to time of diagnosis

Table 3.1: Line Blot and Western Blot Association

				Reactivity of Antigen Biomarkers		
BSID	**Sample ID**	**CA125**	**Test**	**HARS**	**TRIM21**	**CDR2**
674	**P128-Cancer(R)-T2**	**13**	**Western Blot**	**0.1**		**0.21**
			Line Blot			
1740	**P135-Cancer(R)-T2**	**11**	**Western Blot**		***15.15***	***1.75***
			Line Blot		***3***	***4***
1681	**P146-Cancer(R)-T2**	**25**	**Western Blot**	**0.09**	**0.45**	
			Line Blot		**1**	
3905	**P184-Cancer(R)-T2**	**5**	**Western Blot**			**0.2**
			Line Blot			***2***
3776	**P175-Cancer(R)-T2**	**18**	**Western Blot**		***34.5***	**0.3**
			Line Blot		**4**	
784	**P25-Cancer(NR)-T2**	**12**	**Western Blot**	**0.1**		
			Line Blot			
832	**P164-Cancer(NR)-T2**	**28**	**Western Blot**			
			Line Blot			
4012	**P189-Cancer(NR)-T2**	**6**	**Western Blot**	**0.07**	***1.93***	**0.29**
			Line Blot		***2***	**1**
4069	**P206-Cancer(NR)-T2**	**7**	**Western Blot**			
			Line Blot		**1**	
7428	**P281-Cancer(NR)-T2**	**6**	**Western Blot**	**0.06**		
			Line Blot	**1**	**1**	

Table 3.1: Reactivity of 10 samples evaluated on line blot and western blot with TRIM21, HARS, and CDR2 antigens.

Figure 3.4

A.

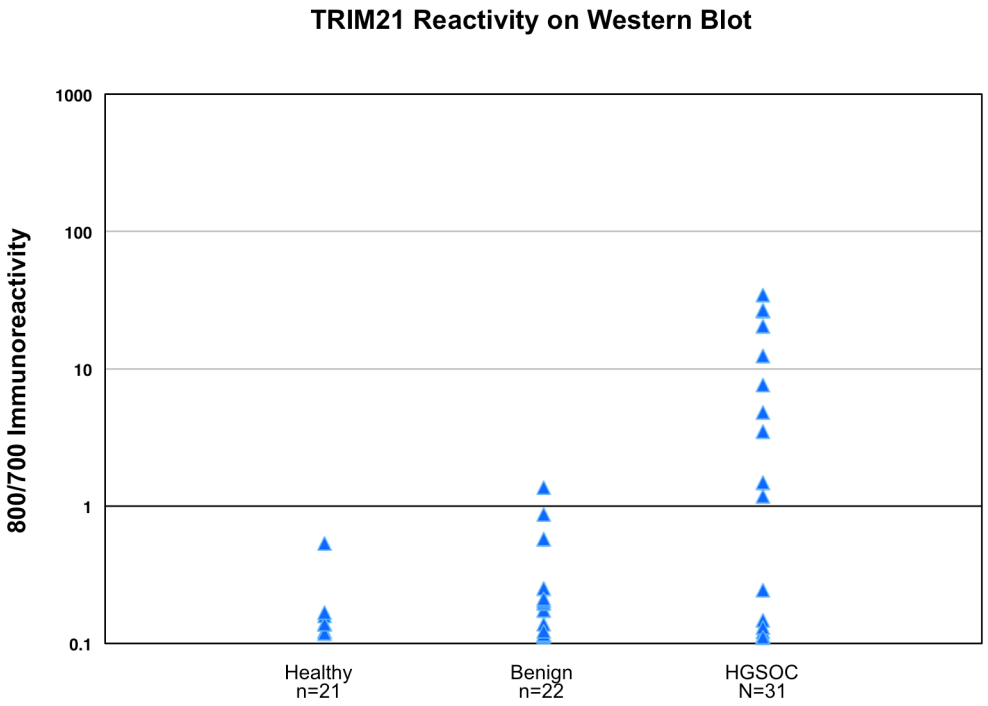

B.

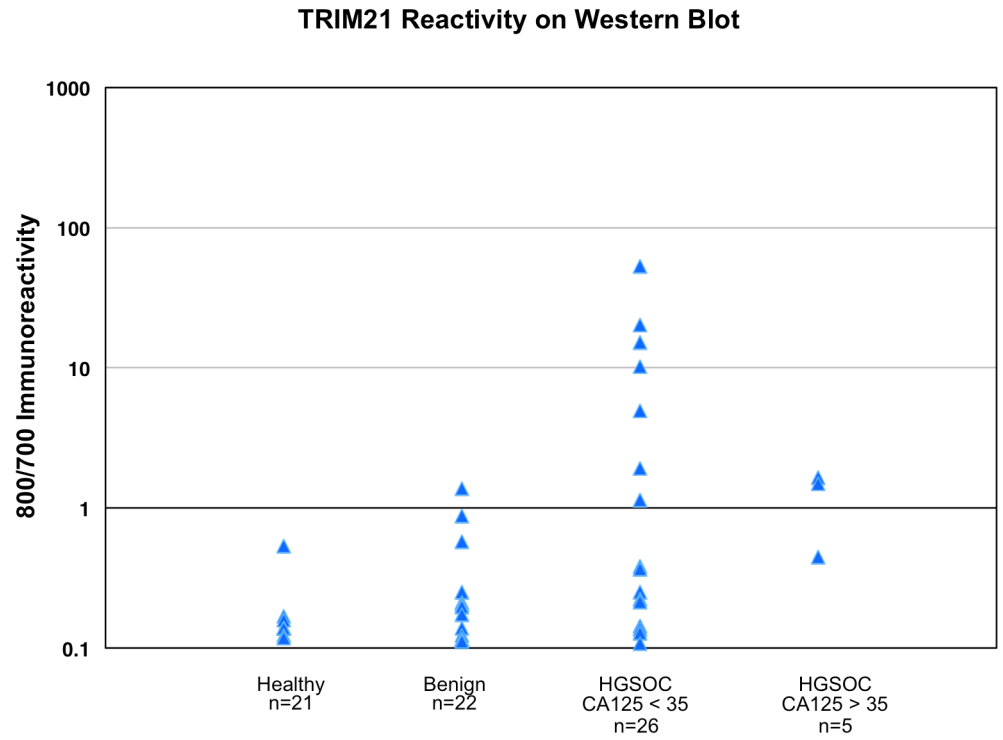

Figure 3.4: TRIM Reactivity and CA125. A. Western blot reactivity with TRIM21. B. Western blot reactivity with TRIM21 with HGSOC cases grouped by CA125 status.

before treatment and most closely matches the serum samples used in our early detection studies. 10/31 (32%) HGSOC ovarian cancer cases were positive for TRIM21 protein, with 0/21 healthy control samples, and 1/22 (0.05%) of samples from women with benign gynecological conditions, shown in **Figure 3.4.** **Figure 3.4:B** shows samples that had CA125 values below clinical cutoff.

3.4. Western blot and ELISA preliminary screening

Next, selected antigens were purified for further analysis on western blot and ELISA. The following antigens were either expressed in E. coli and purified in house, or obtained commercially for quantitation in western blot and ELISA assays: SRP-19, HARS, AARS, CDR2, HuD, TRIM21, TRIM33, CDR2L, CORTACTIN, CKB, NY-ESO-1, PAX8 and TP53 (**Table 3.2**). In addition, the four phage display epitopes with homology to paraneoplastic antigens were sub-cloned, expressed in E. coli and purified [27]. A representative western blot is shown in **Figure 3.5**. Both the homologous epitopes and full-length protein pairs were evaluated; in all cases the full-length protein provided increased sensitivity. Therefore the full-length protein was utilized in future studies rather than the purified epitope peptides.

The serum set of n=36 samples is described in **Table 3.3** and consisted of 12 Healthy control samples, 12 samples representing benign gynecologic conditions including uterine fibroids, endometriosis, and ovarian cysts, and 12 late-stage HGSOC. Western blot was performed first with 11 antigens. HARS, TRIM21, CDR2, and P3F10 had the lowest individual one-way ANOVA p-values. Individual antigen reactivity is shown in a matrix plot in **Figure 3.6**. Each purified antigen was incubated with patient sera autoantibodies, followed by incubation with secondary antibody to human IgG, and

Table 3.2: Description of Paraneoplastic Antigens Evaluated Against HGSOC Sera.

Category	Antigens purified for western blot/ELISA screening	Epitope purified for western blot/ELISA screening	Autoantibodies targeting antigens	Autoimmune conditions associated with Autoantibodies	Cancers types associated with Autoantibodies	Reference
Myositis	**HARS**	**4B7: Epitope**	Jo-1	Myositis, Dermatomyositis	OVCA, lung	[180, 203]
	TRIM21	**4F10: Epitope**	Ro-52	Myositis, Systemic lupus erythematosus, Sjogren's Syndrome	ECC, Basal-like breast cancer	[100, 185]
	SRP-19	**3A9: Epitope**	Anti-SRP-19	Myositis	Breast, endometrial, hepatocellular, bladder	[3, 180]
	CORTACTIN		Anti-Cor	Myositis		[102]
	AlaRS		PL-12	Myositis	Lung, gastric	[180, 197]
	TRIM33		Anti-TIF1-γ	Myositis	Lung, breast, OVCA, stomach	[117, 180, 203]
PCD	**CDR2**		Yo	Paraneoplastic Cerebellar Degeneration	Breast, OVCA	[52, 124]
	CDR2L		Yo	Paraneoplastic Cerebellar Degeneration	Breast, OVCA	[52, 98]
	CKB		Anti-CKB	Paraneoplastic Cerebellar Degeneration	OVCA	[174]
Other PNS	**HuD**	**4E8: Epitope**	Anti-Hu	Encephalomyopathy, sensory neuronopathy	SCLC	[93, 137]
	P3F10		Anti-P3F10	OVCA epitope that binds PNS sera	OVCA	[27]
TAA	**TP53**		Anti-TP53	Systemic lupus erythematosus, Type I Diabetes, AI Thyroid Disease	Pancreatic, Breast, OVCA	[31, 91]
	NY-ESO-1		Anti-NY-ESO-1	N/A, Cancer/Testis Antigen	Lung, Breast, OVCA	[175]
	PAX8		Anti-PAX8	N/A	Antigen overexpression in OVCA	[189]

Table 3.2: Paraneoplastic antigens purified; the 8 antigens shaded in gray are those selected for the large-scale screening on western blot and ELISA. Epitopes identified by phage-display screening of ovarian cancer (OVCA) serum [27]. PNS=Paraneoplastic Neurological Syndrome, PCD=Paraneoplastic Cerebellar Degeneration, TAA=Tumor Associated Antigen.

Figure 3.5

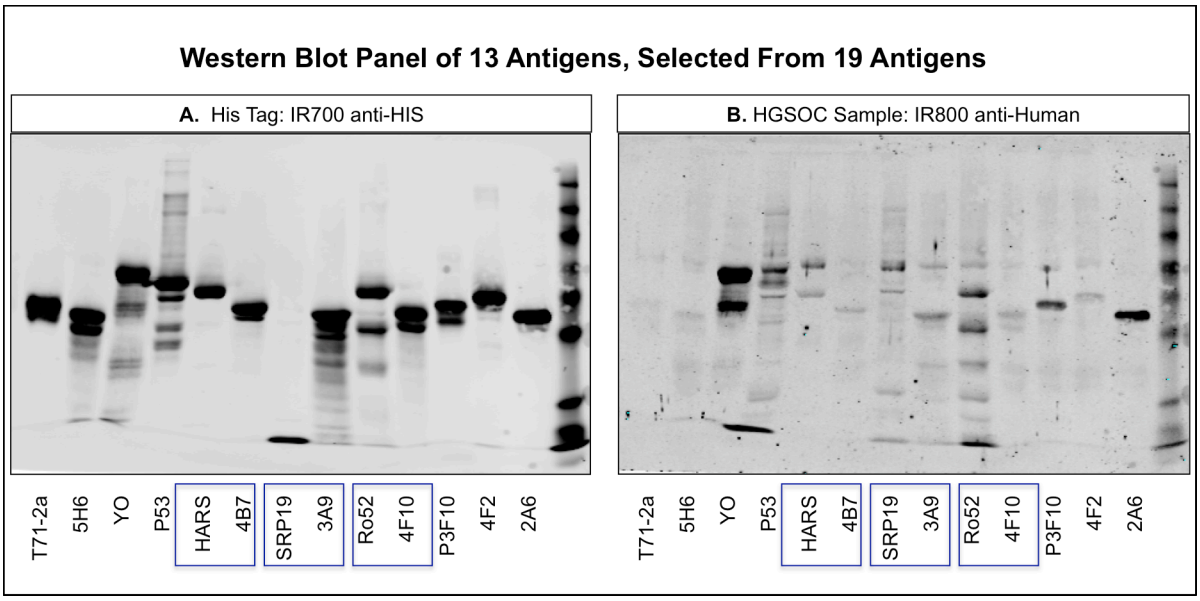

Figure 3.5: Western Blot Image, n=36.
Purified antigens on western blot. Blue boxes indicate full-length protein and corresponding homologous OVCA epitope pair. A. anti-HIS tag antibody. B. Patient serum and anti-Human IgG.

Table 3.3: Serum sample patient population (n=36), analyzed on western blot and ELISA, preliminary screening.

Preliminary Screening Set		
Patient Description	**Number of Samples**	**Age range (Avg)(Median)**
Late Stage HGSOC at time of diagnosis, pre-treatment	12	44-47 (57.4) (56.5)
Benign gynecological condition (ovarian cyst, endometriosis, uterine fibroids)	12	29-72 (50.1) (50.5)
Healthy volunteers from community outreach	12	51-77 (63.6) (64.5)

Table 3.3: Patient Population, n=36. Serum samples analyzed on ELISA and western blot.

Figure 3.6

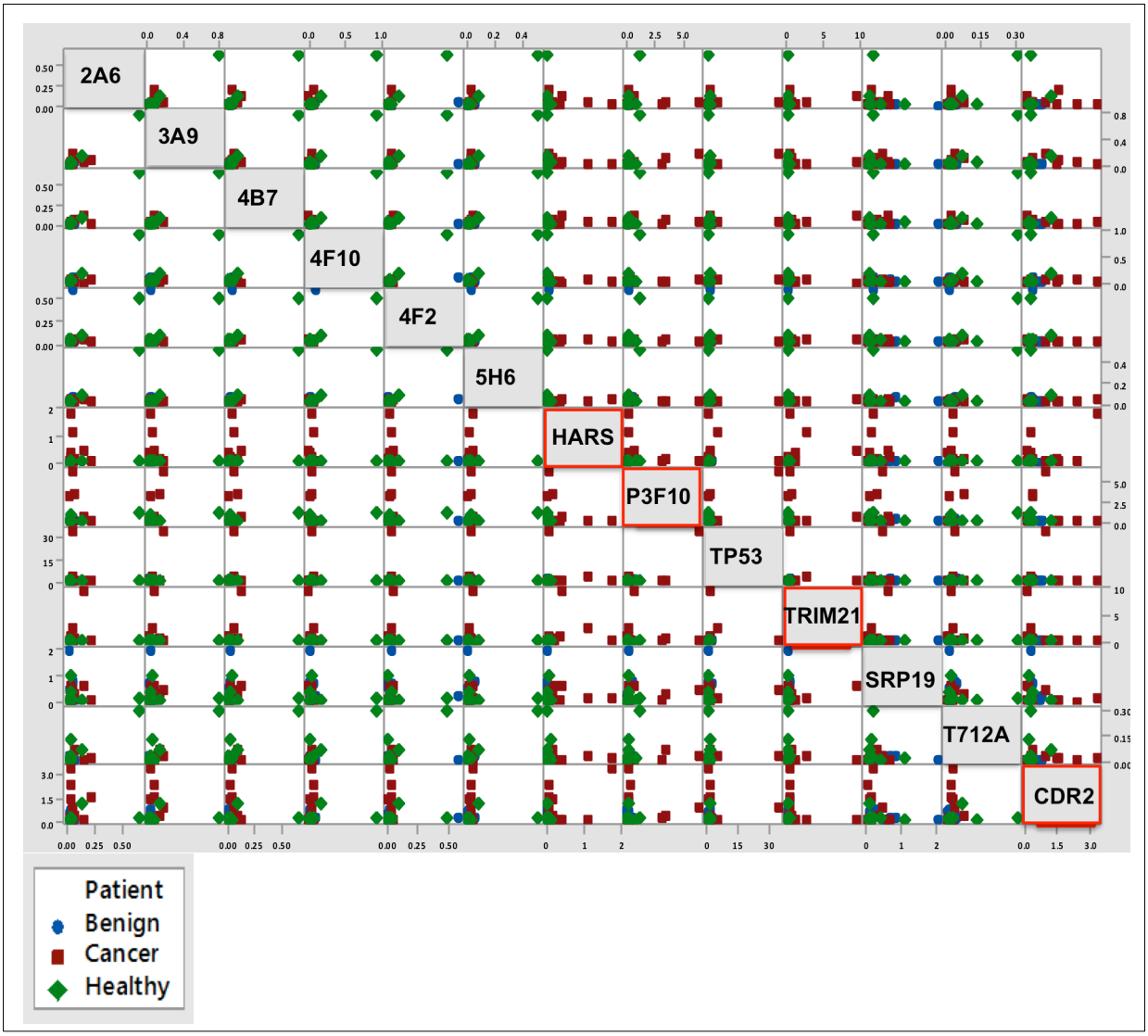

Figure 3.6: Matrix Plot, n=36
Ratio of IR800:IR700 value representing the anti-Human IgG antibody adjusted for protein loading with the anti-HIS tag antibody is plotted on the X and Y axes for each possible marker pair as labeled in the center diagonal gray boxes, with each patient sample represented as a single point. Benign samples are labeled in blue, cancer samples are labled in red, and healthy samples are labled in green. Red boxes represent the pairs which individually significantly separate cancer from healthy and benign by one-way ANOVA.

to 6X Histidine tag. Anti-human antibody intensity is normalized to antibody intensity for each his-tagged antigen. As a visual representation of which marker pairs were compatible, each antigen pair was plotted against the other using a matrix plot in a log scale so that each patient could be represented by a single point defined by two markers, which are labeled as cancer, healthy, or benign in **Figure 3.6**. Certain combinations separated the cancer category to the upper quadrant, so additive effects of marker pairs were then evaluated. Combining the four markers HARS, P3F10, TRIM21, and CDR2 by taking the log of the product (equal to the sum of the four marker values on a log scale), the p-values using one-way ANOVA are: $4.9E^{-06}$ for Healthy vs. HGSOC and $1.2E^{-05}$ for Benign vs. HGSOC.

This set of 36 serum samples was also run on ELISA, 3 times, each time adjusting ELISA conditions. Differences in antigen concentration are shown in **Table 3.4.** Additionally, the number of plates processed per day and the order in which they were processed varied between studies, as we found that variation in plate drying time between washing steps affected results as observed by an order-processed effect. The ELISA procedure established in the third ELISA experiment with the n=36 sample set are the conditions utilized in the large-scale n=164 experiment as described in section 2.5.2.

Results from western blot and ELISA screening with a serum set of n=36 samples are shown in **Table 3.4.** This set of 12, 12, 12 samples was also included in the study of recurrent ovarian cancer described in section 3.1, utilizing the T2 time points as described in section 3.2. This represents western blot 2 as labeled WB2 in **Table 3.4**.

Table 3.4: Results from Preliminary Screening of Purified Recombinant Proteins on Western Blot and ELISA.

	Antigen	HARS					TRIM21					CDR2					P3F10				TP53			NY-ESO-1
	Assay, n=36, Western Blot: W1, W2 ELISA: E1, E2, E3	W1	W2	E1	E2	E3	W1	W2	E1	E2	E3	W1	W2	E1	E2	E3	W2	E1	E2	E3	W2	E2	E3	E3
	Antigen Concentration	1µg	1µg	0.3µg	1µg	3µg	0.6µg	1µg	0.3µg	1µg	0.75µg	1µg	1µg	0.3µg	1µg	1.5µg	1µg	0.3µg	1µg	2µg	1µg	0.3µg	1µg	1µg
Patient ID HGSOC Samples	O1																■	■	■	■				
	O2	■	■	■	■	■																		
	O3																				■	■	■	
	O4																				■	■	■	
	O5																■	■	■	■	■	■	■	
	O6											■	■											■
	O7											■	■											
	O8																							
	O9						■	■																
	O10	■	■	■	■		■	■	■	■														
	O11						■	■	■	■	■										■	■	■	
	O12																							
	HGSOC (+), n=12	2	2	2	2	1	3	3	2	2	1	2	2	0	0	0	2	2	2	2	4	4	4	1
	Sensitivity	0.17	0.17	0.17	0.17	0.08	0.25	0.25	0.17	0.17	0.08	0.17	0.17	0.00	0.00	0.00	0.17	0.17	0.17	0.17	0.33	0.33	0.33	0.08
	Total Sensitivity: 10/12 (83%)			O2, O10 17%					O9, O10, O11 25%					O6, O7 17%					O1, O5 17%				O3, O4, O5, O11 33%		O6 8%

Table 3.4: Positive Samples from 3 ELISA and 2 western blot screening, performed with varying antigen concentrations as shown. A set of 36 sera consisting of 12 healthy, 12 benign gynecological disease, and 12 high-grade serous ovarian cancer was run on three separate ELISA experiments, as well as twice on western blot. Sensitivity is calculated relative to healthy and benign samples at 90% specificity. With these six markers, a total of 10/12 samples were positive using at least one assay. Samples positive for each assay are shaded in gray per antigen.

3.5. Description of Antigens Selected for Large-Scale Validation (n=164)

From the commercial line blot, western blot, and ELISA screenings, three myositis-associated antigens, three paraneoplastic cerebellar degeneration associated antigens, and three tumor-associated antigens were selected for validation on a large-scale western blot and ELISA study using an independent sample set. The 8 selected antigens are highlighted in **Table 2.1**.

HARS, Histidyl-tRNA synthetase.

HARS catalyzes the transfer of Histidine to its cognate tRNA during protein synthesis, and HARS splice variants have reported immuno-modulatory roles [210]. Antibodies against the HARS antigen are termed Jo-1 autoantibodies [193, 203]. Anti-tRNA synthetase antibodies are common in myositis, with Jo-1 autoantibodies having the highest frequency [35].

TRIM21, E3 ubiquitin-protein ligase TRIM21, Sjogren's Syndrome type A antigen.

TRIM21 has E3-ligase activity as well as roles in intracellular pathogen clearance with a potent fc-receptor and activation of the innate immune response [121]. Antibodies against TRIM21 are termed SSA-autoantibodies or Ro-52 autoantibodies and are associated with Sjogren's syndrome, myositis, systemic lupus erythematosis, and systemic sclerosis [133, 134] .

Cortactin, Src substrate cortactin.

Anti-cortactin autoantibodies were identified in sera of patients with polymyositis and in a separate study in myasthenia gravis who were sero-negative for classic paraneoplastic antigens [18]. Cortactin expression as measured by

immunohistochemistry and mRNA analysis of tumor tissues was reported to be associated with poor prognosis in ovarian cancer [108].

CDR2, Cerebellar degeneration-related protein 2.

CDR2 interacts with c-myc and down-regulates c-myc dependent transcription in tumor cells, and is involved in mitotic cell division [130, 171]. Autoantibodies against the CDR2 antigen are termed Yo autoantibodies and are detected in patients with paraneoplastic cerebellar degeneration [46, 52].

CDR2L, Cerebellar degeneration related protein 2-like.

CDR2L (CDR2-Like) shares 50% homology to CDR2; Yo autoantibodies can target both proteins. The function of CDR2L is unknown [52].

TP53, Cellular tumor antigen p53.

TP53 is a tumor suppressor and transcription factor involved in cell cycle regulation, DNA repair activation, apoptosis activation, and senescence. Somatic mutations in p53 are found in approximately half of all human cancers, and in 96% of HGSOC cases [37]; autoantibodies to p53 in HGSOC can be detected against the wild type protein as a polyclonal response [91]. Autoantibodies to p53 are also detected in autoimmune conditions in which DNA antibodies are present, such as SLE, type I diabetes, and autoimmune thyroid disease [31].

NY-ESO-1, Cancer/testis antigen 1.

NY-ESO-1 is involved in cell growth and apoptosis. The restricted expression in testis suggests germ cell self-renewal function. Anti-NY-ESO-1 autoantibodies, originally identified by SEREX technology, have been detected in multiple tumor types including ovarian, breast, lung, and melanoma [33]. NY-ESO-1 is an immunotherapy

target for ovarian cancer with numerous trials evaluating vaccines targeting NY-ESO-1 as well as adoptive transfer of NY-ESO-1 specific T-cells [13, 131].

4. CHAPTER 4: Validation I: 14 Antigens Screened with n=164 Serum Sample Set on ELISA and Western Blot

4.1. Patient Sample Population, n=164, Processed on ELISA and Western Blot

To avoid experimental bias, an independent sample set of 164 samples that had not been used to identify the biomarkers initially was used for validation of the antigens described in chapter 3. The sample population consisting of 50 healthy control samples, 50 benign ovarian cyst samples, 50 late stage HGSOC samples, and 14 early stage HGSOC samples is described in **Table 4.1**, and will be referred to as the Validation I sample set.

4.2. 12 Antigens Evaluated on ELISA or Western Blot with n=164 Sera

4.2.1. Methods: ELISA

4.2.1.1. Antigens

The following 8 antigens were screened on ELISA: TRIM21, HARS, CDR2, CDR2L, NYESO1, TP53, and P3F10 using T712A as a negative control. P3F10 was an epitope selected in chapter 3 based on elevated reactivity with sera from patients with paraneoplastic syndromes. The empty phage control T712A was included as P3F10 epitope includes a portion of this phage coat sequence. The reactivity of P3F10 was determined by subtracting the T712A OD value from the P3F10 OD value. TRIM21 and HARS are antigens associated with myositis/dermatomyositis, CDR2 and CDR2L are associated with paraneoplastic cerebellar degeneration, and TP53 and NY-ESO-1 are tumor-associated antigens previously demonstrated to react with autoantibodies in ovarian cancer serum [6, 173].

Table 4.1: Serum Sample Patient Population (n=164), Analyzed on Western Blot and ELISA, Validation I.

Validation Set I		
Patient Description	**Number of Samples**	**Age range (Avg)(Median)**
Late Stage HGSOC at time of diagnosis, pre-treatment	50	39-81* (62.6) (62)
Early Stage HGSOC at time of diagnosis, pre-treatment	14	44-76 (58.8) (57)
Benign gynecological condition (ovarian cyst)	50	17-76 (48.8) (49.5)
Healthy volunteers from community outreach	50	32-88 (56.2) (53)

Table 4.1: Patient Population, n=164. Serum samples analyzed on ELISA and western blot. *Indicates age not available for 3 cases.

4.2.1.2. Standardization

For the ELISA data analysis, to adjust for day-to-day variability among the 44 ELISA plates measured across 11 days, we utilized the positive control measurements to construct the standard curve, which was measured on all plates. The linear curve consisted of 6 dilutions of a positive control serum sample (The Binding Site, San Diego, CA) measured against TRIM21 in duplicate, as shown in **Figure 4.1**. A linear mixed model with log optical density (OD) as the response; dilution (treated as a factor), protein (either TRIM21 or BKG) and their interaction as the fixed effects; plate nested within day as a random effect; an estimated correlation structure between duplicate observations; and unequal variance within each protein/dilution combination. From this model, we extracted the random effects terms to adjust the observed log(OD) values. After averaging the duplicates and exponenting resultant value, the appropriate control adjusted OD was subtracted to produce the normalized OD measurement. This normalized OD measurement was then used to compare to the values from the western blot analysis.

4.2.2. Methods: Western Blot

4.2.2.1. Antigens

The following 10 antigens were evaluated on western blot: TRIM21, HARS, CDR2, CORTACTIN, CDR2L, NYESO1, TP53, BRCA-1, CMYC, and PAX8. TRIM21, HARS, and CORTACTIN are antigens associated with myositis/dermatomyositis, CDR2 and CDR2L are associated with paraneoplastic cerebellar degeneration, and TP53, NY-ESO-1, BRCA-1, CMYC, and PAX-8 are tumor-associated antigens previously demonstrated to react with autoantibodies in ovarian cancer serum or are over-

Figure 4.1

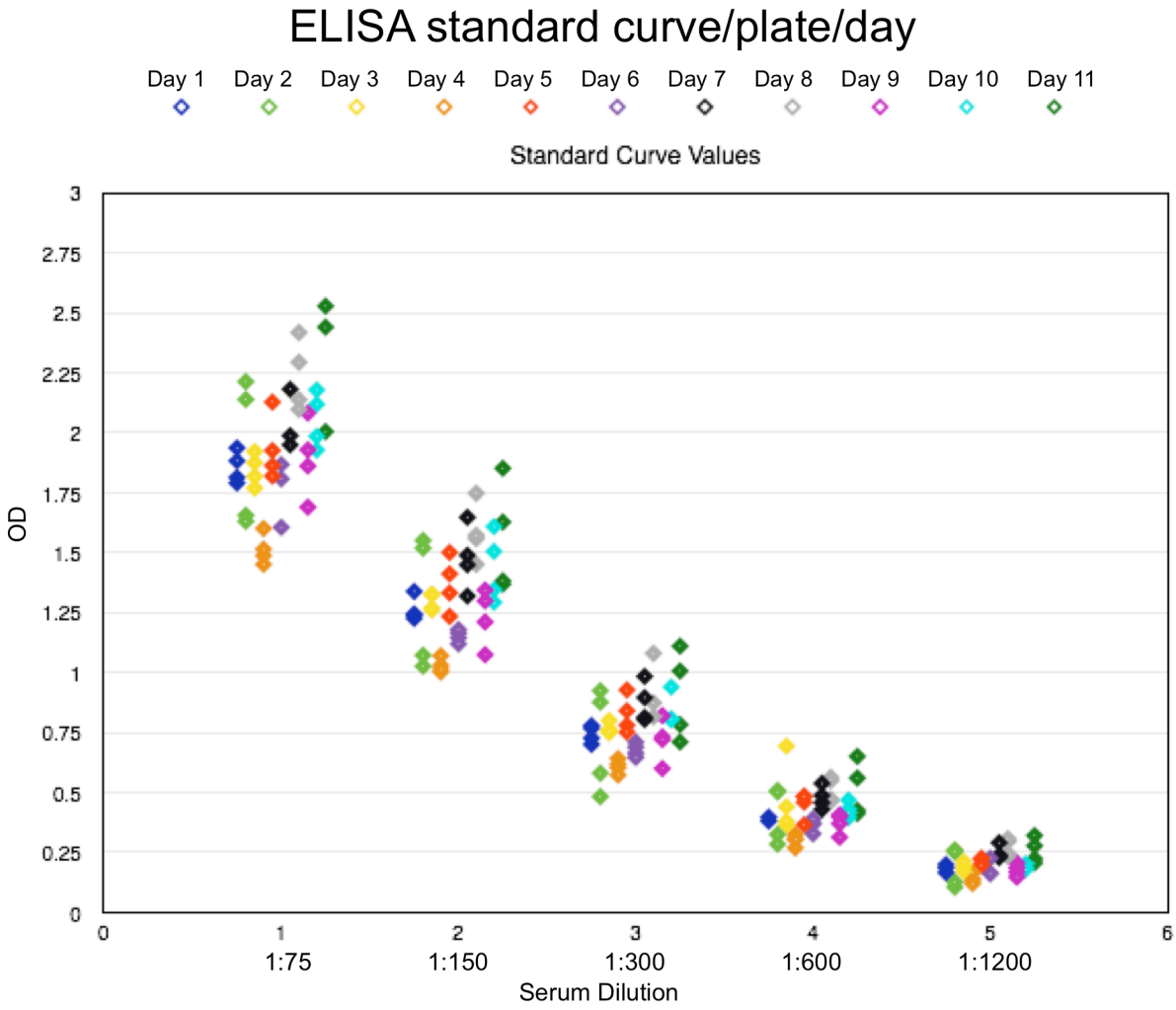

Figure 4.1: ELISA Standard Curve, Validation I, n=164
The ELISA assay was run with a standard curve of 0.75 µg TRIM21 incubated with 5 dilutions (1:1200, 1:600, 1:300, 1:150, 1:75) of the same positive control patient serum per plate. This curve was used to adjust sample values for day-to-day variation. Each color represents one day, each data point represents the average of two duplicate background-corrected measurements per plate, with 4 plates processed per day.

expressed in HGSOC. These 10 antigens were processed on two separate western blot studies; the first study included the 7 antigens TRIM21, HARS, CDR2, CORTACTIN, CDR2L, NYESO1, TP53, and the second study included the 3 antigens BRCA-1, CMYC, and PAX8. **Figure 4.2** shows the first set of 7 antigens on western blot with the Validation I sample set.

4.2.2.2. Standardization

Quantification of autoantibody binding on western blot for each sample was measured over 15 days for Validation I for each of the 8 antigens, and measured over 16 days for Validation II for 4 antigens, utilizing multiple membranes per day. Samples were randomized per category of HGSOC, benign, and healthy with each category evenly distributed per day, and labeled so that the experimenters were blinded to the sample category. The quantification values for both the IRDye700 and IRDye800 channels were log transformed after the addition of a small constant (0.01) to ensure all values were positive. The difference between the log transformed IRDye700 and IRDye800 values for each antigen for each sample is the pre-adjustment analysis metric. We employed a mixed model to develop adjustment factors to account for the between-day variability. We utilized the estimated day-specific random effects (from a model including the log difference as the response, antigen as the fixed effect and day as the random effect) to account for day-to-day variability. The log difference minus the day-specific random effect was used as the final analysis metric. Subsequently, for each antigen, the mean and standard deviation of the analysis metric was computed using the healthy samples. This standardized value was used in the figures and tables presented in this manuscript.

Figure 4.2

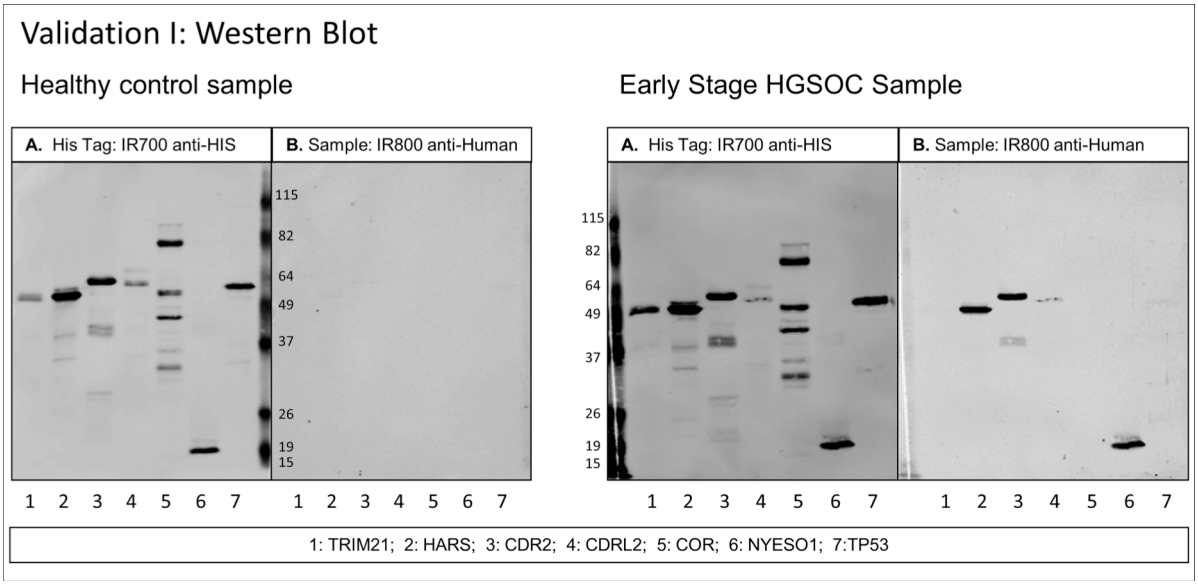

Figure 4.2: Western Blot Image, Validation I, n=164.
Western blot of healthy control serum and early stage HGSOC serum diluted at 1:300 with 7 antigens in Validation I study. A) Secondary antibody anti-HIS tag IgG loading control. B) Secondary antibody anti-human IgG. Scans quantified on Odyssey software; background-corrected integrated intensity of anti-human IgG antibody (IRDye800) normalized as ratio to anti-His tag antibody (IRDye700) per antigen.

4.2.3. Results

4.2.3.1. Individual Antigen Results: ELISA

Individual antigen reactivity is shown in **Figure 4.3**. Positive control serum for HARS, TRIM21, and CDR2 as described in section 3.1.2 were also evaluated on ELISA.

4.2.3.2. ELISA Saturated Signal

Samples that generated a saturated signal on ELISA were assigned a maximum OD value of 4 for analysis. All samples with saturated signal were confirmed as positive on western blot (**Figure 4.4**).

4.2.3.3. Individual Antigen Results: Western Blot

The ratio of anti-human IgG:anti-HIS IgG intensity values are plotted for each antigen for the late-stage HGSOC, early-stage HGSOC, benign ovarian cyst, and healthy control groups in **Figure 4.5.**

4.2.3.4. ELISA and Western Blot Correlation

A threshold based on the 50 healthy control values for each antigen defined positive results. The assay cutoff for both the ELISA assay and the western blot screening is defined as: Mean + 2(StdDev) for the healthy controls. Using this criterion, NY-ESO-1, TP53, and TRIM21 had the highest sensivities and specificities on both platforms. Among all HGSOC samples (n=64), 16/18 samples positive for NY-ESO-1 on ELISA were confirmed by western blot, 14/16 TP53 samples positive on ELISA were confirmed by western blot and 11/13 TRIM21 samples positive on ELISA were confirmed by western blot. However, for the marker TRIM21, 10 additional positive samples were identified on western blot that were not detected by ELISA.

Figure 4.3

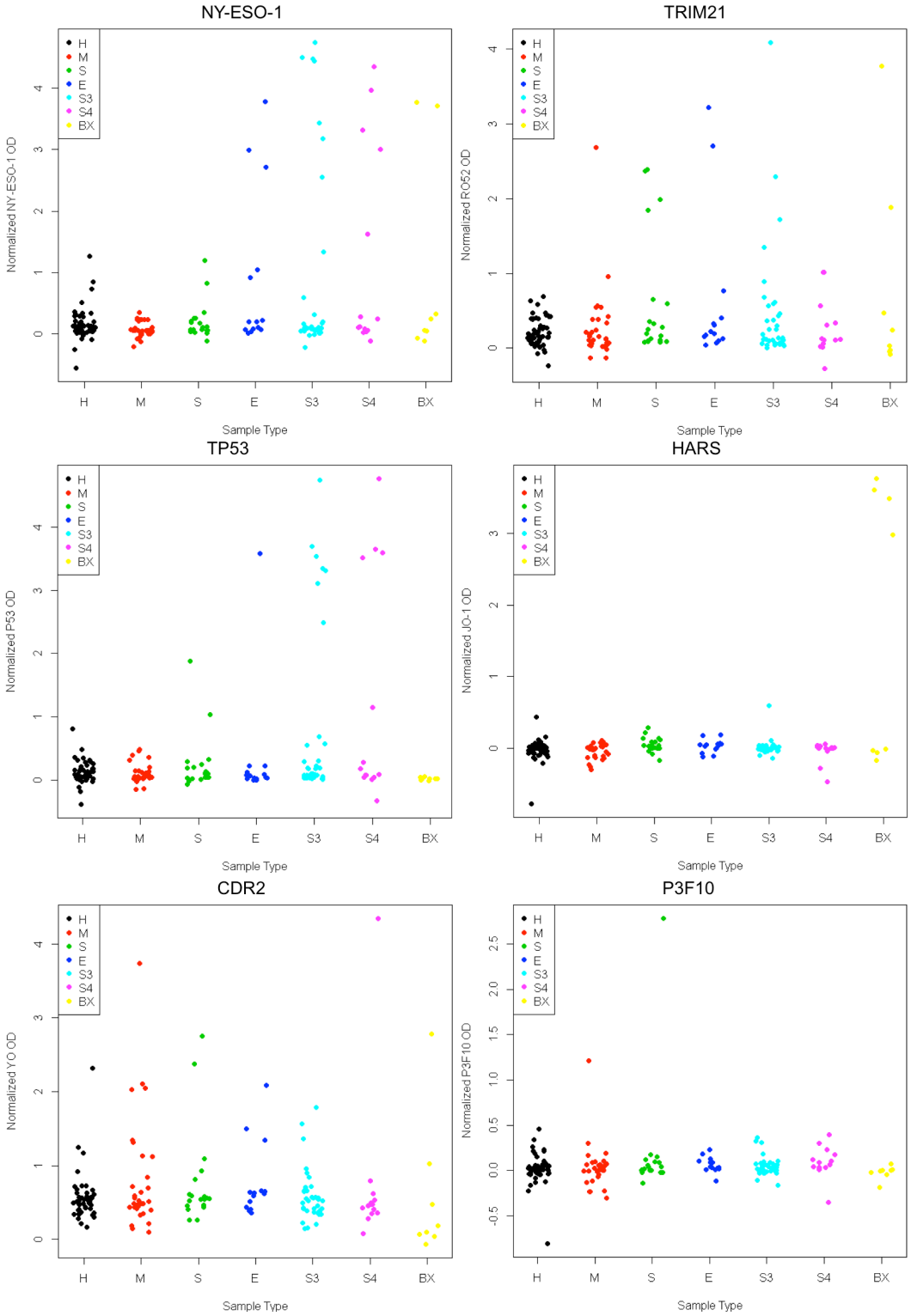

Figure 4.3: ELISA Individual Antigen Graphs, Validation I, n=164. Background-adjusted normalized optical density for each antigen. H=healthy, M=mucinous cyst, S=serous cyst, E=early stage HGSOC, S3=stage 3 HGSOC, S4=stage 4 HGSOC, BX=positive control serum (The Binding Site, San Diego, CA).

Figure 4.4

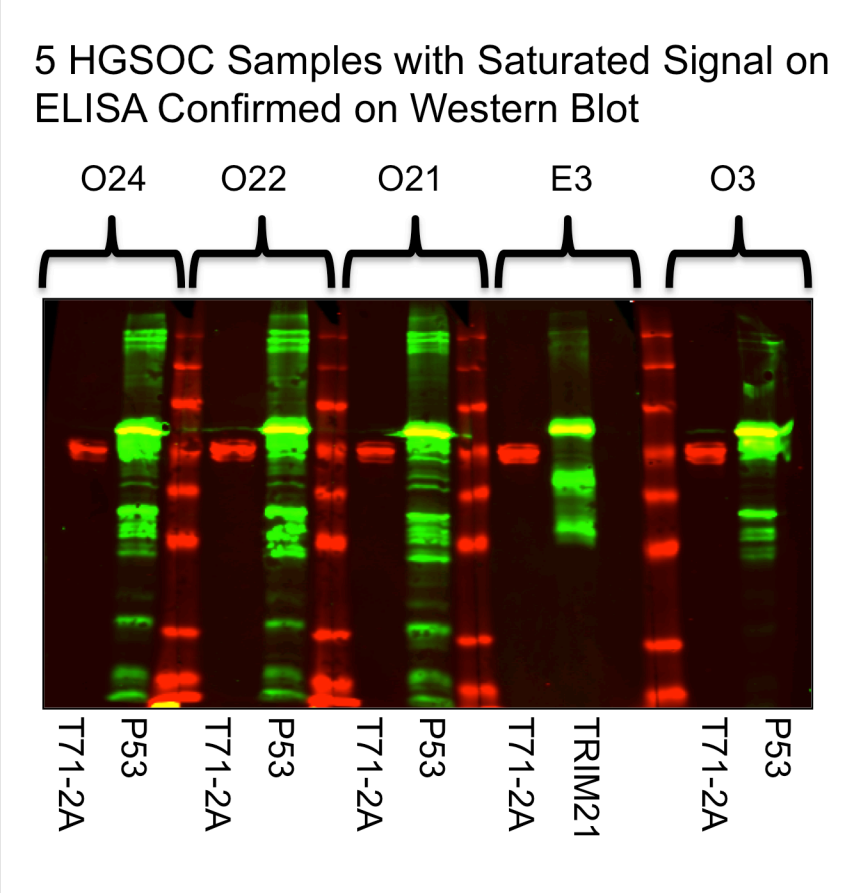

Figure 4.4: Samples with ELISA Saturated Signals Confirmed on Western Blot. ELISA saturated signals for TP53 and TRIM21 confirmed as specific positive reactions on western blot. IR800 anti-human IgG is shown in green, IR700 anti-HIS antibody is shown in red, overlap is shown in yellow.

Figure 4.5

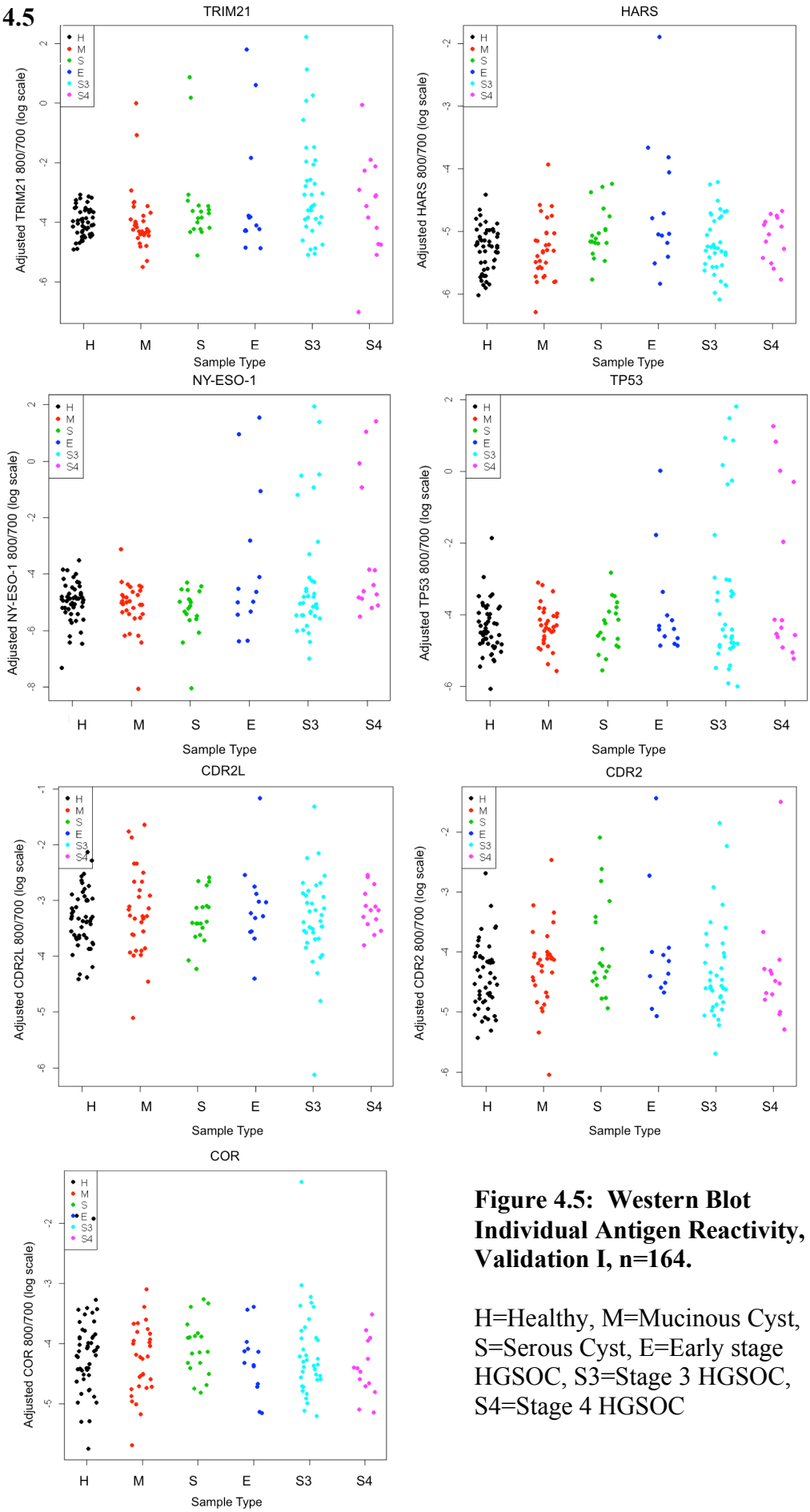

Figure 4.5: Western Blot Individual Antigen Reactivity, Validation I, n=164.

H=Healthy, M=Mucinous Cyst, S=Serous Cyst, E=Early stage HGSOC, S3=Stage 3 HGSOC, S4=Stage 4 HGSOC

Figure 4.6

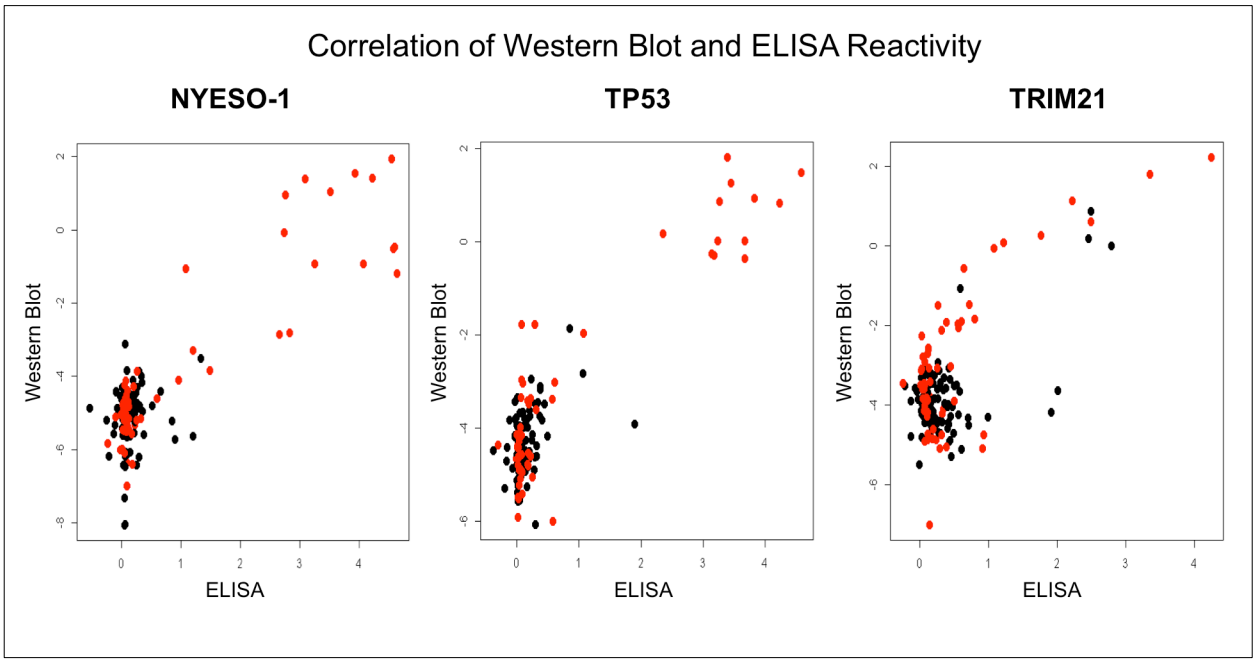

Figure 4.6: Correlation of Western Blot and ELISA. NY-ESO-1, TP53, and TRIM21 western blot values correlated with ELISA values; each sample is represented as a single data point. Red represents HGSOC cases, black indicates healthy or benign cases. Samples in the upper right quadrant were positive on both ELISA and western blot.

4.2.3.5. ELISA Treatment with Reducing Agent DTT

Prior studies have demonstrated enhanced detection of anti-TRIM21 antibodies on ELISA under reducing conditions, including samples with autoantibodies that were undetectable in non-reducing conditions [134, 141]. In Validation I, a threshold based on the 50 healthy control values for each antigen defined positive results. Seven of the positive samples that were identified on western blot but were not detected by ELISA were processed again on ELISA using TRIM21-coated plates that were treated with DTT. Results are shown in **Table 4.2**; treatment with DTT did not affect ELISA reactivity. A representative image of a sample positive for TRIM21 on western blot that was undetectable by ELISA is shown in **Figure 4.7**. Additionally, the marker HARS did not react on ELISA whereas it showed reactivity on western blot. HARS was treated with DTT, and did not show any improvement in ELSA detection for 2 samples that were positive on western blot.

Lack of reactivity can be due to protein binding to the plate and resulting epitope availability on ELISA, as well as increased background noise in the ELISA platform that can interfere with detection of a positive signal. A number of patient samples retained an inherent high background on ELISA regardless of pre-incubation of the serum sample with blocking agent (5% donkey serum) and bacterial extract as described in Methods. It was concluded that western blot eliminates ambiguities introduced by samples with high background noise and is the more reliable platform for detection of patient autoantibodies. Therefore, subsequent analyses employed western blot data.

Table 4.2 ELISA Results: TRIM21 + DTT

Protein	Sample #	N=164 ID	TRIM21 Status, n=164 study	TRIM21 Status, n=164 study	ELISA ABS-BKG NO DTT	ELISA ABS-BKG + DTT	Delta (NO DTT) - (+DTT)
TRIM21	Sample 1	O47	WB +	ELISA -	0.409	0.369	0.041
TRIM21	Sample 2	O40	WB +	ELISA -	0.254	0.275	-0.022
TRIM21	Sample 3	O12	WB +	ELISA -	0.209	0.216	-0.007
TRIM21	Sample 4	O46	WB +	ELISA -	0.305	0.211	0.094
TRIM21	Sample 5	O33	WB +	ELISA -	0.134	0.127	0.007
TRIM21	Sample 6	O3	WB +	ELISA -	0.012	-0.014	0.026
TRIM21	Sample 7	O37	WB +	ELISA +	1.940	1.956	-0.017
TRIM21	Sample 8	O38	WB -	ELISA -	0.042	0.067	-0.025
TRIM21	Sample 9	O42	WB -	ELISA -	-0.014	-0.05	0.036

Table 4.2: Treatment with reducing agent DTT on ELISA. OVCA samples positive on WB and not on ELISA. Addition of DTT had no affect on ELISA sample reactivity.

Figure 4.7

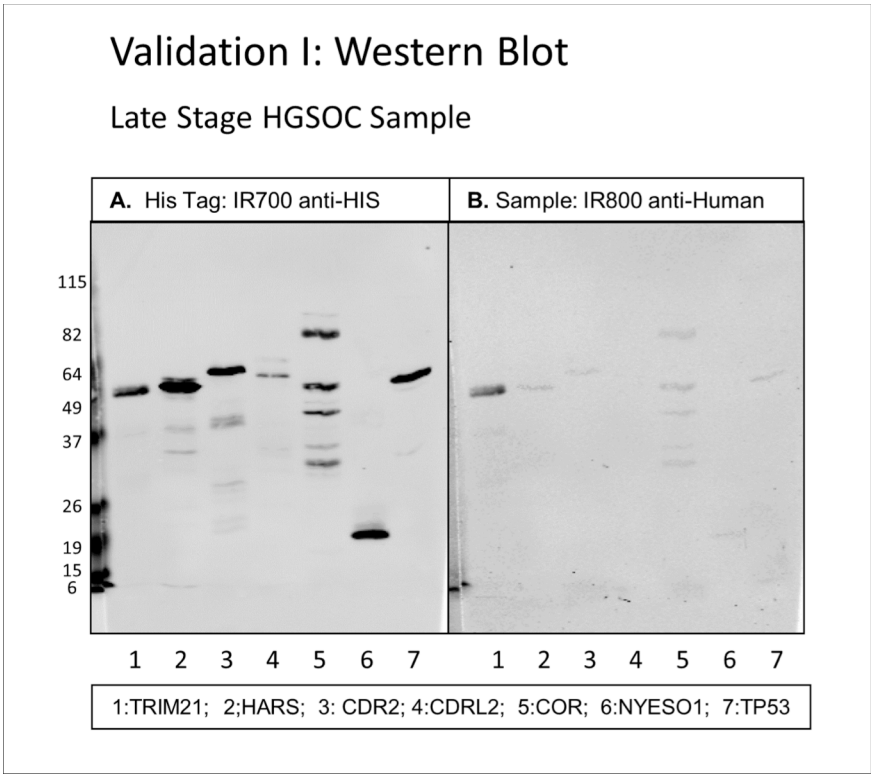

Figure 4.7: Western Blot of Late-Stage HGSOC Sample Positive for TRIM21, Validation I.
Late-Stage HGSOC sample positive for TRIM21 (800:700 standardized ratio > 2) on western blot, which was not detected by ELISA (Standardized background-corrected intensity <2). A) Secondary antibody anti-HIS tag IgG loading control. B) Secondary antibody anti-human IgG.

4.2.3.6. Sensitivity/Specificity: TRIM21 provides highest sensitivity as an individual marker in HGSOC samples.

Sensitivities and specificities as calculated by the standardized thresholds based on mean + 2(StdDev) of the healthy controls and mean + 3(StdDev) of the healthy controls per antigen are reported in **Table 4.3.** The resulting thresholds were applied to all patient groups: healthy, benign, early stage HGSOC, and late stage HGSOC. Applying the assay threshold=2 for western blot to TRIM21 yields 21 positive samples out of 64 HGSOC cases, including both early and late stage. Notably, with 33% sensitivity TRIM21 did not positively react with healthy control samples. Four benign ovarian cyst samples had reactivity above the healthy control threshold. Individual sensitivities and specificities of all markers are shown in **Table 4.3**; the previously established biomarkers NY-ESO-1 and TP53 each detected 16/64 (25%) of HGSOC cases. One healthy control sample with high reactivity to TP53 had self-reported family history of ovarian cancer.

Cortactin (COR), a novel biomarker for myositis, did not show HGSOC specificity [102]. We found that CDR2 and CDR2L had reactivity with healthy and benign samples. Antibodies to CDR2 have previously been reported to have low frequency in ovarian cancer. We observed 5/50 late stage and 2/14 early stage samples positive for CDR2 autoantibodies at the threshold (2)=Mean + 2(StdDev) [124]. Previous studies have shown that Yo-antibody positive patients with paraneoplastic cerebellar degeneration have anti-Yo antibodies that react with both CDR2 and CDR2L [52]. In a study evaluating ovarian cancer sera, anti-Yo positive sera reacted with CDR2L alone, or both CDR2 and CDR2L [52]. In our cohort, the three samples that were positive for both CDR2 and CDR2L were late-stage serous ovarian cancer cases (**Table 4.4**).

Table 4.3 Sensitivity/Specificity for Validation I.

Positive Threshold=2	Late Stage HGSOC (n=50)	Early Stage HGSOC (n=14)	Late and Early Stage HGSOC (n=64)	Benign (n=50)	Healthy (n=50)	Benign and Healthy (n=100)
Antigen	**Sensitivity**	**Sensitivity**	**Sensitivity**	**Specificity**	**Specificity**	**Specificity**
TRIM21	0.34	0.29	0.33	0.90	1.00	0.95
TP53	0.28	0.14	0.25	0.98	0.96	0.97
NYESO1	0.24	0.29	0.25	0.98	0.98	0.98
HARS	0.06	0.29	0.11	0.90	0.98	0.94
CDR2L	0.06	0.14	0.08	0.94	0.96	0.95
CDR2	0.10	0.14	0.11	0.88	0.96	0.92
COR	0.02	0.00	0.02	1.00	0.96	0.98
TRIM21, TP53, NYESO1	0.64	0.43	0.59	0.86	0.94	0.90

Positive Threshold=3	Late Stage HGSOC (n=50)	Early Stage HGSOC (n=14)	Late and Early Stage HGSOC (n=64)	Benign (n=50)	Healthy (n=50)	Benign and Healthy (n=100)
Antigen	**Sensitivity**	**Sensitivity**	**Sensitivity**	**Specificity**	**Specificity**	**Specificity**
TRIM21	0.28	0.21	0.27	0.92	1.00	0.96
TP53	0.26	0.14	0.23	1.00	0.98	0.99
NYESO1	0.22	0.29	0.23	1.00	1.00	1.00
HARS	0.02	0.21	0.06	0.98	1.00	0.99
CDR2L	0.02	0.14	0.05	0.96	1.00	0.98
CDR2	0.06	0.14	0.08	0.94	0.98	0.96
COR	0.02	0.00	0.02	1.00	0.96	0.98
TRIM21, TP53, NYESO1	0.58	0.36	0.53	0.94	0.98	0.96

Table 4.3: Sensitivity and specificity for TRIM21, TP53, NY-ESO-1, HARS, CDR2L, CDR2, and COR evaluated on western blot with n=164 sample set. Threshold (2)=Mean + 2(StdDev) for healthy controls, threshold (3)=Mean + 3(StdDev) for healthy controls.

Table 4.4 CDR2 and CDR2L Combined Reactivity, n=164, Validation I

Antigen	Benign (n=50)	Healthy (n=50)	All HGSOC (n=64)	Early Stage (n=14)	Late Stage (n=50)
CDR2>2	6	2	7	2	5
CDR2L>2	3	2	4	1	3
CDR2>2 + CDR2L>2	0	0	3	1	2

Antigen	Benign (n=50)	Healthy (n=50)	All HGSOC (n=64)	Early Stage (n=14)	Late Stage (n=50)
CDR2>2	6	2	7	2	5
CDR2L>1.5	6	3	6	2	4
CDR2>2 + CDR2L>1.5	0	0	4	2	2

Table 4.4: CDR2 and CDR2L, n=164, Validation I. Samples positive for both CDR2 and CDR2L were all HGSOC cases. Thresholds of 1.5 or 2 shown for individual antigens or the combination of CDR2 and CDR2L.

In cases of myositis, patients that had the combination of TRIM21 and HARS were more likely to have cancer [115, 149]. In our cohort we observed 3/64 HGSOC patients with a combination of HARS and TRIM21 positive values.

4.3. Additional Ovarian Cancer Tumor-Associated Antigens screened with n=164 sample set on western blot: BRCA1, CMYC, PAX8

4.3.1. Study Design

Three additional tumor-associated antigens were evaluated with the Validation I sample set: BRCA1, CMYC, and PAX8.

4.3.1.1. Antigen Description

C-myc, C-myc protein.

In a study by Wang et. al evaluating 12 tumor-associated antigens to identify ovarian cancer biomarkers, C-myc was identified as a top candidate biomarker as measured by ELISA. C-myc was detected in 24/132 (18.2%) of ovarian cancer serum samples, and 3/147 (2%) of healthy control samples, with the positive cutoff defined as mean + 2 standard deviations of the healthy control samples [186].

BRCA1, Breast cancer type I susceptibility protein.

Autoantibodies to BRCA1 were detected in 17/34 ovarian cancer samples on ELISA [211]. BRCA1 and BRCA2 mutations account for the majority of hereditary breast and ovarian cancer cases [136].

PAX8, Paired box protein Pax-8.

Overexpression of PAX8 is associated with HGSOC [20, 189]. The present study is the first to detect anti-PAX8 autoantibodies. The full-length PAX8 protein is 450 aa; the recombinant PAX8 protein used in this study consists of the amino acids 1-287, which are present on isoforms C-E.

4.3.2. Results

Western blot image of patient serum with the three antigens CMYC, BRCA1, and PAX8 is shown in **Figure 4.8**. Individual antigen reactivity is shown in **Figure 4.9**. Of the three markers, PAX8 demonstrated potential to complement NY-ESO-1, TP53, and TRIM21. Alone, PAX8 was positive for 7/64 HGSOC samples, 5 of which were not detected previously. Although previously reported to be elevated in HGSOC patient serum, both BRCA1 and CMYC reacted with HGSOC, healthy control, and benign ovarian cyst samples on western blot (**Figure 4.9**) [186, 211].

4.4. Analysis of 10 antigens Screened with n=164 Sera on Western Blot Identifies Top Panel of 4 Antigens: TRIM21, NY-ESO-1, TP53, and PAX8

4.4.1. Panel of 4 Antigens: TRIM21, NY-ESO-1, TP53, and PAX8 provides highest sensitivity and specificity.

The combination of the four markers TRIM21, NY-ESO-1, TP53, and PAX8 detected 42/64 HGSOC samples. With 94% specificity for the healthy control population, we can achieve 67% sensitivity (threshold=2) for the 4-marker model. At 98% specificity relative to the healthy control population, this 4-marker combination achieves 56% sensitivity (threshold=3). The maximum value among the 4 markers: TRIM21, NY-ESO-1, TP53, and PAX8 for each sample group is plotted in **Figure 4.10.** **Table 4.5** shows performance of the combinations of these 4 markers. ROC Curve analysis of the 4-marker panel is shown in **Figure 4.11**.

Figure 4.8

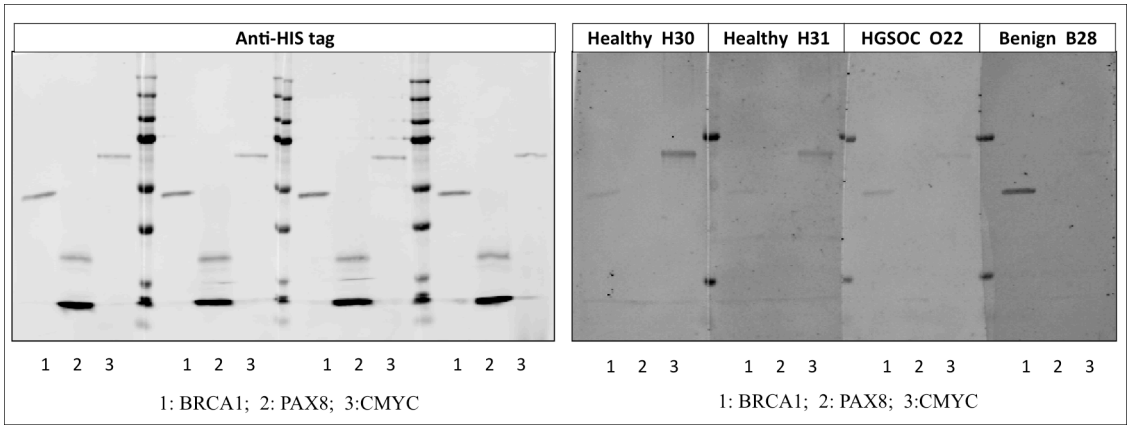

Figure 4.8: Western Blot Images, n=164, Validation I, Additional Tumor-Associated Antigens. BRCA1, PAX8, and CMYC proteins with anti-HIS tag antibody shown on left panel. Healthy, HGSOC, and Benign patient samples with anti-Human IgG antibody shown on right panel. Reactivity of BRCA1 and CMYC is observed in Healthy and Benign samples.

Figure 4.9

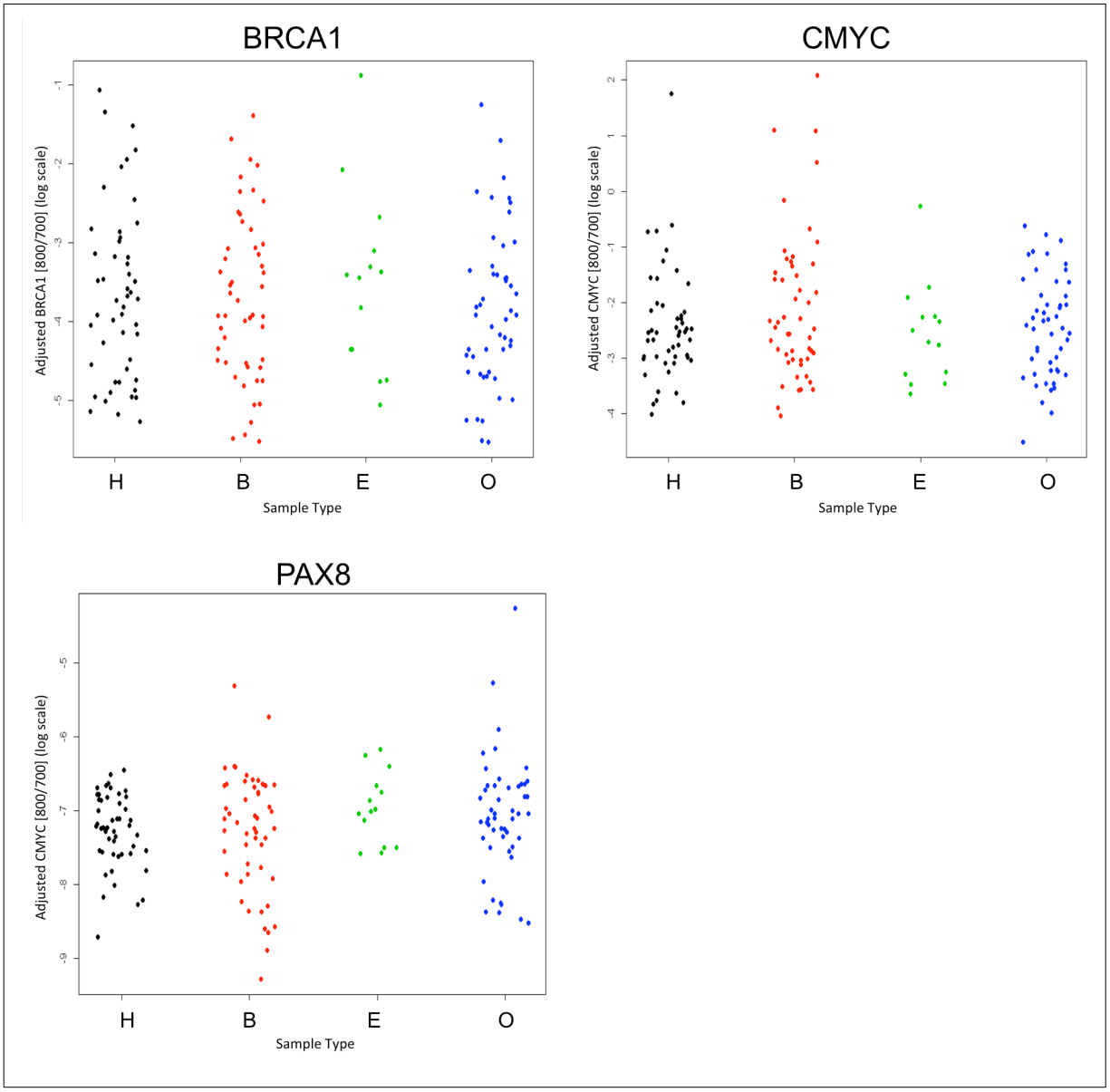

Figure 4.9: Western Blot Individual Antigen Reactivity, n=164, Validation I, Additional Tumor-Associated Antigens. H=Healthy, B=Benign, E=Early Stage HGSOC, O=Late Stage HGSOC. BRCA1 and CMYC react with all sample types.

Figure 4.10

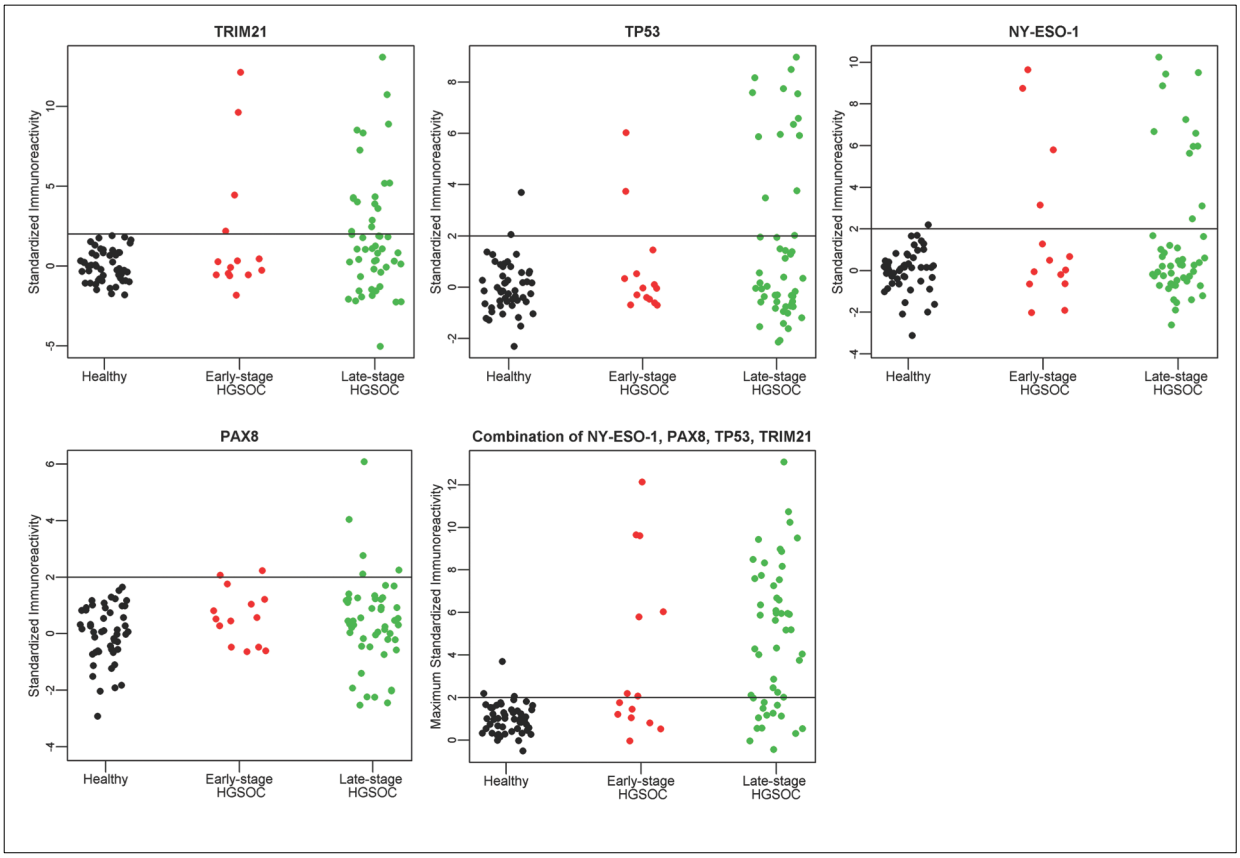

Figure 4.10: Western Blot Individual Antigen Reactivity, 4 Antigens, Validation I, n=164.

A-D) Individual antigen plots for 4 antigens, TRIM21, NY-ESO-1, TP53, and PAX8 in Validation I. E) Maximum value of TRIM21, NY-ESO-1, TP53, or PAX8 in Validation I. The immunoreactivity as defined by the ratio of 800/700 is standardized for each antigen to provide the threshold of Mean + 2(StdDev) for healthy controls, as indicated by the horizontal line at Y=2.

Figure 4.11

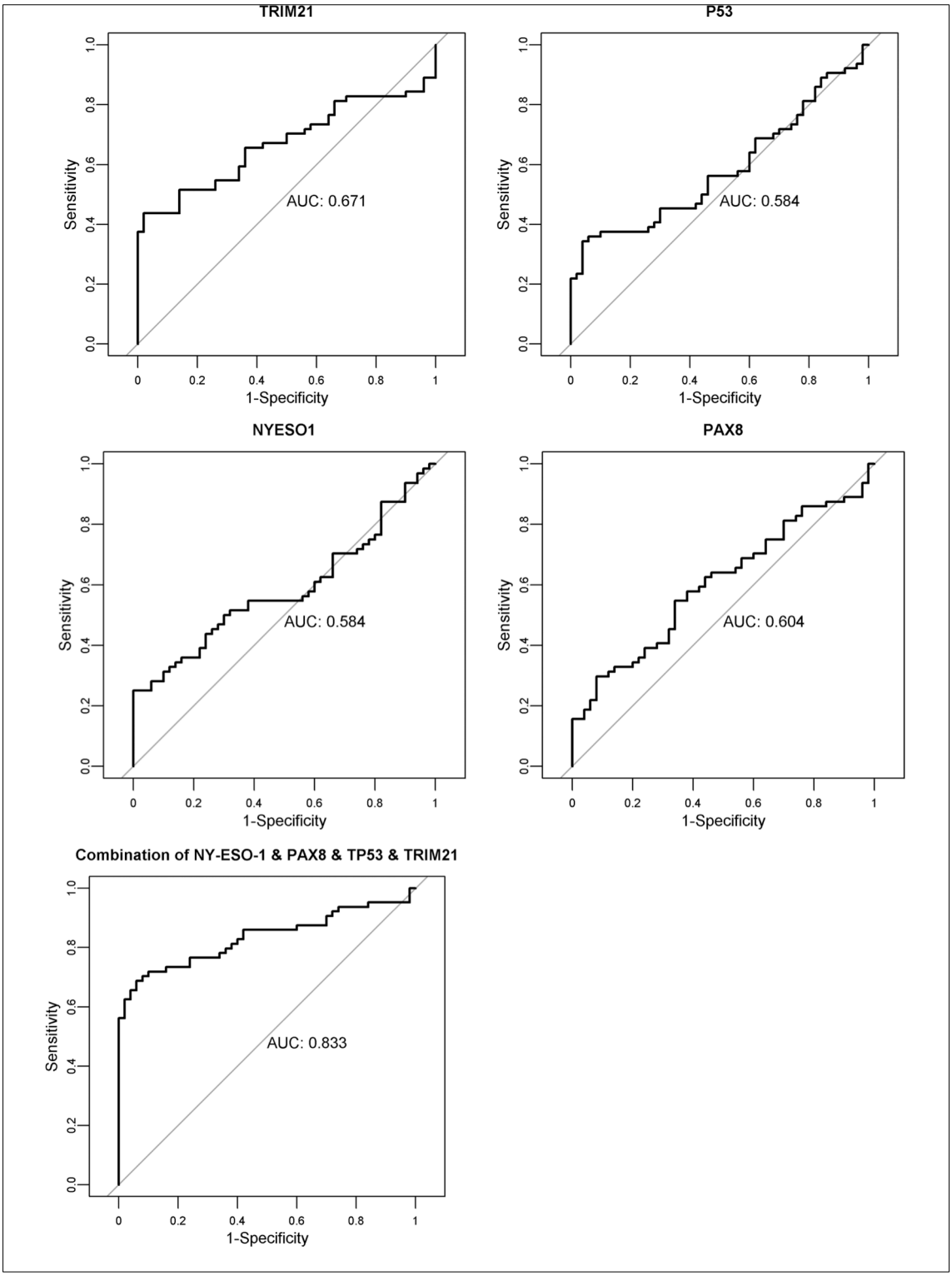

Figure 4.11: ROC Curve Analysis, Validation I, n=164.
ROC curve analysis for the combination of the 4 markers: TRIM21, NY-ESO-1, TP53, and PAX8 in Validation I

4.4.2. TRIM21, HARS, NY-ESO-1, PAX8, and TP53 detected in early stage HGSOC samples.

The Validation I sample set included 14 early stage samples. Individually, NY-ESO-1 and HARS detected 4 early-stage HGSOC samples (29%), TRIM21 detected 3 early-stage HGSOC samples (21%), and TP53 and PAX8 each detected 2 early-stage HGSOC samples (14%). The combination of the 5 markers yielded 50% sensitivity for detecting early stage HGSOC with 94% specificity to discriminate healthy controls. Sensitivities and specificities within each sample group are shown in **Table 4.5**. The combination of markers PAX8, HARS, NY-ESO-1, TP53 and TRIM21 detected 7/14 early-stage HGSOC samples. Among these five antigens, all 7/7 of the positive early stage HGSOC samples were reactive with 2 or more antigens, compared with 12/37 positive late stage HGSOC samples reacting with 2 or more antigens.

Table 4.5 Sensitivity/Specificity for TRIM21, NY-ESO-1, TP53, and PAX8, Validation I.

Positive Threshold=2	Late Stage HGSOC (n=50)	Early Stage HGSOC (n=14)	Late and Early Stage HGSOC (n=64)	Benign (n=50)	Healthy (n=50)	Benign and Healthy (n=100)
Antigen	**Sensitivity**	**Sensitivity**	**Sensitivity**	**Specificity**	**Specificity**	**Specificity**
TRIM21	0.34	0.29	0.33	0.90	1.00	0.95
TP53	0.28	0.14	0.25	0.98	0.96	0.97
NYESO1	0.24	0.29	0.25	0.98	0.98	0.98
PAX8	0.10	0.14	0.11	0.96	1.00	0.98
TRIM21, TP53, NYESO1	0.64	0.43	0.59	0.86	0.94	0.90
TRIM21, TP53, NYESO1, PAX8	0.72	0.50	0.67	0.82	0.94	0.88

Positive Threshold=3	Late Stage HGSOC (n=50)	Early Stage HGSOC (n=14)	Late and Early Stage HGSOC (n=64)	Benign (n=50)	Healthy (n=50)	Benign and Healthy (n=100)
Antigen	**Sensitivity**	**Sensitivity**	**Sensitivity**	**Specificity**	**Specificity**	**Specificity**
TRIM21	0.28	0.21	0.27	0.92	1.00	0.96
TP53	0.26	0.14	0.23	1.00	0.98	0.99
NYESO1	0.22	0.29	0.23	1.00	1.00	1
PAX8	0.04	0.00	0.03	0.96	1.00	0.98
TRIM21, TP53, NYESO1	0.58	0.36	0.53	0.94	0.98	0.96
TRIM21, TP53, NYESO1, PAX8	0.62	0.36	0.56	0.88	0.98	0.93

Table 4.5: Sensitivity and specificity for TRIM21, NY-ESO-1, TP53, and PAX8 evaluated on western blot with n=164 sample set. Threshold (2)=Mean + 2(StdDev) for healthy controls, threshold (3)=Mean + 3(StdDev) for healthy controls.

5. CHAPTER 5: Validation II: Study of 4 Antigens on western blot

A separate serum set consisting of 50 healthy, 50 benign ovarian cyst, and 50 high-grade serous ovarian cancer samples was used for an independent validation of the 4 markers: TRIM21, NY-ESO-1, TP53, and PAX8. This sample set will be referred to as Validation II.

5.1.1. Patient population, n=150

The patient population is described in **Table 5.1.**

5.1.2. Antigens

Antigens were selected based on performance in Validation I for detection of HGSOC autoantibodies. The four markers TRIM21, NY-ESO-1, TP53, and PAX8 achieved the greatest AUC relative to healthy control samples in Validation I.

5.2. Results

5.2.1. Individual Antigen Results

Patient samples were evaluated with the panel of 4 markers: TRIM21, NY-ESO-1, TP53, and PAX8 on western blot (**Figure 5.1).** In this sample set, PAX8 did not complement the 3 markers TRIM21, NY-ESO-1, and TP53. Standardized patient reactivity for each antigen is shown in **Figure 5.2**. This validation screening of the 3 markers TRIM21, NY-ESO-1, and TP53 maintained a specificity of 98% with a sensitivity of 46% as described in **Table 5.2.**

5.2.2. Comparison to Validation I Study

The sensitivity of the combination of the 4 markers: TRIM21, NY-ESO-1, TP53, and PAX8 for all HGSOC cases was lower in the second validation study, 50% vs. 67% with positive threshold=2, and 46% vs. 56% with positive threshold=3. This difference is

Table 5.1: Serum sample patient population (n=150), analyzed on western blot, Validation II.

Validation Set II		
Patient Description	**Number of Samples**	**Age range (Avg)(Median)**
Late Stage HGSOC at time of diagnosis, pre-treatment	45	37-87 (63.6) (64)
Early Stage HGSOC at time of diagnosis, pre-treatment	5	43-66 (51.6) (47)
Benign gynecological condition (ovarian cyst)	50	25-88* (56.5) (55)
Healthy volunteers from community outreach	50	30-82 (55.4) (54)

Table 5.1: Patient population, n=150. Serum samples analyzed on western blot. *Indicates age not available for 5 cases.

Figure 5.1

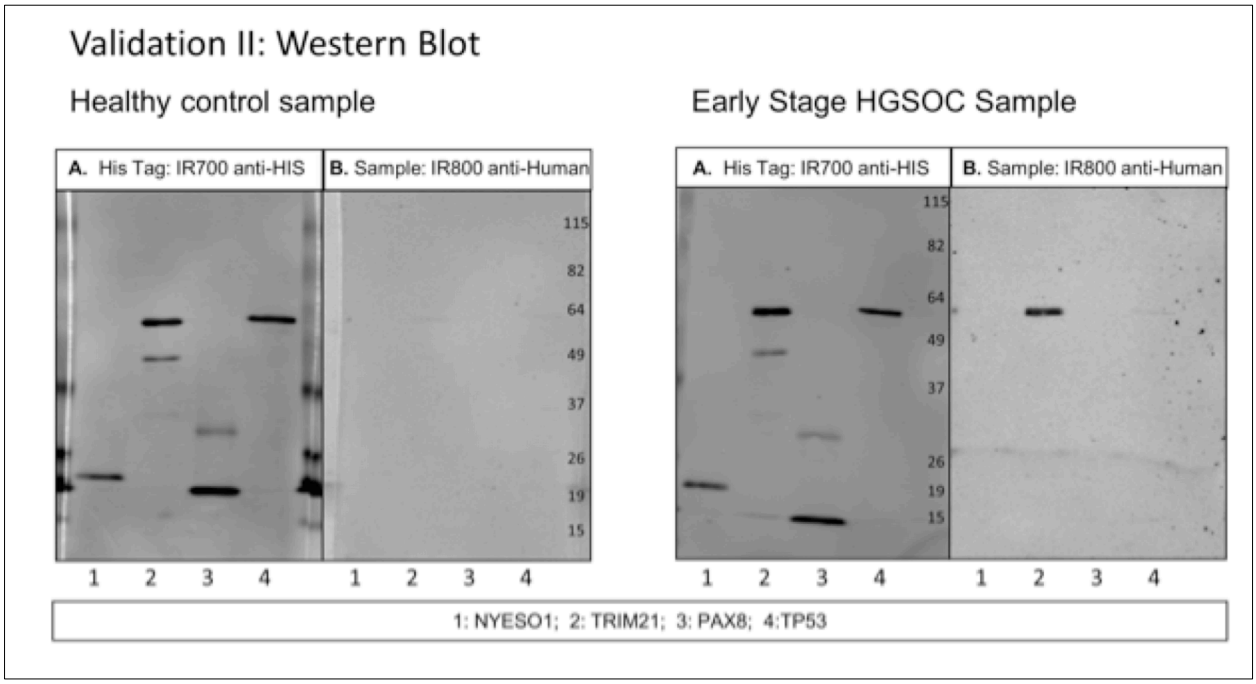

Figure 5.1: Western Blot Images, Validation II, n=150.
Western blot of healthy control serum and early stage HGSOC serum diluted at 1:300 with 4 antigens in Validation II study. A) Secondary antibody anti-HIS tag IgG loading control. B) Secondary antibody anti-human IgG. Scans quantified on Odyssey software; background-corrected integrated intensity of anti-human IgG antibody (IRDye800) normalized as ratio to anti-His tag antibody (IRDye700) per antigen.

Figure 5.2

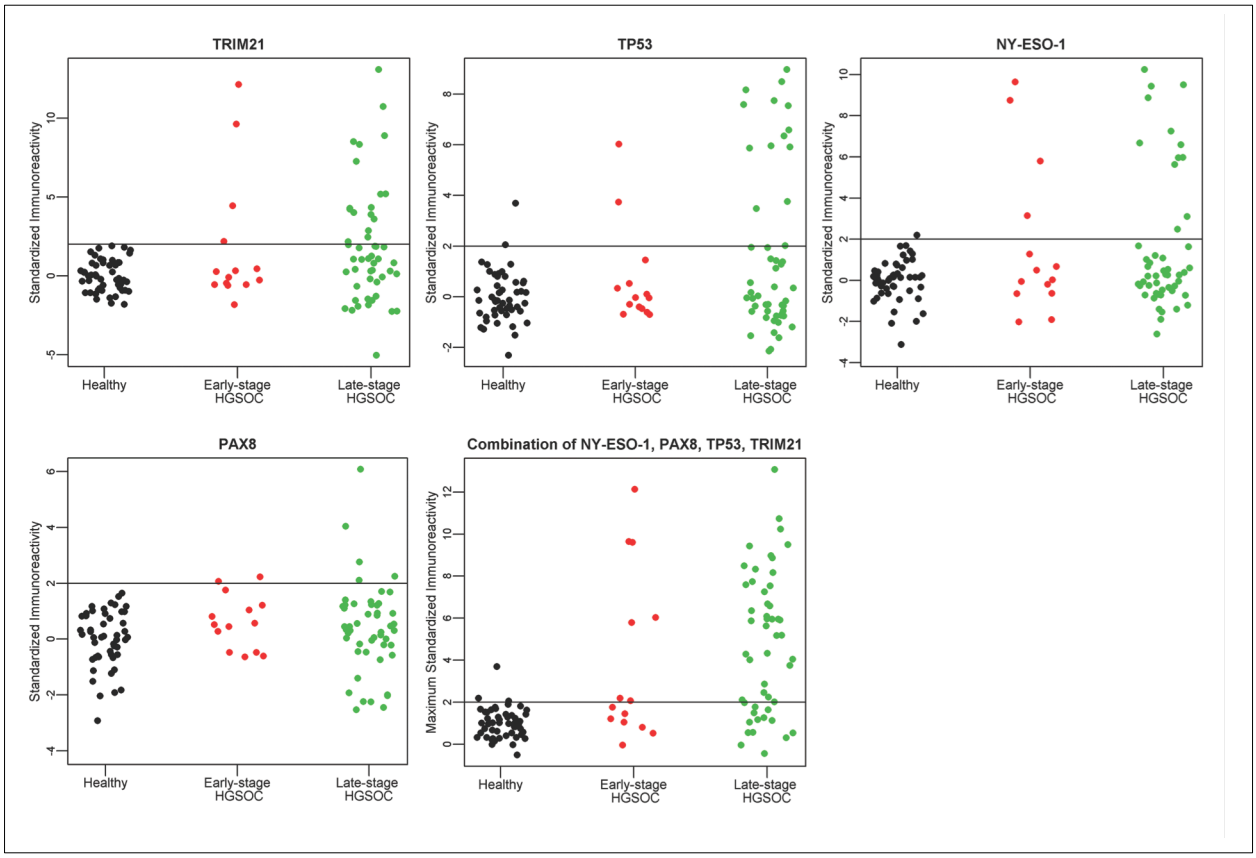

Figure 5.2: Western Blot Individual Antigen Reactivity, 4 Antigens, Validation II, n=150.

A-D) Individual antigen plots for 4 antigens, TRIM21, NY-ESO-1, TP53, and PAX8 in Validation II. E) Maximum value of TRIM21, NY-ESO-1, TP53, or PAX8 in Validation II. The immunoreactivity as defined by the ratio of 800/700 is standardized for each antigen to provide the threshold of Mean + 2(StdDev) for healthy controls, as indicated by the horizontal line at Y=2.

Table 5.2: Sensitivity/Specificity for TRIM21, NY-ESO-1, TP53, and PAX8, Validation II.

Positive Threshold=2	Late Stage HGSOC (n=45)	Early Stage HGSOC (n=5)	Late and Early Stage HGSOC (n=50)	Benign (n=50)	Healthy (n=50)	Benign and Healthy (n=100)
Antigen	**Sensitivity**	**Sensitivity**	**Sensitivity**	**Specificity**	**Specificity**	**Specificity**
TRIM21	0.38	0.20	0.36	0.90	0.96	0.93
TP53	0.16	0.00	0.14	0.96	0.96	0.96
NYESO1	0.20	0.00	0.18	0.94	1.00	0.97
PAX8	0.09	0.00	0.08	0.98	0.96	0.97
TRIM21, TP53, NYESO1	0.51	0.20	0.48	0.80	0.92	0.86
TRIM21, TP53, NYESO1, PAX8	0.53	0.20	0.50	0.80	0.88	0.84

Positive Threshold=3	Late Stage HGSOC (n=45)	Early Stage HGSOC (n=5)	Late and Early Stage HGSOC (n=50)	Benign (n=50)	Healthy (n=50)	Benign and Healthy (n=100)
Antigen	**Sensitivity**	**Sensitivity**	**Sensitivity**	**Specificity**	**Specificity**	**Specificity**
TRIM21	0.24	0.20	0.24	0.98	1.00	0.99
TP53	0.16	0.00	0.14	1.00	0.98	0.99
NYESO1	0.20	0.00	0.18	0.98	1.00	0.99
PAX8	0.04	0.00	0.04	0.98	1.00	0.99
TRIM21, TP53, NYESO1	0.49	0.20	0.46	0.96	0.98	0.97
TRIM21, TP53, NYESO1, PAX8	0.49	0.20	0.46	0.94	0.98	0.96

Table 5.2: Sensitivity and specificity for TRIM21, NY-ESO-1, TP53, PAX8, evaluated on western blot with n=150 sample set. Threshold (2)=Mean + 2(StdDev) for healthy controls, threshold (3)=Mean + 3(StdDev) for healthy controls.

not statistically significant at the 0.05 level (p-value=0.096 and p-value=0.369, respectively, using a 2X2 chi-square contingency table with Yates correction). Receiver Operating Characteristic (ROC) analysis resulted in area under the curve (AUC) of 0.832 for Validation I and 0.701 for Validation II (**Figure 5.3**). For both sample sets, TRIM21 individually provided the highest AUC: 0.671 in Validation I and 0.618 in Validation II.

5.2.3. Reactivity in Early Stage HGSOC Samples

Although the HARS antigen was not evaluated on this entire n=150 sample set, the 5 early stage HGSOC samples were processed with the HARS protein resulting in 1/5 positive samples. TRIM21 was the only other antigen positive in the 5 early stage HGSOC samples; combining TRIM21 and HARS resulted in 2/5 early stage HGSOC samples positive in this set.

5.2.4. Low Grade Serous Ovarian Cancer Samples

As low-grade serous ovarian cancer (LGSOC) can develop step-wise from ovarian serous cystadenoma, it is a possibility that autoantibody positivity in the benign cyst samples may indicate preneoplastic lesions [181, 187]. We evaluated 22 samples from patients with early stage LGSOC with the antigens TRIM21, NY-ESO-1, TP53, PAX8, and HARS. 1/22 early stage LGSOC samples were positive for TP53 autoantibodies and 1/22 samples were positive for TRIM21 autoantibodies. LGSOC has a distinct protein expression and mutational profile from HGSOC however, and our markers were selected with HGSOC samples.

Figure 5.3

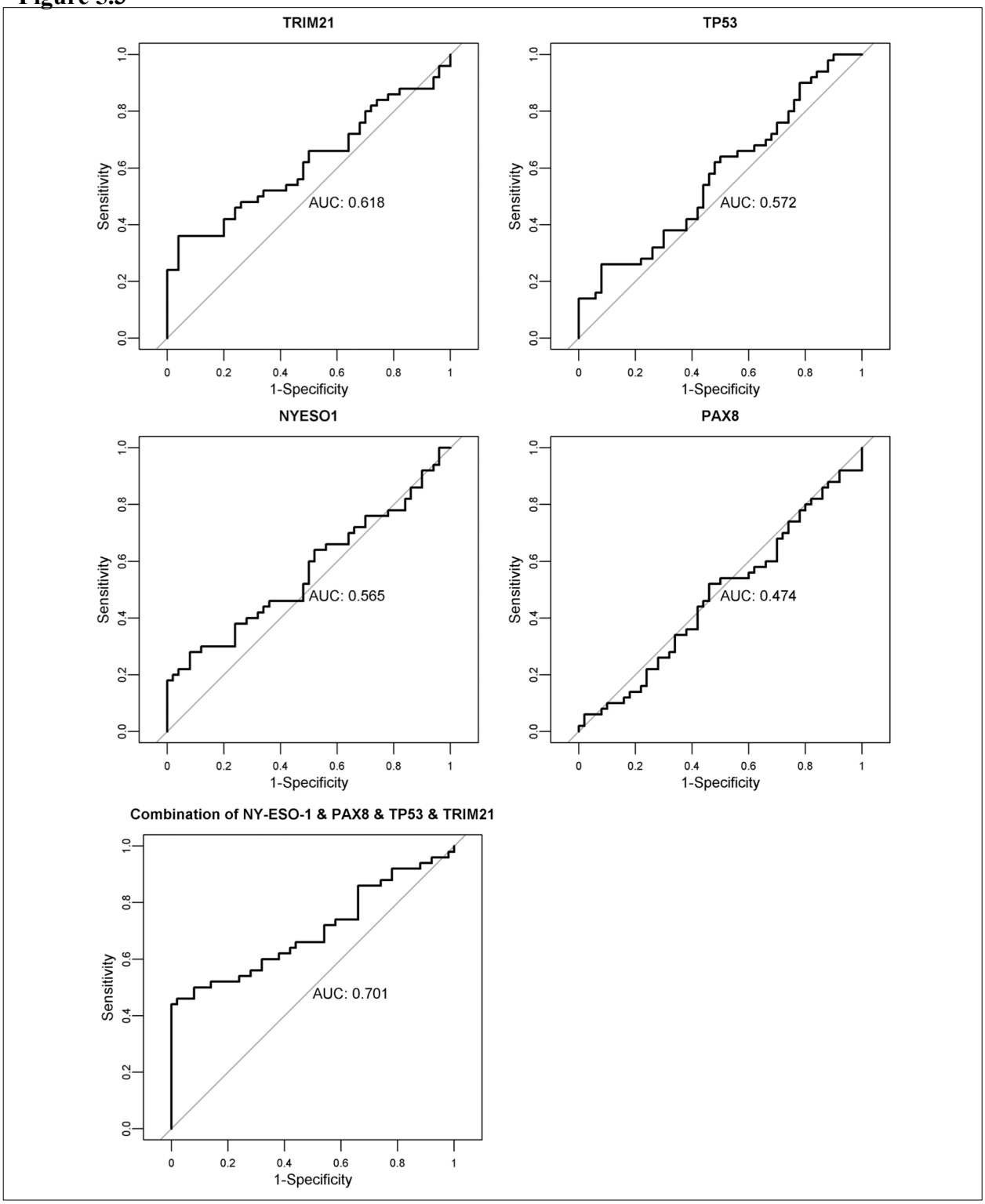

Figure 5.3: ROC Curve Analysis, Validation II, n=150.
ROC curve analysis for the combination of the 4 markers: TRIM21, NY-ESO-1, TP53, and PAX8 in Validation II

5.2.5. Stage Distributions Validation I and Validation II

Stage distributions for the two samples populations are shown in. **Table 5.3**. Although Validation I set had a higher number of stage 4 cases than the Validation set, within Validation I, Stage 3 sensitivity is 72% compared with sensitivity among stage 4 cases of 71%.

Table 5.3: Antigen Reactivity by Tumor Stage for HGSOC samples.

Validation I, n=64

Stage	Stage 1A	Stage 1B	Stage 1C	Stage 3A	Stage 3B	Stage 3C	Stage 3 NOS	Stage 4A	Stage 4B	Stage 4 NOS
# Positive	3	1	3	1	2	22	1	3	3	4
Total samples	4	1	9	1	3	31	1	3	5	6
%	0.75	1.00	0.33	1.00	0.67	0.71	1.00	1.00	0.60	0.67

	TOTAL				
Stage	Stage 1	Stage 3	Stage 4	Stage 3 or 4	All Stages
# Positive	7	26	10	36	43
Total samples	14	36	14	50	64
%	0.50	0.72	0.71	0.72	0.67

Validation II, n=50

Stage	Stage 1A	Stage 1C	Stage 3B	Stage 3C	Stage 3 NOS	Stage 4 NOS	Late stage NOS
# Positive	0	1	0	22	0	1	1
Total samples	3	2	1	36	2	4	2
%	0.00	0.50	0.00	0.61	0.00	0.25	0.50

	TOTAL					
Stage	Stage 1	Stage 3	Stage 4	Late stage NOS	Stage 3 or 4	All Stages
# Positive	1	22	1	1	24	25
Total samples	5	39	4	2	45	50
%	0.20	0.56	0.25	0.50	0.53	0.50

NOS=Not otherwise specified

Table 5.3: Antigen Reactivity by Tumor Stage for HGSOC samples.

6. CHAPTER 6: TRIM21 AUTOANTIBODIES IN HGSOC

6.1. Summary of TRIM21 Reactivity with HGSOC Sera

TRIM21 consistently showed superior reactivity in multiple patient sample populations, including on line blots in section 1.1, on western blot and ELISA with a set of n=36 samples in section 3.2, and on western blot in Validation I in section 5.2 and in Validation II in section 6.2. TRIM21 was identified as a novel biomarker for ovarian cancer, with the highest individual sensitivity of 33% for all HGSOC samples at 100% specificity compared to healthy controls in Validation I, and 36% sensitivity at 96% specificity in Validation II.

6.2. TRIM21 Function as Intracellular Pathogen Sensor and Potent Fc Receptor

TRIM21 consists of 4 domains: a RING domain involved in ubiquitination, B-box domain, coiled-coiled domain, and a c-terminal PRY-SPRY domain which is an immunoglobulin Fc receptor [94]. TRIM21 is the most potent mammalian Fc receptor. The PRY-SPRY domain alone binds with ~200 nM affinity, but when it binds as a dimer to the immunoglobulin heavy chain, the affinity is sub-nanomolar, at approximately 0.6 nM [94]. There are 68 members in the TRIM protein family, however only TRIM21 has Fc binding ability [22]. This Fc binding function allows TRIM21 to neutralize antibody-bound virus or bacteria. Binding of TRIM21 to an antibody-bound pathogen initiates innate immune signaling as a multi-step process. It neutralizes the virus by targeting for degradation and detection by RIG1 or cGAS, and activates NFKB and TLR signaling [49].

The recent discovery that TRIM21 participates in neutralization of intracellular antibody-bound virus or bacteria has prompted studies to take advantage of this activity

for therapeutics. One group has demonstrated the ability of TRIM21 to disrupt tau aggregation using anti-tau antibodies, with potential for therapeutics for neurodegenerative diseases with protein aggregates [120]. Another technology has been proposed for degradation of endogenous proteins has been engineered around TRIM21 neutralization and is named the Trim-Away approach, which targets any protein by introduction of the target-specific antibody and over-expression of TRIM21 [120].

Autoantibodies are targeted to the Fc-binding domain [22]. It has been proposed that autoantibodies can be generated against TRIM21 when it is in complex with antibody-bound pathogens. Burbelo et al. have generated mutant TRIM21 proteins that are deficient in Fc-binding function, and demonstrated specific autoantibody binding to these mutants [22]. Additionally, TRIM21 positive serum was blocked with TRIM21 and other TRIM protein family members to demonstrate specific binding. The Fc binding function of TRIM21 is conformation dependent; our studies utilized denatured protein. Studies with native TRIM21 demonstrated a low level of background signal present in all sample types, yet still observed specific TRIM21 autoantibodies in positive control sera with reactivity that was significantly elevated compared with controls [22]. We have demonstrated specific antibody binding by blocking a TRIM21 autoantibody positive control serum sample (The Binding Site, San Diego, CA) with TRIM21 antigen, shown in **Figure 6.1**.

6.3. Screening for TRIM21 Autoantibodies in Samples from Patients with Pelvic Inflammatory Disease and other Benign Gynecologic Conditions.

To determine if TRIM21 autoantibodies can be detected in the setting of pelvic infection and inflammation, we evaluated 12 serum samples from patients that had self-

Figure 6.1

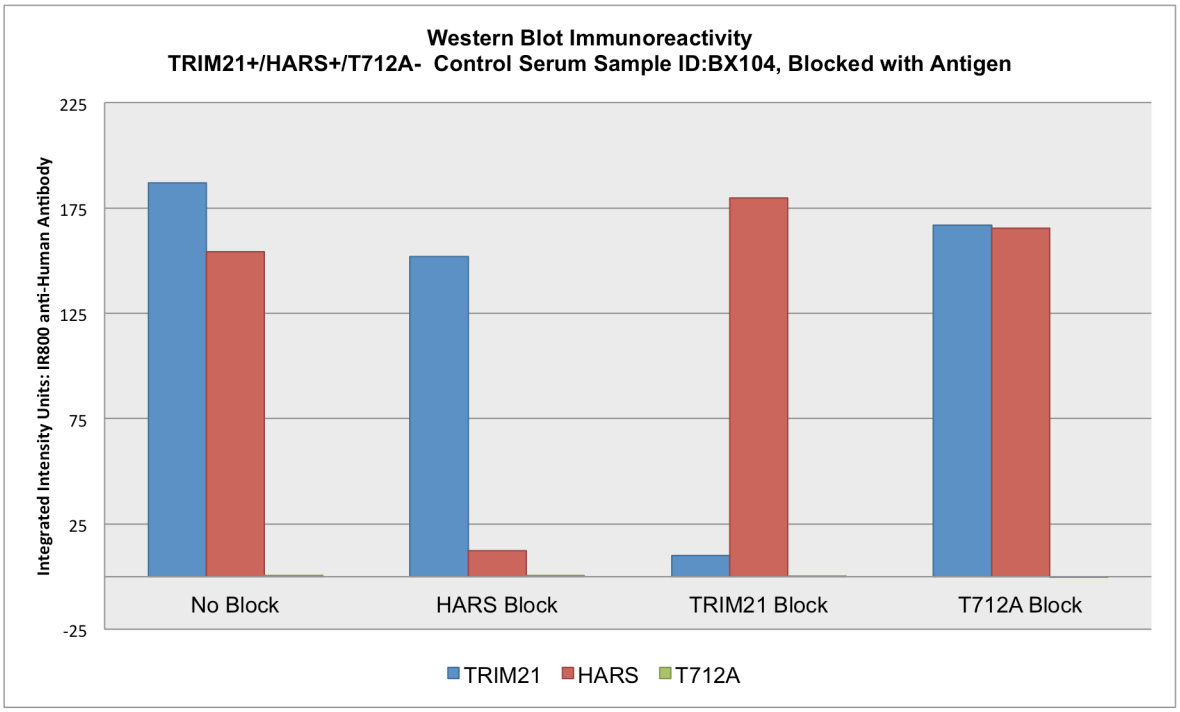

Figure 6.1: Western Blot Evaluating TRIM21 Autoantibody Binding Specificity
Positive control patient serum, sample ID:BX104 (The Binding Site, San Diego, CA) was pre-incubated with purified antigen prior to incubation on western blot. Without pre-incubation with antigen, BX104 reacts with HARS and TRIM21, and does not react with T712A on western blot. Pre-incubation of BX104 with HARS specifically reduces reactivity with HARS, pre-incubation of BX104 with TRIM21 specifically reduces reactivity with TRIM21, and pre-incubation of BX-104 with T712A has no effect on HARS or TRIM21 on western blot.

reported pelvic inflammatory disease (PID). Patients with PID have bacterial or viral infection of the pelvis. None of the 12 samples displayed reactivity with TRIM21 on western blot (**Figure 6.2**). TRIM21 was detected in 5/50 benign ovarian cyst samples in Validation I and 5/50 ovarian cyst samples in Validation II.

6.4. TRIM21 Reactivity in Ovarian Cancer Serum Samples

In a study of HGSOC serum samples that utilized high-density programmable protein microarrays containing 10,247 antigens, TRIM21 was identified as one of the top 39 candidate tumor antigens, which passed three rounds of serum screening in independent sample sets [92]. From the top 39 candidate antigens, the authors selected a final panel of 11 antigens, which did not include TRIM21. Performance of TRIM21 relative to the top 39 antigens is shown in **Table 6.1**. TRIM21 has equal or greater performance than several antigens included in the final panel of 11 antigens. These studies were performed on a rapid ELISA platform, and in our experiments TRIM21 was undetectable o ELISA in 10 HGSOC serum samples that reacted with TRIM21 on western blot.

6.5. TRIM21 Autoantibodies in Other Cancer Types

TRIM21 has previously been reported as a biomarker for esophageal squamous cell carcinoma (ESCC) and basal-like breast cancer [100, 185]. To identify autoantibody biomarkers for ESCC, a SEREX library created with cDNA from an ESCC cell line and screened with ESCC sera. TRIM21 was identified from the SEREX screening and reactivity with patient serum was confirmed on ELISA and western blot [100]. TRIM21 autoantibodies were also detected in colon, gastric, and breast cancer serum samples [100]. In a protein array screen of 10,000 human proteins, TRIM21 was

selected in a set of 71 candidate autoantibody biomarkers for basal like breast cancer [185]. After 3 rounds of ELISA screening with basal like breast cancer sera, TRIM21 was identified as a top marker in a set of 13 markers [185].

Figure 6.2

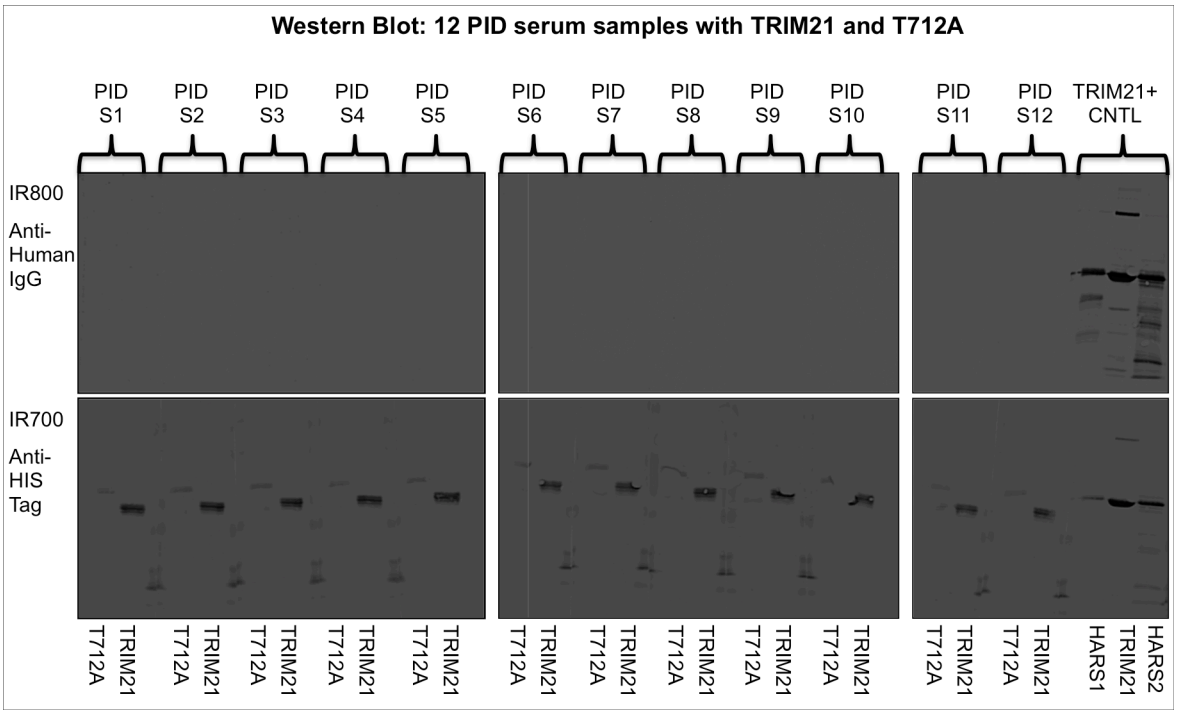

Figure 6.2: Western Blot: 12 PID Serum samples with TRIM21 and T712A. Positive control BX sera (The Binding Site, LLC), positive for TRIM21 and HARS is shown in the last column, with two HARS antigens, HARS1 (Novus Biologicals) and HARS2 (purified in lab), as well as the TRIM21 antigen which was included on PID samples 1-12. Negative control antigen T712A was included on each membrane incubated with patient serum. Serum samples diluted 1:300 in 5% milk.

Table 6.1 TRIM21 Reactivity on Rapid ELISA

A. Healthy Threshold (Mean + 2 Std. Dev) per Antigen

Antigens	Cancer (n=29)	Benign (n=30)	Healthy (n=28)
NUDT11	8	1	1
STYXL1	7	2	0
PVR (B)	6	2	0
CA4	5	2	0
POMC	5	4	1
UHMK1	4	4	0
TRIM21	3	3	0
NY-ESO-1	3	4	1
TP53	2	1	1
NXF3	2	4	0
ICAM3	1	0	1
TRIM39	1	0	1
SAP18	3	2	1
TNFRSF11B	3	2	0
AKT1	3	3	1
BRD3	3	1	2
PRMT5	2	2	0
MLH1	2	0	1
TUBB	1	3	1
KCNH2	1	0	2
CHRM4	1	1	2
LRRFIP1	1	1	1
WSB1	1	2	2
ELOVL2	1	0	2
AARS	1	2	1
MIB2	1	0	2
KSR1	0	0	1

B. Benign Threshold (Mean + 2 Std. Dev) per Antigen

Antigens	Cancer (n=29)	Benign (n=30)	Healthy (n=28)
NUDT11	8	1	2
TRIM39	7	1	4
STYXL1	4	2	0
PVR (B)	4	1	0
KSR1	4	3	3
CA4	3	2	0
NY-ESO-1	3	2	0
TRIM21	2	1	0
P53	2	1	0
POMC	2	1	0
ICAM3	1	0	1
UHMK1	1	2	0
NXF3	1	2	0
TNFRSF11B	2	1	0
KCNH2	1	2	2
CHRM4	1	1	3
MAP3K7	1	1	1
PVR-A	1	1	2
TIMP3	1	1	2
SAP18	1	2	0
PRMT5	1	2	0
NDUFA3	1	1	2
AKT1	1	1	1
MIB2	4	1	5
BRD3	3	1	3
NPTX2	3	3	3
MLH1	3	2	4

Table 6.1: Analysis of Supplemental Data from: *Katchman BA, Chowell D, Wallstrom G, et al. Autoantibody biomarkers for the detection of serous ovarian cancer. Gynecol Oncol. 2017;146(1):129–136.* Thresholds calculated using values from A) healthy controls and B) benign samples. Of the top 39 antigens selected from original 10,247 antigens, shown are those Positive count indicates sample value > threshold. Antigens highlighted in yellow indicated final panel of 11 antigens selected by authors. TRIM21 highlighted in turquoise, shows equal or greater performance to the 11 antigens highlighted in yellow.

7. CHAPTER 7: Discussion

7.1. Ovarian Cancer Early Detection Biomarker Performance

Early detection of ovarian cancer has the potential to improve patient outcome, as late stage disease is associated with widespread metastasis, complication of surgery, and drastically reduced prognosis. Screening for ovarian cancer is currently not recommended for the general population, and there are no approved tests or markers for early diagnosis. One method which has been evaluated in clinical trials is ROCA, which consists of a two-step test that involves measurement of circulating antigen CA125 at an increased level relative to each patient's baseline interpreted with patient age, followed by imaging such as TVUS. Having a sequential test process of orthogonal measurements reduces the rate of false-positives. However, the initial step of CA125 detection in this two-step process misses approximately 20% of all cases as 20% of all ovarian cancers do not shed CA125 [166]. Moreover, 40-50% of early stage cases with low-volume disease do not shed CA125 at levels high enough to be detected [194]. Autoantibodies to tumor antigens, produced at small tumor volumes, can be combined with serum screening of CA125 to improve sensitivity in early detection. TP53 autoantibodies have been detected in 16% of cases that were not detectable with CA125 in preclinical samples [194]. We have found that NY-ESO-1 and TRIM21 autoantibodies are present in a higher percentage of early stage samples than autoantibodies to TP53.

7.1.1. PPV Calculations

The positive and negative predictive values were estimated using a range of OVCA prevalence representing 10 to 20-fold increases relative to the general

population level risk (1/2500). We combined values from Validation I and Validation II for analysis of n=214 HGSOC cases and n=100 healthy cases for the three markers TRIM21, TP53, and NY-ESO-1, resulting in a sensitivity of 52% with a specificity of 98%. For a 10-fold increase in prevalence of OVCA (0.4%) relative to population prevalence, using a sensitivity of 52% and a specificity of 98%, we estimated the PPV and NPV. PPV at 10, 15, or 20-fold increased prevalence was 9.4%, 13.5%, and 17.2%, respectively, with NPV 99.8%, 99.6%, and 99.7%. Additionally, in practice, these biomarkers would be combined with CA125 values presumably resulting in increased sensitivity, followed by TVUS, which would result in increased specificity. These results indicate that the panel could be useful for screening in a high-risk population, including BRCA1/2 mutation carriers and women with a family history of OVCA.

7.1.2. High-risk population

In three recent studies within the population of women with an increased risk of ovarian cancer that evaluated CA125 using the ROCA method at intervals of 3 or 4 months, an increase in detection sensitivity for early stage tumors was observed [147, 166]. The goal of identifying autoantibody biomarkers is both to complement CA125, and to provide lead-time to CA125 detection. The serum set used in this study had limited samples with data for CA125 values. Autoantibodies to TP53 have been shown by Yang et al. to be elevated in pre-diagnostic patient samples up to 11 months before detection of CA125, and in samples taken 23 months before diagnosis of ovarian cancer for cases that were not detected by CA125 [194]. In our cohort anti-TP53 antibodies were present in 2/19 early stage samples. The markers TRIM21, HARS, NY-

ESO-1, and PAX8, detected 9/19 additional early stage samples. Addition of these markers to TP53 improves sensitivity, and may improve lead-time, thus addressing the ultimate goal of a diagnosis at an earlier stage. Determining whether TRIM21, HARS, NY-ESO-1, and PAX8 autoantibodies are also detectable in addition to TP53 in pre-diagnostic sera will be a critical step in evaluating these biomarkers for clinical use. Early detection of HGSOC has potential to provide a mortality reduction [86].

7.2. Autoantibodies as predictors of neurologic irAEs

In addition to early detection, this work also describes the frequency of paraneoplastic antibodies in HGSOC patients without a neurological syndrome. In lung cancer, the frequency of the anti-Hu antibody has been reported to be 16-25% in patients without a syndrome [93]. Assessing the frequency of autoantibodies in cancers associated with paraneoplastic syndromes can contribute to understanding the etiology of paraneoplastic syndromes.

With increasing success of immunotherapy for cancer treatment, determining if patients can be stratified into those likely develop a paraneoplastic syndrome as a result of immunotherapy will be critical for optimal patient care. Baseline levels of autoantibodies have been assessed for their utility to predict risk of neurologic irAEs with immune-checkpoint therapy [10]. As described in section 1.2.3., immunotherapy strategies are being developed for ovarian cancer including CAR-T cell, vaccines, CTLA-4 and PD-1-inhibiton in combination with Parp-inhibition. Although markers such as CDR2 and CDR2L did not provide early detection diagnostic ability, they may serve as markers to identify patients undergoing anti-CTLA4 checkpoint blockade therapy who

may be at risk of developing neurologic irAEs, particularly paraneoplastic cerebellar degeneration.

7.3. Conformational Considerations

The antigens used in this study were purified form E. coli and were denatured with both urea and heat. These methods limit the ability to detect antibodies against conformation-dependent epitopes. Production of protein in E. coli results in lack of posttranslational modifications and proper folding as observed in human cells [88]. Additionally, treatment with heat and urea results in unfolded protein. Follow up studies to determine if native protein will detect additional cases are warranted. Antibody-antigen binding is also limited due to solid surface immobilization of our antigen, which can restrict epitope availability [13]. Due to variability in performance between antibody detection platforms, confirmation of positive results on a separate platform may be necessary [172].

Additionally, autoantibodies can be in complex with antigen has been described for ovarian cancer biomarkers HE-4 and CA125 [40, 195]. In the case of CA125, presence of CA125 immune complexes were associated with decreased antigen concentration, presumably due to assay interference [40]. Whether antigen-autoantibody complexes hamper autoantibody detection can be assessed with pre-treatment of samples to dissociate complexes.

7.4. Sources for Novel Autoantigen Discovery

Rather than screening serum against protein libraries, novel methods of antibody discovery aim at directly sequencing the autoantibody content from serum samples. There are multiple platforms for sequencing of the B-cell antibody receptor, however

results have been shown to not accurately represent circulating IgG [21]. Supplementing with protein-level data is necessary to identify relevant antibodies [34]. One approach involves top-down mass spectrometry analysis of intact immunoglobulins purified from serum. IgG can also be digested and the Fab-fragment which binds antigen is then sequenced, with bottom-up data analysis with alignment of sequences to a reference library. Top-down and bottom-up approaches can be integrated for a more complete analysis of the antibody repertoire in a single sample [48]

Sources of antibody discovery include samples from patients that were sero-negative for existing biomarkers. This approach has been used for discovery of novel paraneoplastic autoantibodies that were common among samples sero-negative for the classical markers [102, 174]. Within our Validation I and Validation II sample sets, the HGSOC samples that did not react with our panel of 4 antigens could be pooled as a discovery sample resource.

The precursor of the majority of high-grade serous ovarian cancers is widely recognized as serous tubal intraepithelial carcinoma. These lesions have been identified in the fallopian tubes of patients who underwent RRSO. Gene expression profiling has identified HGSOC signatures to better correlate with normal fallopian tube than ovarian surface epithelium [50]. Tissue from resected serous tubal intraepithelial carcinoma are excellent sources for biomarker discovery as they represent the earliest phases of tumor progression which have been reported to be present years prior to development of HGSOC.

8. CHAPTER 8: Conclusions and Future Directions

The goal of this dissertation work was to evaluate the serum autoantibody levels to paraneoplastic antigens in HGSOC in order to identify candidate biomarkers for early detection. A panel of autoantibody biomarkers can be useful in complementing current screening methods for the early detection of ovarian cancer in women with an increased genetic risk of ovarian cancer. Our laboratory has previously identified epitopes reactive with ovarian cancer patient serum using phage-display technology. As described in Chapter 3, we identified phage-borne epitopes that were homologous to antigens associated with paraneoplastic neurological syndromes. In Chapter 3, the presence of paraneoplastic antibodies in HGSOC sera was evaluated. We screened a panel of 20 paraneoplastic antigens against patient serum samples and identified candidate antigens reactive with HGSOC sera: TRIM21, HARS, AlaRS, SRP, CDR2, and HuD. We further sub-cloned full-length HIS-tagged protein of these markers as well as 4 epitopes with homology to HARS, TRIM21, SRP, and HuD. These proteins were purified from E. coli using HIS tag and T7 tag, and evaluated on western blot and ELISA. In Chapter 4, we performed a screening of n=164 patient samples against 9 selected antigens on western blot and ELISA: TRIM21, HARS, CDR2, CDR2L, CORTACTIN, NY-ESO-1, TP53, P3F10, and T712A. Autoantibodies against the HARS antigen were more frequently detected in early stage sera than in late stage sera, and autoantibodies against TRIM21 were observed at the highest frequency. An additional 3 tumor-associated antigens were processed with the n=164 sample set: BRCA1, CMYC, and PAX8. We determined that the combination of 4 markers: TRIM21, NY-ESO-1, TP53, and PAX8, provide sensitivity of 67% at 95% specificity. In Chapter 5, we validated this

panel of 4 markers on an independent serum set consisting of n=150 patient serum samples on western blot. In this study, the combination of TRIM-21, NY-ESO-1, TP53, and PAX8 provided a sensitivity of 46% with 98% specificity.

This study is the first to demonstrate accuracy of TRIM21 autoantibodies as a biomarker for HGSOC in a large-scale screening. TRIM21 was previously identified as a relevant tumor-associated antigen in basal-like breast cancer, ESCC, and serous ovarian cancer through proteomics-based discovery. In Validation I and Validation II, autoantibodies to TRIM21 were detected at 33% and 36% sensitivity in all HGSOC cases with 100% and 96% specificity compared to healthy controls. Somatic mutations in TP53 are found in in 96% of HGSOC cases [37]; autoantibodies to TP53 in HGSOC can be detected against the wild type protein as a polyclonal response [91]. NY-ESO-1 is an immunotherapy target for ovarian cancer with numerous trials evaluating vaccines targeting NY-ESO-1 as well as adoptive transfer of NY-ESO-1 specific T-cells [131]. PAX8 is expressed in the majority of HGSOCs [20]. The present study is the first to detect anti-PAX8 autoantibodies.

These studies provide evidence that autoantibodies associated with paraneoplastic syndromes can be identified in the serum of patients diagnosed with cancer who do not present with paraneoplastic symptoms. We found that although a number of paraneoplastic antibodies are present in HGSOC sera, the anti-TRIM21 antibodies provided the best sensitivity and specificity for use in early detection. Combination of TRIM21 with established tumor antigens NY-ESO-1 and TP53 enhanced sensitivity and specificity. Furthermore, we demonstrated that anti-PAX8 autoantibodies are present in the serum of patients with ovarian cancer.

The identified autoantibody biomarkers should be validated with pre-diagnostic serum samples to determine the time prior to diagnosis that the autoantibodies can be detected. Another area for further study is to expand the current panel by identification of autoantibodies in those serum samples that did not react with our set of 4 markers. Additionally, assessment of these markers in companion with CA125 will be performed with the Validation I and Validation II sample sets, which is essential for determination of clinical utility of these markers.

REFERENCES

[1] Y. Akisawa, I. Nishimori, K. Taniuchi, N. Okamoto, T. Takeuchi, H. Sonobe, Y. Ohtsuki and S. Onishi, Expression of carbonic anhydrase-related protein CA-RP VIII in non-small cell lung cancer, *Virchows Arch* **442** (2003), 66-70.

[2] M.L. Albert, J.C. Darnell, A. Bender, L.M. Francisco, N. Bhardwaj and R.B. Darnell, Tumor-specific killer cells in paraneoplastic cerebellar degeneration, *Nat Med* **4** (1998), 1321-4.

[3] Y. Allenbach, J. Keraen, A.M. Bouvier, V. Jooste, N. Champtiaux, B. Hervier, Y. Schoindre, A. Rigolet, L. Gilardin, L. Musset, J.L. Charuel, O. Boyer, F. Jouen, L. Drouot, J. Martinet, T. Stojkovic, B. Eymard, P. Laforet, A. Behin, E. Salort-Campana, O. Fain, A. Meyer, N. Schleinitz, K. Mariampillai, A. Grados and O. Benveniste, High risk of cancer in autoimmune necrotizing myopathies: usefulness of myositis specific antibody, *Brain* **139** (2016), 2131-5.

[4] R. Amampai and P. Suprasert, Cancer Antigen 125 during Pregnancy in Women without Ovarian Tumor Is Not Often Rising, *Obstet Gynecol Int* **2018** (2018), 8141583.

[5] M.R. Andersen, B.A. Goff, K.A. Lowe, N. Scholler, L. Bergan, C.W. Dresher, P. Paley and N. Urban, Combining a symptoms index with CA 125 to improve detection of ovarian cancer, *Cancer* **113** (2008), 484-9.

[6] K.S. Anderson, J. Wong, A. Vitonis, C.P. Crum, P.M. Sluss, J. Labaer and D. Cramer, p53 autoantibodies as potential detection and prognostic biomarkers in serous ovarian cancer, *Cancer Epidemiol Biomarkers Prev* **19** (2010), 859-68.

[7] J.C. Antoine, L. Absi, J. Honnorat, J.M. Boulesteix, T. de Brouker, C. Vial, M. Butler, P. De Camilli and D. Michel, Antiamphiphysin antibodies are associated with various paraneoplastic neurological syndromes and tumors, *Arch Neurol* **56** (1999), 172-7.

[8] J.C. Antoine and J.P. Camdessanche, Peripheral nervous system involvement in patients with cancer, *Lancet Neurol* **6** (2007), 75-86.

[9] D.K. Armstrong, R.D. Alvarez, J.N. Bakkum-Gamez, L. Barroilhet, K. Behbakht, A. Berchuck, J.S. Berek, L.M. Chen, M. Cristea, M. DeRosa, A.C. ElNaggar, D.M. Gershenson, H.J. Gray, A. Hakam, A. Jain, C. Johnston, C.A. Leath, III, J. Liu, H. Mahdi, D. Matei, M. McHale, K. McLean, D.M. O'Malley, R.T. Penson, S. Percac-Lima, E. Ratner, S.W. Remmenga, P. Sabbatini, T.L. Werner, E. Zsiros, J.L. Burns and A.M. Engh, NCCN Guidelines Insights: Ovarian Cancer, Version 1.2019, *J Natl Compr Canc Netw* **17** (2019), 896-909.

[10] E. Arriola, M. Wheater, I. Galea, N. Cross, T. Maishman, D. Hamid, L. Stanton, J. Cave, T. Geldart, C. Mulatero, V. Potter, S. Danson, P.J. Woll, R. Griffiths, L. Nolan and C. Ottensmeier, Outcome and Biomarker Analysis from a Multicenter Phase 2 Study of Ipilimumab in Combination with Carboplatin and Etoposide as First-Line Therapy for Extensive-Stage SCLC, *J Thorac Oncol* (2016).

[11] A. Aspatwar, M.E. Tolvanen, C. Ortutay and S. Parkkila, Carbonic anhydrase related protein VIII and its role in neurodegeneration and cancer, *Curr Pharm Des* **16** (2010), 3264-76.

[12] A. Ayed, F.A. Mulder, G.S. Yi, Y. Lu, L.E. Kay and C.H. Arrowsmith, Latent and active p53 are identical in conformation, *Nat Struct Biol* **8** (2001), 756-60.

[13] S.M. Aziz F., Blackburn J.M., Autoantibody-Based Diagnostic Biomarkers: Technological Approaches to Discovery and Validation, in: *Autoantibodies and Cytokines*, W.A. Khan, ed. eds., IntechOpen, 2018, pp. 159-180.

[14] L. Bataller, F. Graus, A. Saiz and J. Vilchez, Clinical outcome in adult onset idiopathic or paraneoplastic opsoclonus-myoclonus, *Brain* **124** (2001), 437-43.

[15] R. Bei, L. Masuelli, C. Palumbo, M. Modesti and A. Modesti, A common repertoire of autoantibodies is shared by cancer and autoimmune disease patients: Inflammation in their induction and impact on tumor growth, *Cancer Lett* **281** (2009), 8-23.

[16] M. Benvenuto, R. Mattera, L. Masuelli, I. Tresoldi, M.G. Giganti, G.V. Frajese, V. Manzari, A. Modesti and R. Bei, The crossroads between cancer immunity and autoimmunity: antibodies to self antigens, *Front Biosci (Landmark Ed)* **22** (2017), 1289-1329.

[17] M. Berger, D.E. McCallus and C.S. Lin, Rapid and reversible responses to IVIG in autoimmune neuromuscular diseases suggest mechanisms of action involving competition with functionally important autoantibodies, *J Peripher Nerv Syst* **18** (2013), 275-96.

[18] S. Berrih-Aknin, Cortactin: a new target in autoimmune myositis and Myasthenia Gravis, *Autoimmun Rev* **13** (2014), 1001-2.

[19] F. Blaes, Paraneoplastic brain stem encephalitis., *Curr Treat Options Neurol* **2** (2013), 201-9.

[20] D.D. Bowtell, S. Bohm, A.A. Ahmed, P.J. Aspuria, R.C. Bast, Jr., V. Beral, J.S. Berek, M.J. Birrer, S. Blagden, M.A. Bookman, J.D. Brenton, K.B. Chiappinelli, F.C. Martins, G. Coukos, R. Drapkin, R. Edmondson, C. Fotopoulou, H. Gabra, J. Galon, C. Gourley, V. Heong, D.G. Huntsman, M. Iwanicki, B.Y. Karlan, A. Kaye, E. Lengyel, D.A. Levine, K.H. Lu, I.A. McNeish, U. Menon, S.A. Narod, B.H. Nelson, K.P. Nephew, P. Pharoah, D.J. Powell, Jr., P. Ramos, I.L. Romero, C.L. Scott, A.K. Sood, E.A. Stronach and F.R. Balkwill, Rethinking ovarian cancer II: reducing mortality from high-grade serous ovarian cancer, *Nat Rev Cancer* **15** (2015), 668-79.

[21] S.D. Boyd and J.E. Crowe, Jr., Deep sequencing and human antibody repertoire analysis, *Curr Opin Immunol* **40** (2016), 103-9.

[22] P.D. Burbelo, L.Y. Teos, J.L. Herche, M.J. Iadarola and I. Alevizos, Autoantibodies against the Immunoglobulin-Binding Region of Ro52 Link its Autoantigenicity with Pathogen Neutralization, *Sci Rep* **8** (2018), 3345.

[23] S.S. Buys, E. Partridge, A. Black, C.C. Johnson, L. Lamerato, C. Isaacs, D.J. Reding, R.T. Greenlee, L.A. Yokochi, B. Kessel, E.D. Crawford, T.R. Church, G.L. Andriole, J.L. Weissfeld, M.N. Fouad, D. Chia, B. O'Brien, L.R. Ragard, J.D. Clapp, J.M. Rathmell, T.L. Riley, P. Hartge, P.F. Pinsky, C.S. Zhu, G. Izmirlian, B.S. Kramer, A.B. Miller, J.L. Xu, P.C. Prorok, J.K. Gohagan, C.D. Berg and P.P. Team, Effect of screening on ovarian cancer mortality: the Prostate, Lung, Colorectal and Ovarian (PLCO) Cancer Screening Randomized Controlled Trial, *JAMA* **305** (2011), 2295-303.

[24] P.L. Carl, B.R. Temple and P.L. Cohen, Most nuclear systemic autoantigens are extremely disordered proteins: implications for the etiology of systemic autoimmunity, *Arthritis Res Ther* **7** (2005), R1360-74.

[25] P.O. Carstens and J. Schmidt, Diagnosis, pathogenesis and treatment of myositis: recent advances, *Clin Exp Immunol* **175** (2014), 349-58.

[26] L. Casciola-Rosen, K. Nagaraju, P. Plotz, K. Wang, S. Levine, E. Gabrielson, A. Corse and A. Rosen, Enhanced autoantigen expression in regenerating muscle cells in idiopathic inflammatory myopathy, *J Exp Med* **201** (2005), 591-601.

[27] M. Chatterjee, G. Dyson, N.K. Levin, J.P. Shah, R. Morris, A. Munkarah and M.A. Tainsky, Tumor autoantibodies as biomarkers for predicting ovarian cancer recurrence, *Cancer Biomark* **11** (2012), 59-73.

[28] M. Chatterjee, L.C. Hurley, N.K. Levin, M. Stack and M.A. Tainsky, Utility of paraneoplastic antigens as biomarkers for surveillance and prediction of recurrence in ovarian cancer, *Cancer Biomark* **20** (2017), 369-387.

[29] M. Chatterjee, L.C. Hurley and M.A. Tainsky, Paraneoplastic antigens as biomarkers for early diagnosis of ovarian cancer, *Gynecol Oncol Rep* **21** (2017), 37-44.

[30] M. Chatterjee, S. Mohapatra, A. Ionan, G. Bawa, R. Ali-Fehmi, X. Wang, J. Nowak, B. Ye, F.A. Nahhas, K. Lu, S.S. Witkin, D. Fishman, A. Munkarah, R. Morris, N.K. Levin, N.N. Shirley, G. Tromp, J. Abrams, S. Draghici and M.A. Tainsky, Diagnostic markers of ovarian cancer by high-throughput antigen cloning and detection on arrays, *Cancer Res* **66** (2006), 1181-90.

[31] R. Chauhan, R. Handa, T.P. Das and U. Pati, Over-expression of TATA binding protein (TBP) and p53 and autoantibodies to these antigens are features of systemic sclerosis, systemic lupus erythematosus and overlap syndromes, *Clin Exp Immunol* **136** (2004), 574-84.

[32] A. Chefdeville, I. Treilleux, M.E. Mayeur, C. Couillault, G. Picard, C. Bost, K. Mokhtari, A. Vasiljevic, D. Meyronet, V. Rogemond, D. Psimaras, B. Dubois, J. Honnorat and V. Desestret, Immunopathological characterization of ovarian teratomas associated with anti-N-methyl-D-aspartate receptor encephalitis, *Acta Neuropathol Commun* **7** (2019), 38.

[33] Y.T. Chen, M.J. Scanlan, U. Sahin, O. Tureci, A.O. Gure, S. Tsang, B. Williamson, E. Stockert, M. Pfreundschuh and L.J. Old, A testicular antigen aberrantly expressed in human cancers detected by autologous antibody screening, *Proc Natl Acad Sci U S A* **94** (1997), 1914-8.

[34] W.C. Cheung, S.A. Beausoleil, X. Zhang, S. Sato, S.M. Schieferl, J.S. Wieler, J.G. Beaudet, R.K. Ramenani, L. Popova, M.J. Comb, J. Rush and R.D. Polakiewicz, A proteomics approach for the identification and cloning of monoclonal antibodies from serum, *Nat Biotechnol* **30** (2012), 447-52.

[35] H. Chinoy, N. Fertig, C.V. Oddis, W.E. Ollier and R.G. Cooper, The diagnostic utility of myositis autoantibody testing for predicting the risk of cancer-associated myositis, *Ann Rheum Dis* **66** (2007), 1345-9.

[36] H. Choi, D. Kim, S. Yang, H. Sung and S. Choi, A case of paraneoplastic vasculitic neuropathy associated with gastric cancer, *Clin Neurol* **115** (2013), 218-21.

[37] A.J. Cole, T. Dwight, A.J. Gill, K.A. Dickson, Y. Zhu, A. Clarkson, G.B. Gard, J. Maidens, S. Valmadre, R. Clifton-Bligh and D.J. Marsh, Assessing mutant p53 in primary high-grade serous ovarian cancer using immunohistochemistry and massively parallel sequencing, *Sci Rep* **6** (2016), 26191.

[38] J.P. Corradi, C. Yang, J.C. Darnell, J. Dalmau and R.B. Darnell, A post-transcriptional regulatory mechanism restricts expression of the paraneoplastic cerebellar degeneration antigen cdr2 to immune privileged tissues, *J Neurosci* **17** (1997), 1406-15.

[39] K.L. Cox, V. Devanarayan, A. Kriauciunas, J. Manetta, C. Montrose and S. Sittampalam, Immunoassay Methods, in: *Assay Guidance Manual*, G.S. Sittampalam, N.P. Coussens, K. Brimacombe, A. Grossman, M. Arkin, D. Auld, C. Austin, J. Baell, B. Bejcek, J.M.M. Caaveiro, T.D.Y. Chung, J.L. Dahlin, V. Devanaryan, T.L. Foley, M. Glicksman, M.D. Hall, J.V. Haas, J. Inglese, P.W. Iversen, S.D. Kahl, S.C. Kales, M. Lal-Nag, Z. Li, J. McGee, O. McManus, T. Riss, O.J. Trask, Jr., J.R. Weidner, M.J. Wildey, M. Xia and X. Xu, eds., Bethesda (MD), 2004.

[40] D.W. Cramer, D.J. O'Rourke, A.F. Vitonis, U.A. Matulonis, D.A. Dijohnson, P.M. Sluss, C.P. Crum and B.C. Liu, CA125 immune complexes in ovarian cancer patients with low CA125 concentrations, *Clin Chem* **56** (2010), 1889-92.

[41] M.G. Cruellas, S. Viana Vdos, M. Levy-Neto, F.H. Souza and S.K. Shinjo, Myositis-specific and myositis-associated autoantibody profiles and their clinical associations in a large series of patients with polymyositis and dermatomyositis, *Clinics (Sao Paulo)* **68** (2013), 909-14.

[42] T. Cui, M. Hurtig, G. Elgue, S.C. Li, G. Veronesi, A. Essaghir, J.B. Demoulin, G. Pelosi, M. Alimohammadi, K. Oberg and V. Giandomenico, Paraneoplastic antigen Ma2 autoantibodies as specific blood biomarkers for detection of early recurrence of small intestine neuroendocrine tumors, *PLoS One* **5** (2010), e16010.

[43] J.M. Cunningham, M.S. Cicek, N.B. Larson, J. Davila, C. Wang, M.C. Larson, H. Song, E.M. Dicks, P. Harrington, M. Wick, B.J. Winterhoff, H. Hamidi, G.E. Konecny, J. Chien, M. Bibikova, J.B. Fan, K.R. Kalli, N.M. Lindor, B.L. Fridley, P.P. Pharoah and E.L. Goode, Clinical characteristics of ovarian cancer classified by BRCA1, BRCA2, and RAD51C status, *Sci Rep* **4** (2014), 4026.

[44] M.C. Dalakas, Inflammatory disorders of muscle: progress in polymyositis, dermatomyositis and inclusion body myositis, *Curr Opin Neurol* **17** (2004), 561-7.

[45] J. Dalmau, E. Lancaster, E. Martinez-Hernandez, M.R. Rosenfeld and R. Balice-Gordon, Clinical experience and laboratory investigations in patients with anti-NMDAR encephalitis, *Lancet Neurol* **10** (2011), 63-74.

[46] J.C. Darnell, M.L. Albert and R.B. Darnell, Cdr2, a target antigen of naturally occuring human tumor immunity, is widely expressed in gynecological tumors, *Cancer Res* **60** (2000), 2136-9.

[47] J.W. de Beukelaar and P.A. Sillevis Smitt, Managing paraneoplastic neurological disorders. Oncologist *Oncologist* **11** (2006), 292-305.

[48] L. Dekker, S. Wu, M. Vanduijn, N. Tolic, C. Stingl, R. Zhao, T. Luider and L. Pasa-Tolic, An integrated top-down and bottom-up proteomic approach to characterize the antigen-binding fragment of antibodies, *Proteomics* **14** (2014), 1239-48.

[49] C. Dickson, A.J. Fletcher, M. Vaysburd, J.C. Yang, D.L. Mallery, J. Zeng, C.M. Johnson, S.H. McLaughlin, M. Skehel, S. Maslen, J. Cruickshank, N. Huguenin-Dezot, J.W. Chin, D. Neuhaus and L.C. James, Intracellular antibody signalling is regulated by phosphorylation of the Fc receptor TRIM21, *Elife* **7** (2018).

[50] J. Ducie, F. Dao, M. Considine, N. Olvera, P.A. Shaw, R.J. Kurman, I.M. Shih, R.A. Soslow, L. Cope and D.A. Levine, Molecular analysis of high-grade serous ovarian carcinoma with and without associated serous tubal intra-epithelial carcinoma, *Nat Commun* **8** (2017), 990.

[51] S. Ehrlich, C.M. Fassbender, C. Blaes, C. Finke, A. Gunther, L. Harms, F. Hoffmann, K. Jahner, R. Klingel, A. Kraft, T. Lempert, M. Tesch, J. Thomsen, H. Topka, J. Jochim, C. Veauthier and W. Kohler, Therapeutic apheresis for autoimmune encephalitis: a nationwide data collection, *Nervenarzt* **84** (2013), 498-507.

[52] T.W. Eichler, C. Totland, M. Haugen, T.H. Qvale, K. Mazengia, A. Storstein, B.I. Haukanes and C.A. Vedeler, CDR2L Antibodies: A New Player in Paraneoplastic Cerebellar Degeneration, *PLoS One* **8** (2013), e66002.

[53] K.M. Elias, W. Fendler, K. Stawiski, S.J. Fiascone, A.F. Vitonis, R.S. Berkowitz, G. Frendl, P. Konstantinopoulos, C.P. Crum, M. Kedzierska, D.W. Cramer and D. Chowdhury, Diagnostic potential for a serum miRNA neural network for detection of ovarian cancer, *Elife* **6** (2017).

[54] K.M. Elias, J. Guo and R.C. Bast, Jr., Early Detection of Ovarian Cancer, *Hematol Oncol Clin North Am* **32** (2018), 903-914.

[55] A. Espinosa, W. Zhou, M. Ek, M. Hedlund, S. Brauner, K. Popovic, L. Horvath, T. Wallerskog, M. Oukka, F. Nyberg, V.K. Kuchroo and M. Wahren-Herlenius, The Sjogren's syndrome-associated autoantigen Ro52 is an E3 ligase that regulates proliferation and cell death, *J Immunol* **176** (2006), 6277-85.

[56] A. Finch, K.A. Metcalfe, J.K. Chiang, L. Elit, J. McLaughlin, C. Springate, R. Demsky, J. Murphy, B. Rosen and S.A. Narod, The impact of prophylactic salpingo-oophorectomy on menopausal symptoms and sexual function in women who carry a BRCA mutation, *Gynecol Oncol* **121** (2011), 163-8.

[57] D.F. Fiorentino, L.S. Chung, L. Christopher-Stine, L. Zaba, S. Li, A.L. Mammen, A. Rosen and L. Casciola-Rosen, Most patients with cancer-associated dermatomyositis have antibodies to nuclear matrix protein NXP-2 or transcription intermediary factor 1gamma, *Arthritis Rheum* **65** (2013), 2954-62.

[58] J. Fleisher, M. Richie, R. Price, S. Scherer, J. Dalmau and E. Lancaster, Acquired neuromyotonia heralding recurrent thymoma in myasthenia gravis, *JAMA Neurol* **70** (2013), 1311-4.

[59] K. Fon Tacer, M.C. Montoya, M.J. Oatley, T. Lord, J.M. Oatley, J. Klein, R. Ravichandran, H. Tillman, M. Kim, J.P. Connelly, S.M. Pruett-Miller, A.L. Bookout, E. Binshtock, M.M. Kaminski and P.R. Potts, MAGE cancer-testis antigens protect the mammalian germline under environmental stress, *Sci Adv* **5** (2019), eaav4832.

[60] A.P. Forgy, T.L. Ewing and J. Flaningam, Two paraneoplastic syndromes in a patient with ovarian cancer: nephrotic syndrome and paraneoplastic cerebellar degeneration, *Gynecol Oncol* **80** (2001), 96-8.

[61] R.T. Fortner, A. Damms-Machado and R. Kaaks, Systematic review: Tumor-associated antigen autoantibodies and ovarian cancer early detection, *Gynecol Oncol* **147** (2017), 465-480.

[62] M. Frings, G. Antoch, P. Knorn, L. Freudenberg, U. Bier, D. Timmann and M. Maschke, Strategies in detection of the primary tumour in anti-Yo associated paraneoplastic cerebellar degeneration, *J Neurol* **252** (2005), 197-201.

[63] M. Gieron, L. Margraf, J. Korthals, A. Gonzalvo, R. Murtagh and E. Hvizdala, Progressive necrotizing myelopathy associated with leukemia: clinical, pathologic, and MRI correlation, *J Child Neurol* **1987**, 44-9.

[64] C.C. Goodnow, J. Sprent, B. Fazekas de St Groth and C.G. Vinuesa, Cellular and genetic mechanisms of self tolerance and autoimmunity, *Nature* **435** (2005), 590-7.

[65] P. Gozzard, M. Woodhall, C. Chapman, A. Nibber, P. Waters, A. Vincent, B. Lang and P. Maddison, Paraneoplastic neurologic disorders in small cell lung carcinoma: A prospective study, *Neurology* **85** (2015), 235-9.

[66] F. Graus and J. Dalmau, Paraneoplastic neurological syndromes in the era of immune-checkpoint inhibitors, *Nat Rev Clin Oncol* **16** (2019), 535-548.

[67] F. Graus, J.Y. Delattre, J.C. Antoine, J. Dalmau, B. Giometto, W. Grisold, J. Honnorat, P.S. Smitt, C. Vedeler, J.J. Verschuuren, A. Vincent and R. Voltz, Recommended diagnostic criteria for paraneoplastic neurological syndromes, *J Neurol Neurosurg Psychiatry* **75** (2004), 1135-40.

[68] J.E. Greenlee, S.A. Clawson, K.E. Hill, B. Wood, S.L. Clardy, I. Tsunoda and N.G. Carlson, Anti-Yo antibody uptake and interaction with its intracellular target antigen causes Purkinje cell death in rat cerebellar slice cultures: a possible mechanism for paraneoplastic cerebellar degeneration in humans with gynecological or breast cancers, *PLoS One* **10** (2015), e0123446.

[69] J.E. Greenlee, S.A. Clawson, K.E. Hill, B. Wood, S.L. Clardy, I. Tsunoda, T.D. Jaskowski and N.G. Carlson, Neuronal uptake of anti-Hu antibody, but not anti-Ri antibody, leads to cell death in brain slice cultures, *J Neuroinflammation* **11** (2014), 160.

[70] W. Grisold, B. Giometto, R. Vitaliani and S. Oberndorfer, Current approaches to the treatment of paraneoplastic encephalitis, *Ther Adv Neurol Disord* **4** (2011), 237-248.

[71] S. Gultekin, M. Rosenfeld, R. Voltz, J. Eichen, J. Posner and J. Dalmau, Paraneoplastic limbic encephalitis: neurological symptoms, immunological findings and tumour association in 50 patients., *Brain* **123** (2000), 1481-1494.

[72] P. Gupta, C. Chen, P. Chaluvally-Raghavan and S. Pradeep, B Cells as an Immune-Regulatory Signature in Ovarian Cancer, *Cancers (Basel)* **11** (2019).

[73] T. Hainzl, S. Huang and A.E. Sauer-Eriksson, Structure of the SRP19 RNA complex and implications for signal recognition particle assembly, *Nature* **417** (2002), 767-71.

[74] I. Hellstrom, J. Raycraft, M. Hayden-Ledbetter, J.A. Ledbetter, M. Schummer, M. McIntosh, C. Drescher, N. Urban and K.E. Hellstrom, The HE4 (WFDC2) protein is a biomarker for ovarian carcinoma, *Cancer Res* **63** (2003), 3695-700.

[75] J.T. Henderson, E.M. Webber and G.F. Sawaya, Screening for Ovarian Cancer: Updated Evidence Report and Systematic Review for the US Preventive Services Task Force, *JAMA* **319** (2018), 595-606.

[76] K.A. Henry, C. Zwieb and H.M. Fried, Purification and biochemical characterization of the 19-kDa signal recognition particle RNA-binding protein expressed as a hexahistidine-tagged polypeptide in Escherichia coli, *Protein Expr Purif* **9** (1997), 15-26.

[77] Y. Hiasa, M. Kunishige, T. Mitsui, S. Kondo, R. Kuriwaka and S. Shigekiyo, et al., Complicated paraneoplastic neurological syndromes: a report of two patients with small cell or non-small cell lung cancer., *Clin Neurol Neurosurg* **90** (2003), 213-6.

[78] O. Hocar, E. Poszepczynska-Guigne, O. Faye, J. Wechsler, M. Bagot and V. Buffard, Severe necrotizing myopathy subsequent to Merkel cell carcinoma, *Ann Dermatol Venereol* **138** (2011), 130-4.

[79] R. Hoftberger, L. Sabater, F. Velasco, R. Ciordia, J. Dalmau and F. Graus, Carbonic anhydrase-related protein VIII antibodies and paraneoplastic cerebellar degeneration, *Neuropathol Appl Neurobiol* **40** (2014), 650-3.

[80] R. Houtmeyers, J. Souopgui, S. Tejpar and R. Arkell, The ZIC gene family encodes multi-functional proteins essential for patterning and morphogenesis, *Cell Mol Life Sci* **70** (2013), 3791-811.

[81] R.Y. Huang, A. Francois, A.R. McGray, A. Miliotto and K. Odunsi, Compensatory upregulation of PD-1, LAG-3, and CTLA-4 limits the efficacy of single-agent checkpoint blockade in metastatic ovarian cancer, *Oncoimmunology* **6** (2017), e1249561.

[82] J.K. Hwang, F.W. Alt and L.S. Yeap, Related Mechanisms of Antibody Somatic Hypermutation and Class Switch Recombination, *Microbiol Spectr* **3** (2015), MDNA3-0037-2014.

[83] R. Iorio, G. Spagni and G. Masi, Paraneoplastic neurological syndromes, *Semin Diagn Pathol* **36** (2019), 279-292.

[84] A. Ishikawa, Y. Muro, K. Sugiura and M. Akiyama, Development of an ELISA for detection of autoantibodies to nuclear matrix protein 2, *Rheumatology (Oxford)* **51** (2012), 1181-7.

[85] I. Jacobs, Steady, relentless progress towards effective, safe screening for early detection of cancer of the ovary, *BJOG* **125** (2018), 526-528.

[86] I.J. Jacobs, U. Menon, A. Ryan, A. Gentry-Maharaj, M. Burnell, J.K. Kalsi, N.N. Amso, S. Apostolidou, E. Benjamin, D. Cruickshank, D.N. Crump, S.K. Davies, A. Dawnay, S. Dobbs, G. Fletcher, J. Ford, K. Godfrey, R. Gunu, M. Habib, R. Hallett, J. Herod, H. Jenkins, C. Karpinskyj, S. Leeson, S.J. Lewis, W.R. Liston, A. Lopes, T. Mould, J. Murdoch, D. Oram, D.J. Rabideau, K. Reynolds, I. Scott, M.W. Seif, A. Sharma, N. Singh, J. Taylor, F. Warburton, M. Widschwendter, K. Williamson, R. Woolas, L. Fallowfield, A.J. McGuire, S. Campbell, M. Parmar and S.J. Skates, Ovarian cancer screening and mortality in the UK Collaborative Trial of Ovarian Cancer Screening (UKCTOCS): a randomised controlled trial, *Lancet* **387** (2016), 945-956.

[87] J.R. Jett, L.J. Peek, L. Fredericks, W. Jewell, W.W. Pingleton and J.F. Robertson, Audit of the autoantibody test, EarlyCDT(R)-lung, in 1600 patients: an evaluation of its performance in routine clinical practice, *Lung Cancer* **83** (2014), 51-5.

[88] B. Jia and C.O. Jeon, High-throughput recombinant protein expression in Escherichia coli: current status and future perspectives, *Open Biol* **6** (2016).

[89] V. Jindal, E. Arora, S. Gupta, A. Lal, M. Masab and R. Potdar, Prospects of chimeric antigen receptor T cell therapy in ovarian cancer, *Med Oncol* **35** (2018), 70.

[90] L.E. Kandalaft, K. Odunsi and G. Coukos, Immunotherapy in Ovarian Cancer: Are We There Yet?, *J Clin Oncol* **37** (2019), 2460-2471.

[91] B.A. Katchman, R. Barderas, R. Alam, D. Chowell, M.S. Field, L.J. Esserman, G. Wallstrom, J. LaBaer, D.W. Cramer, M.A. Hollingsworth and K.S. Anderson, Proteomic mapping of p53 immunogenicity in pancreatic, ovarian, and breast cancers, *Proteomics Clin Appl* **10** (2016), 720-31.

[92] B.A. Katchman, D. Chowell, G. Wallstrom, A.F. Vitonis, J. LaBaer, D.W. Cramer and K.S. Anderson, Autoantibody biomarkers for the detection of serous ovarian cancer, *Gynecol Oncol* **146** (2017), 129-136.

[93] M. Kazarian and I.A. Laird-Offringa, Small-cell lung cancer-associated autoantibodies: potential applications to cancer diagnosis, early detection, and therapy, *Mol Cancer* **10** (2011), 33.

[94] A.H. Keeble, Z. Khan, A. Forster and L.C. James, TRIM21 is an IgG receptor that is structurally, thermodynamically, and kinetically conserved, *Proc Natl Acad Sci U S A* **105** (2008), 6045-50.

[95] A. Kerasnoudis, M. Rockhoff, J. Federlein, R. Gold and C. Krogias, Isolated ZIC4 antibodies in paraneoplastic cerebellar syndrome with an underlying ovarian tumor, *Arch Neurol* **68** (2011), 1073.

[96] V. Keyvani, M. Farshchian, S.A. Esmaeili, H. Yari, M. Moghbeli, S.K. Nezhad and M.R. Abbaszadegan, Ovarian cancer stem cells and targeted therapy, *J Ovarian Res* **12** (2019), 120.

[97] H. Kobayashi, Y. Yamada, T. Sado, M. Sakata, S. Yoshida, R. Kawaguchi, S. Kanayama, H. Shigetomi, S. Haruta, Y. Tsuji, S. Ueda and T. Kitanaka, A randomized study of screening for ovarian cancer: a multicenter study in Japan, *Int J Gynecol Cancer* **18** (2008), 414-20.

[98] T. Krakenes, I. Herdlevaer, M. Raspotnig, M. Haugen, M. Schubert and C.A. Vedeler, CDR2L Is the Major Yo Antibody Target in Paraneoplastic Cerebellar Degeneration, *Ann Neurol* **86** (2019), 316-321.

[99] D.R. Kroeger, K. Milne and B.H. Nelson, Tumor-Infiltrating Plasma Cells Are Associated with Tertiary Lymphoid Structures, Cytolytic T-Cell Responses, and Superior Prognosis in Ovarian Cancer, *Clin Cancer Res* **22** (2016), 3005-15.

[100] M. Kuboshima, H. Shimada, T.L. Liu, F. Nomura, M. Takiguchi, T. Hiwasa and T. Ochiai, Presence of serum tripartite motif-containing 21 antibodies in patients with esophageal squamous cell carcinoma, *Cancer Sci* **97** (2006), 380-6.

[101] R.J. Kurman and M. Shih Ie, The Dualistic Model of Ovarian Carcinogenesis: Revisited, Revised, and Expanded, *Am J Pathol* **186** (2016), 733-47.

[102] M. Labrador-Horrillo, M.A. Martinez, A. Selva-O'Callaghan, E. Trallero-Araguas, J.M. Grau-Junyent, M. Vilardell-Tarres and C. Juarez, Identification of a novel myositis-associated antibody directed against cortactin, *Autoimmun Rev* **13** (2014), 1008-12.

[103] E. Lancaster, Paraneoplastic Disorders, *Continuum (Minneap Minn)* **23** (2017), 1653-1679.

[104] V.A. Lennon, T.J. Kryzer, G.E. Griesmann, P.E. O'Suilleabhain, A.J. Windebank, A. Woppmann, G.P. Miljanich and E.H. Lambert, Calcium-channel antibodies in the Lambert-Eaton syndrome and other paraneoplastic syndromes, *N Engl J Med* **332** (1995), 1467-74.

[105] F. Leypoldt and K.-P. Wandinger, Paraneoplastic neurological syndromes, *Clinical & Experimental Immunology* **175** (2014), 336-348.

[106] S. Lheureux, C. Gourley, I. Vergote and A.M. Oza, Epithelial ovarian cancer, *Lancet* **393** (2019), 1240-1253.

[107] A. Li, M. Yi, S. Qin, Q. Chu, S. Luo and K. Wu, Prospects for combining immune checkpoint blockade with PARP inhibition, *J Hematol Oncol* **12** (2019), 98.

[108] A. Li, L. Zhang, X. Zhang, W. Jin and Y. Ren, Expression and clinical significance of cortactin protein in ovarian neoplasms, *Clin Transl Oncol* **18** (2016), 220-7.

[109] S.S. Lingawi, J.H. Bilbey, P.L. Munk, P.Y. Poon, B.M. Allan and I.A. Olivotto, et al., MR imaging of brachial plexopathy in breast cancer patients without palpable recurrence., *Skeletal Radiol* **48** (1999), 836-7.

[110] M.Y. Liu, H. Su, H.L. Huang and J.Q. Chen, Cancer stem-like cells with increased expression of NY-ESO-1 initiate breast cancer metastasis, *Oncol Lett* **18** (2019), 3664-3672.

[111] P. Maat, E. Brouwer, E. Hulsenboom, M. VanDuijn, M.W. Schreurs, H. Hooijkaas and P.A. Smitt, Multiplex serology of paraneoplastic antineuronal antibodies, *J Immunol Methods* **391** (2013), 125-32.

[112] P.L. Mai, M. Piedmonte, P.K. Han, R.P. Moser, J.L. Walker, G. Rodriguez, J. Boggess, T.J. Rutherford, O. Zivanovic, D.E. Cohn, J.T. Thigpen, R.M. Wenham, M.L. Friedlander, C.A. Hamilton, J. Bakkum-Gamez, A.B. Olawaiye, M.L. Hensley, M.H. Greene, H.Q. Huang and L. Wenzel, Factors associated with deciding between risk-reducing salpingo-oophorectomy and ovarian cancer screening among high-risk women enrolled in GOG-0199: An NRG Oncology/Gynecologic Oncology Group study, *Gynecol Oncol* **145** (2017), 122-129.

[113] C. Mallecourt and J. Delattre, Paraneoplastic neuropathies, *Presse Med* **29** (2000), 447-52.

[114] R. Mari, E. Mamessier, E. Lambaudie, M. Provansal, D. Birnbaum, F. Bertucci and R. Sabatier, Liquid Biopsies for Ovarian Carcinoma: How Blood Tests May Improve the Clinical Management of a Deadly Disease, *Cancers (Basel)* **11** (2019).

[115] I. Marie, P.Y. Hatron, S. Dominique, P. Cherin, L. Mouthon, J.F. Menard, H. Levesque and F. Jouen, Short-term and long-term outcome of anti-Jo1-positive patients with anti-Ro52 antibody, *Semin Arthritis Rheum* **41** (2012), 890-9.

[116] C. Marth, V. Wieser, I. Tsibulak and A.G. Zeimet, Immunotherapy in ovarian cancer: fake news or the real deal?, *Int J Gynecol Cancer* **29** (2019), 201-211.

[117] A. Masiak, J. Kulczycka, Z. Czuszynska and Z. Zdrojewski, Clinical characteristics of patients with anti-TIF1-gamma antibodies, *Reumatologia* **54** (2016), 14-8.

[118] R.M. Mathew, R. Vandenberghe, A. Garcia-Merino, T. Yamamoto, J.C. Landolfi, M.R. Rosenfeld, J.E. Rossi, B. Thiessen, E.J. Dropcho and J. Dalmau, Orchiectomy for suspected microscopic tumor in patients with anti-Ma2-associated encephalitis, *Neurology* **68** (2007), 900-5.

[119] M. Matz, M.P. Coleman, H. Carreira, D. Salmeron, M.D. Chirlaque, C. Allemani and C.W. Group, Worldwide comparison of ovarian cancer survival: Histological group and stage at diagnosis (CONCORD-2), *Gynecol Oncol* **144** (2017), 396-404.

[120] W.A. McEwan, B. Falcon, M. Vaysburd, D. Clift, A.L. Oblak, B. Ghetti, M. Goedert and L.C. James, Cytosolic Fc receptor TRIM21 inhibits seeded tau aggregation, *Proc Natl Acad Sci U S A* **114** (2017), 574-579.

[121] W.A. McEwan and L.C. James, TRIM21-dependent intracellular antibody neutralization of virus infection, *Prog Mol Biol Transl Sci* **129** (2015), 167-87.

[122] A. Mitchell, C. Bakhos and E. Zimmerman, Anti-Ri-associated paraneoplastic brainstem cerebellar syndrome with coexisting limbic encephalitis in a patient with mixed large cell neuroendocrine lung carcinoma, *J Clin Neurosci* **22** (2015), 421-3.

[123] P. Modaffari, R. Ponzone, A. Ferrari, I. Cipullo, V. Liberale, M. D'Alonzo, F. Maggiorotto and N. Biglia, Concerns and Expectations of Risk-Reducing Surgery in Women with Hereditary Breast and Ovarian Cancer Syndrome, *J Clin Med* **8** (2019).

[124] S.E. Monstad, A. Storstein, A. Dorum, A. Knudsen, P.E. Lonning, H.B. Salvesen, J.H. Aarseth and C.A. Vedeler, Yo antibodies in ovarian and breast cancer patients detected by a sensitive immunoprecipitation technique, *Clin Exp Immunol* **144** (2006), 53-8.

[125] A. Montfort, O. Pearce, E. Maniati, B.G. Vincent, L. Bixby, S. Bohm, T. Dowe, E.H. Wilkes, P. Chakravarty, R. Thompson, J. Topping, P.R. Cutillas, M. Lockley, J.S. Serody, M. Capasso and F.R. Balkwill, A Strong B-cell Response Is Part of the Immune Landscape in Human High-Grade Serous Ovarian Metastases, *Clin Cancer Res* **23** (2017), 250-262.

[126] K. Musunuru and S. Kesari, Paraneoplastic opsoclonus-myoclonus ataxia associated with non-small-cell lung carcinoma., *J Neurooncol* **90** (2008), 213-6.

[127] A. Neal, M. Qian, A. Clinch and B. Le, Orthostatic hypotension secondary to CRMP-5 paraneoplastic autonomic neuropathy, *J Clin Neurosci* **21** (2014), 885-6.

[128] D.R. Nebgen, K.H. Lu and R.C. Bast, Jr., Novel Approaches to Ovarian Cancer Screening, *Curr Oncol Rep* **21** (2019), 75.

[129] S.S. Neelapu, S. Tummala, P. Kebriaei, W. Wierda, C. Gutierrez, F.L. Locke, K.V. Komanduri, Y. Lin, N. Jain, N. Daver, J. Westin, A.M. Gulbis, M.E. Loghin, J.F. de Groot, S. Adkins, S.E. Davis, K. Rezvani, P. Hwu and E.J. Shpall, Chimeric antigen receptor T-cell therapy - assessment and management of toxicities, *Nat Rev Clin Oncol* **15** (2018), 47-62.

[130] K.J. O'Donovan, J. Diedler, G.C. Couture, J.J. Fak and R.B. Darnell, The onconeural antigen cdr2 is a novel APC/C target that acts in mitosis to regulate c-myc target genes in mammalian tumor cells, *PLoS One* **5** (2010), e10045.

[131] K. Odunsi, Immunotherapy in ovarian cancer, *Ann Oncol* **28** (2017), viii1-viii7.

[132] K. Odunsi, J. Matsuzaki, S.R. James, P. Mhawech-Fauceglia, T. Tsuji, A. Miller, W. Zhang, S.N. Akers, E.A. Griffiths, A. Miliotto, A. Beck, C.A. Batt, G. Ritter, S. Lele, S. Gnjatic and A.R. Karpf, Epigenetic potentiation of NY-ESO-1 vaccine therapy in human ovarian cancer, *Cancer Immunol Res* **2** (2014), 37-49.

[133] V. Oke and M. Wahren-Herlenius, The immunobiology of Ro52 (TRIM21) in autoimmunity: a critical review, *J Autoimmun* **39** (2012), 77-82.

[134] I. Peene, Meheus, L, De Keyser, S, Humbel, R, Veys, EM, De Keyser, F, Anti-Ro52 reactivity is an independent and additional
serum marker in connective tissue disease, *Ann Rheum Dis* **61** (2002), 929-933.

[135] K. Peterson, M.K. Rosenblum, H. Kotanides and J.B. Posner, Paraneoplastic cerebellar degeneration. I. A clinical analysis of 55 anti-Yo antibody-positive patients, *Neurology* **42** (1992), 1931-7.

[136] N. Petrucelli, M.B. Daly and G.L. Feldman, Hereditary breast and ovarian cancer due to mutations in BRCA1 and BRCA2, *Genet Med* **12** (2010), 245-59.

[137] B.S. Pignolet, C.M. Gebauer and R.S. Liblau, Immunopathogenesis of paraneoplastic neurological syndromes associated with anti-Hu antibodies: A beneficial antitumor immune response going awry, *Oncoimmunology* **2** (2013), e27384.

[138] I. Pinal-Fernandez, D.R. Amici, C.A. Parks, A. Derfoul, M. Casal-Dominguez, K. Pak, R. Yeker, P. Plotz, J.C. Milisenda, J.M. Grau-Junyent, A. Selva-O'Callaghan, J.J. Paik, J. Albayda, A.M. Corse, T.E. Lloyd, L. Christopher-Stine and A.L. Mammen, Myositis Autoantigen Expression Correlates With Muscle Regeneration but Not Autoantibody Specificity, *Arthritis Rheumatol* **71** (2019), 1371-1376.

[139] P.H. Plotz, The autoantibody repertoire: searching for order, *Nat Rev Immunol* **3** (2003), 73-8.

[140] A. Polans, D. Witkowska, T. Haley, D. Amundson, L. Baizer and G. Adamus, Recoverin, a photoreceptor-specific calcium-binding protein, is expressed by the tumor of a patient with cancer-associated retinopathy, *Proc Natl Acad Sci USA* **92** (1995), 9176-80.

[141] N. Pourmand and I. Pettersson, The Zn2+ binding domain of the human Ro 52 kDa protein is a target for conformation-dependent autoantibodies, *J Autoimmun* **11** (1998), 11-7.

[142] R. Pourmand, Lambert-eaton myasthenic syndrome., *Front Neurol Neurosci* **26** (2009), 120-5.

[143] J. Prat and F.C.o.G. Oncology, FIGO's staging classification for cancer of the ovary, fallopian tube, and peritoneum: abridged republication, *J Gynecol Oncol* **26** (2015), 87-9.

[144] W.A. Rocca, L. Gazzuola-Rocca, C.Y. Smith, B.R. Grossardt, S.S. Faubion, L.T. Shuster, J.L. Kirkland, E.A. Stewart and V.M. Miller, Accelerated Accumulation of Multimorbidity After Bilateral Oophorectomy: A Population-Based Cohort Study, *Mayo Clin Proc* **91** (2016), 1577-1589.

[145] A.H. Ropper and K.C. Gorson, Neuropathies Associated with Paraproteinemia, *N Engl J Med* **338** (1998), 1601-1607.

[146] B. Rosen, J. Kwon, M. Fung Kee Fung, A. Gagliardi, A. Chambers and G. Cancer Care Ontario's Practice Guidelines Initiative Gynecology Cancer Disease Site, Systematic review of management options for women with a hereditary predisposition to ovarian cancer, *Gynecol Oncol* **93** (2004), 280-6.

[147] A.N. Rosenthal, L.S.M. Fraser, S. Philpott, R. Manchanda, M. Burnell, P. Badman, R. Hadwin, I. Rizzuto, E. Benjamin, N. Singh, D.G. Evans, D.M. Eccles, A. Ryan, R. Liston, A. Dawnay, J. Ford, R. Gunu, J. Mackay, S.J. Skates, U. Menon, I.J. Jacobs and c. United Kingdom Familial Ovarian Cancer Screening Study, Evidence of Stage Shift in Women Diagnosed With Ovarian Cancer During Phase II of the United Kingdom Familial Ovarian Cancer Screening Study, *J Clin Oncol* **35** (2017), 1411-1420.

[148] A. Ruffatti, S. Aversa, T. Del Ross, S. Tonetto, M. Fiorentino and S. Todesco, Antiphospholipid antibody syndrome associated with ovarian cancer. A new paraneoplastic syndrome?, *J Rheumatol* **21** (1994), 2162-3.

[149] S.A. Rutjes, W.T. Vree Egberts, P. Jongen, F. Van Den Hoogen, G.J. Pruijn and W.J. Van Venrooij, Anti-Ro52 antibodies frequently co-occur with anti-Jo-1 antibodies in sera from patients with idiopathic inflammatory myopathy, *Clin Exp Immunol* **109** (1997), 32-40.

[150] L. Sabater, M. Titulaer, A. Saiz, J. Verschuuren, A. Gure and F. Graus, SOX1 antibodies are markers of paraneoplastic Lambert-Eaton myasthenic syndrome, *Neurology* **70** (2008), 924-8.

[151] T. Sakurai, K. Wakida, A. Kimura, T. Inuzuka and H. Nishida, Anti-Hu antibody-positive paraneoplastic limbic encephalitis with acute motor sensory neuropathy resembling Guillain-Barre syndrome: a case study, *Rinsho Shinkeigaku* **55** (2015), 921-5.

[152] A.D. Salama, T. Chitnis, J. Imitola, M.J. Ansari, H. Akiba, F. Tushima, M. Azuma, H. Yagita, M.H. Sayegh and S.J. Khoury, Critical role of the programmed death-1 (PD-1) pathway in regulation of experimental autoimmune encephalomyelitis, *J Exp Med* **198** (2003), 71-8.

[153] N. Scholler and N. Urban, CA125 in ovarian cancer, *Biomark Med* **1** (2007), 513-23.

[154] R.D. Schreiber, L.J. Old and M.J. Smyth, Cancer immunoediting: integrating immunity's roles in cancer suppression and promotion, *Science* **331** (2011), 1565-70.

[155] M. Schubert, D. Panja, M. Haugen, C.R. Bramham and C.A. Vedeler, Paraneoplastic CDR2 and CDR2L antibodies affect Purkinje cell calcium homeostasis, *Acta Neuropathol* **128** (2014), 835-52.

[156] M.F. Seldin, The genetics of human autoimmune disease: A perspective on progress in the field and future directions, *J Autoimmun* **64** (2015), 1-12.

[157] V.L. Sergio Prieto-González, Ernesto Trallero-Araguás, Albert Selva-O'Callaghan and Josep M Grau, Myositis and Cancer, in: *Idiopathic Inflammatory Myopathies - Recent Developments*, P.J.T. Gran, ed. eds., InTech, Europe, 2011, pp. 111-122.

[158] S. Shams'ili, J. Grefkens, B. de Leeuw, M. van den Bent, H. Hooijkaas, B. van der Holt, C. Vecht and P. Sillevis Smitt, Paraneoplastic cerebellar degeneration associated with antineuronal antibodies: analysis of 50 patients., *Brain : a journal of neurology* **126** (2003), 1409-18.

[159] S. Sheik Ali, A.L. Goddard, J.J. Luke, H. Donahue, D.J. Todd, A. Werchniak and R.A. Vleugels, Drug-associated dermatomyositis following ipilimumab therapy: a novel immune-mediated adverse event associated with cytotoxic T-lymphocyte antigen 4 blockade, *JAMA Dermatol* **151** (2015), 195-9.

[160] J.X. Shi, J.J. Qin, H. Ye, P. Wang, K.J. Wang and J.Y. Zhang, Tumor associated antigens or anti-TAA autoantibodies as biomarkers in the diagnosis of ovarian cancer: a systematic review with meta-analysis, *Expert Rev Mol Diagn* **15** (2015), 829-52.

[161] T. Shirafuji, F. Kanda, K. Sekiguchi, M. Higuchi, H. Yokozaki and K. Tanaka, et al, Anti-Hu-associated paraneoplastic encephalomyelitis with esophageal small cell carcinoma, *Intern Med* **51** (2012), 2423-7.

[162] Y. Shu, W. Qiu, J. Zheng, X. Sun, J. Yin, X. Yang, X. Yue, C. Chen, Z. Deng, S. Li, Y. Yang, F. Peng, Z. Lu, X. Hu, F. Petersen and X. Yu, HLA class II allele DRB1*16:02 is associated with anti-NMDAR encephalitis, *J Neurol Neurosurg Psychiatry* **90** (2019), 652-658.

[163] L. Sigalotti, A. Covre, S. Zabierowski, B. Himes, F. Colizzi, P.G. Natali, M. Herlyn and M. Maio, Cancer testis antigens in human melanoma stem cells: expression, distribution, and methylation status, *J Cell Physiol* **215** (2008), 287-91.

[164] A.R. Simmons, E.O. Fourkala, A. Gentry-Maharaj, A. Ryan, M.N. Sutton, K. Baggerly, H. Zheng, K.H. Lu, I. Jacobs, S. Skates, U. Menon and R.C. Bast, Jr., Complementary Longitudinal Serum Biomarkers to CA125 for Early Detection of Ovarian Cancer, *Cancer Prev Res (Phila)* **12** (2019), 391-400.

[165] S.J. Skates, EPIC Early Detection of Ovarian Cancer, *Clin Cancer Res* **22** (2016), 4542-4.

[166] S.J. Skates, M.H. Greene, S.S. Buys, P.L. Mai, P. Brown, M. Piedmonte, G. Rodriguez, J.O. Schorge, M. Sherman, M.B. Daly, T. Rutherford, W.R. Brewster, D.M. O'Malley, E. Partridge, J. Boggess, C.W. Drescher, C. Isaacs, A. Berchuck, S. Domchek, S.A. Davidson, R. Edwards, S.A. Elg, K. Wakeley, K.A. Phillips, D. Armstrong, I. Horowitz, C.J. Fabian, J. Walker, P.M. Sluss, W. Welch, L. Minasian, N.K. Horick, C.H. Kasten, S. Nayfield, D. Alberts, D.M. Finkelstein and K.H. Lu, Early Detection of Ovarian Cancer using the Risk of Ovarian Cancer Algorithm with Frequent CA125 Testing in Women at Increased Familial Risk - Combined Results from Two Screening Trials, *Clin Cancer Res* **23** (2017), 3628-3637.

[167] M. Small, I. Treilleux, C. Couillault, D. Pissaloux, G. Picard, S. Paindavoine, V. Attignon, Q. Wang, V. Rogemond, S. Lay, I. Ray-Coquard, J. Pfisterer, F. Joly, A. Du Bois, D. Psimaras, N. Bendriss-Vermare, C. Caux, B. Dubois, J. Honnorat and V. Desestret, Genetic alterations and tumor immune attack in Yo paraneoplastic cerebellar degeneration, *Acta Neuropathol* **135** (2018), 569-579.

[168] M. Stangel and R. Pul, Basic principles of intravenous immunoglobulin (IVIg) treatment, *J Neurol* **253 Suppl 5** (2006), V18-24.

[169] S. Suzuki, A. Nishikawa, M. Kuwana, H. Nishimura, Y. Watanabe, J. Nakahara, Y.K. Hayashi, N. Suzuki and I. Nishino, Inflammatory myopathy with anti-signal recognition particle antibodies: case series of 100 patients, *Orphanet J Rare Dis* **10** (2015), 61.

[170] L. Sweeney and T. Howe, Paraneoplastic syndromes, *Medicine* **44** (2016), 69-72.

[171] H. Takanaga, H. Mukai, H. Shibata, M. Toshimori and Y. Ono, PKN interacts with a paraneoplastic cerebellar degeneration-associated antigen, which is a potential transcription factor, *Exp Cell Res* **241** (1998), 363-72.

[172] C. Tanase, R. Albulescu and M. Neagu, Highlights of new immunoassay-based technologies, *J Immunoassay Immunochem* **38** (2017), 1.

[173] D.D. Taylor, C. Gercel-Taylor and L.P. Parker, Patient-derived tumor-reactive antibodies as diagnostic markers for ovarian cancer, *Gynecol Oncol* **115** (2009), 112-120.

[174] S. Tetsuka, K. Tominaga, E. Ohta, K. Kuroiwa, E. Sakashita, K. Kasashima, T. Hamamoto, M. Namekawa, M. Morita, S. Natsui, T. Morita, K. Tanaka, Y. Takiyama, I. Nakano and H. Endo, Paraneoplastic cerebellar degeneration associated with an onconeural antibody against creatine kinase, brain-type, *J Neurol Sci* **335** (2013), 48-57.

[175] R. Thomas, G. Al-Khadairi, J. Roelands, W. Hendrickx, S. Dermime, D. Bedognetti and J. Decock, NY-ESO-1 Based Immunotherapy of Cancer: Current Perspectives, *Front Immunol* **9** (2018), 947.

[176] E. Tuzun, D. Kinay, Y. Hacohen, F. Aysal and A. Vincent, Guillain-Barre-like syndrome associated with lung adenocarcinoma and CASPR2 antibodies, *Muscle Nerve* **48** (2013), 836-7.

[177] M. Uchuya, F. Graus, F. Vega, R. Rene and J.Y. Delattre, Intravenous immunoglobulin treatment in paraneoplastic neurological syndromes with antineuronal autoantibodies, *J Neurol Neurosurg Psychiatry* **60** (1996), 388-92.

[178] K. Uluc, M. Kocak, P. Koytak, D. Borucu, B. Isak and S. Aktan, et al, Paraneoplastic pandysautonomia as a manifestation of non-small cell lung cancer, *Neurol Sci* **31** (2010), 813-6.

[179] M.H. van Coevorden-Hameete, M.J. Titulaer, M.W. Schreurs, E. de Graaff, P.A. Sillevis Smitt and C.C. Hoogenraad, Detection and Characterization of Autoantibodies to Neuronal Cell-Surface Antigens in the Central Nervous System, *Front Mol Neurosci* **9** (2016), 37.

[180] S.H. van Dooren, W.J. van Venrooij and G.J. Pruijn, Myositis-specific autoantibodies: detection and clinical associations, *Auto Immun Highlights* **2** (2011), 5-20.

[181] R. Vang, M. Shih Ie and R.J. Kurman, Ovarian low-grade and high-grade serous carcinoma: pathogenesis, clinicopathologic and molecular biologic features, and diagnostic problems, *Adv Anat Pathol* **16** (2009), 267-82.

[182] G.J. Verschueren A, Boucraut J, Honnorat J, Pouget J, Attarian S., Paraneoplastic subacute lower motor neuron syndrome associated with solid cancer, *J Neurol Sci* (2015), 413-6.

[183] C.V. Verschuur, A.J. Kooi and D. Troost, Anti-aquaporin 4 related paraneoplastic neuromyelitis optica in the presence of adenocarcinoma of the lung, *Clin Neuropathol* **34** (2015), 232-6.

[184] J. Viallard, A. Vincent, J. Moreau, M. Parrens, J. Pellegrin and E. Ellie, Thymoma-associated neuromyotonia with antibodies against voltage-gated potassium channels presenting as chronic intestinal pseudo-obstruction, *Eur Neurol* **53** (2005), 60-3.

[185] J. Wang, J.D. Figueroa, G. Wallstrom, K. Barker, J.G. Park, G. Demirkan, J. Lissowska, K.S. Anderson, J. Qiu and J. LaBaer, Plasma Autoantibodies Associated with Basal-like Breast Cancers, *Cancer Epidemiol Biomarkers Prev* **24** (2015), 1332-40.

[186] P. Wang, J. Qin, H. Ye, L. Li, X. Wang and J. Zhang, Using a panel of multiple tumor-associated antigens to enhance the autoantibody detection in the immunodiagnosis of ovarian cancer, *J Cell Biochem* **120** (2019), 3091-3100.

[187] Y. Wang, S. Hong, J. Mu, Y. Wang, J. Lea, B. Kong and W. Zheng, Tubal Origin of "Ovarian" Low-Grade Serous Carcinoma: A Gene Expression Profile Study, *J Oncol* **2019** (2019), 8659754.

[188] T.J. Williams, D.R. Benavides, K.A. Patrice, J.O. Dalmau, A.L. de Avila, D.T. Le, E.J. Lipson, J.C. Probasco and E.M. Mowry, Association of Autoimmune Encephalitis With Combined Immune Checkpoint Inhibitor Treatment for Metastatic Cancer, *JAMA Neurol* **73** (2016), 928-33.

[189] L. Xiang and B. Kong, PAX8 is a novel marker for differentiating between various types of tumor, particularly ovarian epithelial carcinomas, *Oncol Lett* **5** (2013), 735-738.

[190] K. Xie, C. Fu, S. Wang, H. Xu, S. Liu, Y. Shao, Z. Gong, X. Wu, B. Xu, J. Han, J. Xu, P. Xu, X. Jia and J. Wu, Cancer-testis antigens in ovarian cancer: implication for biomarkers and therapeutic targets, *J Ovarian Res* **12** (2019), 1.

[191] S. Yadav, N. Kashaninejad, M.K. Masud, Y. Yamauchi, N.T. Nguyen and M.J.A. Shiddiky, Autoantibodies as diagnostic and prognostic cancer biomarker: Detection techniques and approaches, *Biosens Bioelectron* **139** (2019), 111315.

[192] W. Yan, H. Hu and B. Tang, Advances Of Chimeric Antigen Receptor T Cell Therapy In Ovarian Cancer, *Onco Targets Ther* **12** (2019), 8015-8022.

[193] H. Yang, Q. Peng, L. Yin, S. Li, J. Shi, Y. Zhang, X. Lu, X. Shu, S. Zhang and G. Wang, Identification of multiple cancer-associated myositis-specific autoantibodies in idiopathic inflammatory myopathies: a large longitudinal cohort study, *Arthritis Res Ther* **19** (2017), 259.

[194] W.L. Yang, A. Gentry-Maharaj, A. Simmons, A. Ryan, E.O. Fourkala, Z. Lu, K.A. Baggerly, Y. Zhao, K.H. Lu, D. Bowtell, I. Jacobs, S.J. Skates, W.W. He, U. Menon, R.C. Bast, Jr. and A.S. Group, Elevation of TP53 Autoantibody Before CA125 in Preclinical Invasive Epithelial Ovarian Cancer, *Clin Cancer Res* **23** (2017), 5912-5922.

[195] W.L. Yang, Z. Lu, J. Guo, B.M. Fellman, J. Ning, K.H. Lu, U. Menon, M. Kobayashi, S.M. Hanash, J. Celestino, S.J. Skates and R.C. Bast, Jr., Human epididymis protein 4 antigen-autoantibody complexes complement cancer antigen 125 for detecting early-stage ovarian cancer, *Cancer* (2019).

[196] T. Yawata, E. Nakai, K.C. Park, T. Chihara, A. Kumazawa, S. Toyonaga, T. Masahira, H. Nakabayashi, T. Kaji and K. Shimizu, Enhanced expression of cancer testis antigen genes in glioma stem cells, *Mol Carcinog* **49** (2010), 532-44.

[197] T.N. Yoichiro Akiyama, Masahiro Iwamoto, and Seiji Minota, Clinical features of seven Japanese patients with anti-PL-12 antibody: frequent positivity for anti-cyclic citrullinated peptide antibody, *Jichi Medical University Journal* **38** (2015), 41-45.

[198] A. Yokoi, Y. Yoshioka, A. Hirakawa, Y. Yamamoto, M. Ishikawa, S.I. Ikeda, T. Kato, K. Niimi, H. Kajiyama, F. Kikkawa and T. Ochiya, A combination of circulating miRNAs for the early detection of ovarian cancer, *Oncotarget* **8** (2017), 89811-89823.

[199] Y. Yoshida, M. Kinuta, T. Abe, S. Liang, K. Araki, O. Cremona, G. Di Paolo, Y. Moriyama, T. Yasuda, P. De Camilli and K. Takei, The stimulatory action of amphiphysin on dynamin function is dependent on lipid bilayer curvature, *EMBO J* **23** (2004), 3483-91.

[200] L.M. Yshii, C.M. Gebauer, B. Pignolet, E. Maure, C. Queriault, M. Pierau, H. Saito, N. Suzuki, M. Brunner-Weinzierl, J. Bauer and R. Liblau, CTLA4 blockade elicits paraneoplastic neurological disease in a mouse model, *Brain* **139** (2016), 2923-2934.

[201] M.P. Zaborowski and S. Michalak, Cell-mediated immune responses in paraneoplastic neurological syndromes, *Clin Dev Immunol* **2013** (2013), 630602.

[202] M.P. Zaborowski, M. Spaczynski, E. Nowak-Markwitz and S. Michalak, Paraneoplastic neurological syndromes associated with ovarian tumors, *Journal of Cancer Research and Clinical Oncology* **141** (2015), 99-108.

[203] Z.A. Zahr and A.N. Baer, Malignancy in myositis, *Curr Rheumatol Rep* **13** (2011), 208-15.

[204] S. Zampieri, D. Biral, N. Adami, A. Ghirardello, M.E. Rampudda, M. Tonello and A. Doria, Expression of myositis specific autoantigens during post-natal myogenesis, *Neurol Res* **30** (2008), 145-8.

[205] A. Zekeridou and V.A. Lennon, Neurologic Autoimmunity in the Era of Checkpoint Inhibitor Cancer Immunotherapy, *Mayo Clin Proc* **94** (2019), 1865-1878.

[206] D.Q. Zhang, R. Wang, T. Li, X. Li, Y. Qi and e.a. Wang J, Remarkably increased resistin levels in anti-AChR antibody-positive myasthenia gravis, *J Neuroimmunol* **283** (2015), 7-10.

[207] L. Zhang, J.R. Conejo-Garcia, D. Katsaros, P.A. Gimotty, M. Massobrio, G. Regnani, A. Makrigiannakis, H. Gray, K. Schlienger, M.N. Liebman, S.C. Rubin and G. Coukos, Intratumoral T cells, recurrence, and survival in epithelial ovarian cancer, *N Engl J Med* **348** (2003), 203-13.

[208] X. Zhang, H. Li, X. Yu, S. Li, Z. Lei, C. Li, Q. Zhang, Q. Han, Y. Li, K. Zhang, Y. Wang, C. Liu, Y. Mao, X. Wang, D.M. Irwin, H. Guo, G. Niu and H. Tan, Analysis of Circulating Tumor Cells in Ovarian Cancer and Their Clinical Value as a Biomarker, *Cell Physiol Biochem* **48** (2018), 1983-1994.

[209] H. Zheng, L. Zhang, Y. Zhao, D. Yang, F. Song, Y. Wen, Q. Hao, Z. Hu, W. Zhang and K. Chen, Plasma miRNAs as diagnostic and prognostic biomarkers for ovarian cancer, *PLoS One* **8** (2013), e77853.

[210] J.J. Zhou, F. Wang, Z. Xu, W.S. Lo, C.F. Lau, K.P. Chiang, L.A. Nangle, M.A. Ashlock, J.D. Mendlein, X.L. Yang, M. Zhang and P. Schimmel, Secreted histidyl-tRNA synthetase splice variants elaborate major epitopes for autoantibodies in inflammatory myositis, *J Biol Chem* **289** (2014), 19269-75.

[211] Q. Zhu, S.X. Han, C.Y. Zhou, M.J. Cai, L.P. Dai and J.Y. Zhang, Autoimmune response to PARP and BRCA1/BRCA2 in cancer, *Oncotarget* **6** (2015), 11575-84.

ABSTRACT

EVALUATION OF AUTOANTIBODIES TO PARANEOPLASTIC ANTIGEN AS EARLY DETECTION BIOMARKERS FOR HIGH-GRADE SEROUS OVARIAN CANCER

by

LAURA CATHERINE HURLEY

May 2020

Advisor: Dr. Michael A. Tainsky

Major: Cancer Biology

Degree: Doctor of Philosophy

The majority of ovarian cancer cases are diagnosed at an advanced stage metastatic disease with poor prognosis due to non-specific symptoms and lack of early detection methods. This study evaluates autoantibodies against tumor antigens to identify candidate biomarkers for the early detection of ovarian cancer in high-risk women. We examined antigens associated with paraneoplastic neurological synromes, which are autoimmune diseases that develop when the unregulated immune response against a tumor also targets healthy cells. Notably, a set of autoantibodies have been previously detected in paraneoplastic neurological syndrome patients with concurrent or subsequent diagnosis of ovarian cancer, identifying highly immunogenic antigens in the tumor.

In this dissertation work, we have detected paraneoplastic antibodies present in serum samples from patients with high-grade serous ovarian cancer (HGSOC) without paraneoplastic neurological syndromes using line blots, western blots, and ELISA. A panel of five paraneoplastic antigens (HARS, TRIM21, COR, CDR2, CDR2L) along with 2 established tumor antigens (NY-ESO-1, p53) were purified from E. coli for screening

on western blot and ELISA. Screening was performed with a patient serum set consisting of: 50 late stage HGSOC, 14 early stage HGSOC, 50 benign ovarian cyst, and 50 healthy volunteer samples. On western blot, the paraneoplastic antigen with the best performance was TRIM21 with 35% sensitivity. Combining TRIM21 with p53 and NY-ESO-1 yielded a sensitivity of 60% with 90% specificity. In the early stage HGSOC sample set, HARS demonstrated 31% sensitivity individually, and 46% sensitivity with 98% specificity when combined with p53 and NY-ESO-1. The identified markers will were tested in an independent validation serum set consisting of n=150 samples. The work in this dissertation identified the paraneoplastic antigen TRIM21 that can enhance autoantibody biomarker panels for the early detection of HGSOC.

AUTOBIOGRAPHICAL STATEMENT

EDUCATION

The University of Michigan, Ann Arbor
2007-2011
Bachelor of Science: Biology

FELLOWSHIPS/SCHOLARSHIPS

DeRoy Testamentary Foundation Predoctoral Fellowship in Cancer Research
Detroit, Michigan
2018-2019

Wayne State University Rumble Graduate Research Assistantship
Detroit, Michigan
2018-2019

Ruth L. Kirschenstein Research Training Grant (T32-CA009531)
Detroit, Michigan
2016-2018

Okayama University Research Exchange Fellowship
Detroit, Michigan
Okayama University, Okayama, Japan
Enrichment of cancer stem cells from ovarian cancer cell lines
2015-2016

Cancer Biology Graduate Program Director's Award
Detroit, Michigan
2014-2015

University of Michigan College of Literature Science and the Arts International Opportunities Scholarship
Ann Arbor, Michigan
San Raffaelle Scientific Institute, Milan, Italy
Study of ADAM10 autoantibodies in epithelial cancer patient serum
2010